2020-06-05

BYU Diesel Engine Lab Setup and Parasitic Losses of the Water Pump and Vacuum Pump on a Cummins 2.8L Engine

Eric Ashton Jessup
Brigham Young University

BYU Diesel Engine Lab Setup and Parasitic Losses of the Water Pump

and Vacuum Pump on a Cummins 2.8 L Engine

Eric Ashton Jessup

A thesis submitted to the faculty of
Brigham Young University
in partial fulfillment of the requirements for the degree of

Master of Science

Dale R. Tree, Chair
Bradley R. Adams
Brian D. Iverson

Department of Mechanical Engineering

Brigham Young University

ABSTRACT

BYU Diesel Engine Lab Setup and Parasitic Losses of the Water Pump
and Vacuum Pump on a Cummins 2.8 L Engine

Eric Ashton Jessup
Department of Mechanical Engineering, BYU
Master of Science

The need to minimize carbon dioxide (CO_2) emissions is becoming increasingly important with the total number of vehicles throughout the world exceeding one billion. Carbon dioxide emissions can be reduced by improving vehicle fuel efficiency. While electric transportation is gaining popularity, most passenger vehicles are still powered by gasoline or diesel engines. The main objective of this work was to provide opportunities for studying and improving the fuel efficiency of internal combustion engines (ICE). This was achieved by 1) Designing, building and testing auxiliary systems necessary to run a Cummins 2.8 L engine in a an engine test cell; 2) Creating educational labs for the ICE class; and 3) Measuring the parasitic losses of the vacuum pump and water pump on the installed Cummins 2.8 L diesel engine. All auxiliary systems were completed at a hardware cost of $8100 and are rated to support an engine with the power output capacity of 233 kW (312 hp). The educational laboratories enable future engineers to measure and assess the efficiency of internal combustions engines. The parasitic losses of the vacuum pump and water pump were found to impact the relative brake fuel conversion efficiency by 1.3% and 1.5% respectively over the Federal Test Procedure (FTP) cycle.

Keywords: parasitic losses, water pump, vacuum pump, internal combustion engine (ICE)

ACKNOWLEDGEMENTS

TABLE OF CONTENTS

LIST OF TABLES

LIST OF FIGURES

1 INTRODUCTION

Internal Combustion Engine (ICE) powered vehicles provide an inexpensive and convenient mode of transportation for hundreds of millions of people in the United States. During combustion, the gasoline or diesel fuel used to power an ICE reacts with air to release energy and is converted into carbon dioxide (CO_2) and water (H_2O). Carbon dioxide is a greenhouse gas, which is considered a contributor to global climate change and is therefore a global pollutant. If a vehicle is more efficient, it uses less fuel, saves money, and emits less CO_2 into the atmosphere.

In 2012, the Environmental Protection Agency, Department of Transportation, and National Highway Traffic Safety Administrations issued regulations requiring automotive manufacturers to meet emissions levels culminating in "an average industry fleet-wide level of 163 grams/mile of CO_2 in model year 2025, which is equivalent to 54.5 miles per gallon (mpg)" [1]. While these targets are currently under political and legal evaluation [2], [3], reduction of CO_2 emissions is clearly a national interest.

Engines are complex systems that have been under development for over a century. In order for efficiency improvements to be made, engineers should seek to understand the fundamental principles of operation and have opportunities to explore changes through experimental work. BYU has the opportunity to contribute to future engine design and research through the use of a new facility designed for internal combustion engine testing and research. The facility provided

space, an AC motoring dynamometer, a 2.8 L Cummins diesel engine, chilled water supply, air supply, and exhaust fans. The facility provided an opportunity for several objectives.

The first objective was to design, fabricate and test the auxiliary systems necessary run the Cummins engine in the test cell. Fulfillment of this objective required the design and installation of the following engine auxiliary systems: 1) Engine coupling system, 2) Cooling system, 3) Intake and Exhaust system, 4) Fuel system, 5) Controls and Data Acquisition system.

The second objective was to set up instructional laboratories for the internal combustion engines (ICE) class. One lab was to demonstrate the brake fuel conversion efficiency of a diesel engine at a constant speed and variable loads (fuel flow rates). A second lab was to demonstrate the emissions of the engine for the same speed and loads. The understanding of the correlation between fuel efficiency and emissions will enable current, and future, students to become informed engineers that will make efficiency improvements in the future.

The third objective was to measure the parasitic losses of the water pump and vacuum pump on the Cummins 2.8 L diesel engine. The water pump and vacuum pumps were selected for parasitic loss testing in compliance to a request from Cummins, who donated the engine.

Figure 1-1 [4] is a schematic demonstrating how fuel energy is used in an internal combustion engine. Fuel enters the engine (top arrow) and is combusted, 16% - 25% of that energy is used to propel the vehicle forward (green arrow), while the rest of the energy is lost. Most energy, 68% - 72%, (red arrow) is lost as heat. Other vehicle losses such as wind drag remove 5% - 6% (blue arrow on left). The last 4% - 6% of the energy is considered parasitic losses (yellow arrow). Parasitic losses consist of auxiliary pumps that remove energy from the engine; examples of these are water pumps, vacuum pumps, oil pumps, and AC compressors.
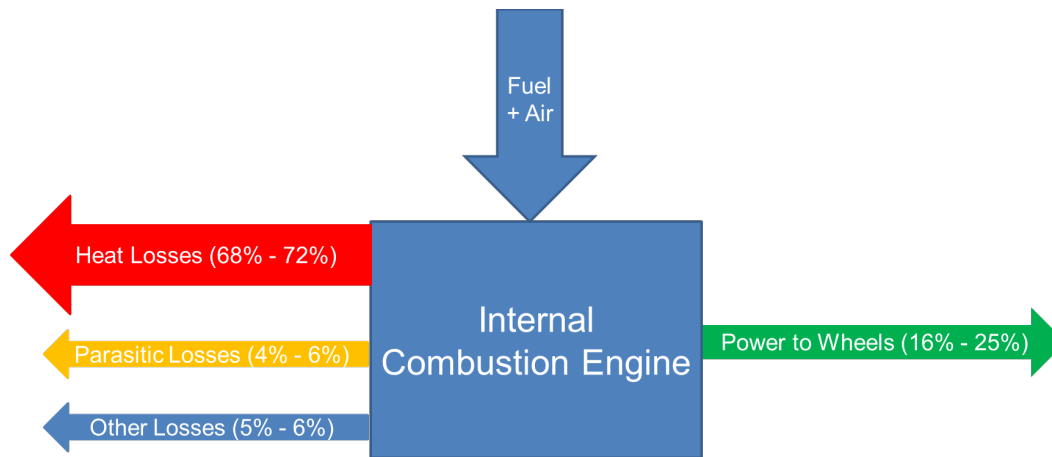
Figure 1-1: Schematic showing how fuel energy is used, or lost, during combustion in an ICE vehicle.

Many methods have been explored for improving the fuel conversion efficiency of ICE vehicles by reducing the heat losses (red arrow) because it shows the largest potential for improvements. There are significantly fewer studies published that explore reducing parasitic losses (yellow arrow), which would improve the overall conversion of fuel energy to engine shaft output energy. While parasitic losses promise smaller potential improvements in overall brake thermal efficiency, it is critical to understand the energy consumption of each component in order to take a system level design approach to maximize efficiency. Fuel conversion efficiency can be improved by removing the parasitic pumps from the engine and powering them with electric motors, that are powered by regenerative energy sources such as exhaust or braking.

The objectives of this work can be summarized as follows: 1) Set up a functioning engine test cell by specifying, designing, and installing all auxiliary engine systems necessary to run the engine in the test cell. 2) Create instructional laboratory experiments to test the fuel efficiency and emissions in the ICE class. 3) Measure the parasitic losses of the water pump and vacuum

pump on a Cummins 2.8 L diesel engine to determine the brake fuel conversion efficiency

improvement possible by removing the vacuum pump and water pump from the engine.

2 LITERATURE REVIEW

This chapter focuses on ways that the parasitic losses of automotive pumps have been measured in the literature. Results of these articles are shared in terms of relative efficiency gains rather than absolute engine efficiency gains. Relative efficiency gain is defined as the power increase of the engine without the pump divided by the original engine power. This definition is shown in Equation (2-1). The brake thermodynamic efficiency of an engine is defined as the engine power output divided by the rate of fuel energy input. Dividing all of the terms (numerator and denominator) in Equation (2-1) by $\dot{m}_f Q_{HV}$ (product of the fuel flow rate and the fuel heating value) gives the same relative efficiency result and is shown in Equation (2-2).

$$\eta_{rel} = \frac{Engine\ Power_{without\ pump} - Engine\ Power_{with\ pump}}{Engine\ Power_{with\ pump}} \qquad (2\text{-}1)$$

$$\eta_{rel} = \frac{\eta_{without\ pump} - \eta_{with\ pump}}{\eta_{with\ pump}} \qquad (2\text{-}2)$$

The change in absolute engine efficiency is simply the numerator of Equation (2-2), or the difference between the efficiency with and without the pump as shown in Equation (2-3). It is important to understand which change in efficiency, relative or absolute, is being referenced when considering the literature regarding parasitic losses.

$$\eta_{abs} = \eta_{without\ pump} - \eta_{with\ pump} \qquad (2\text{-}3)$$

2.1 Measurements of Water Pump Parasitic Losses

The water pump moves coolant through the engine and the radiator to cool engine components and prevent engine failure; it is normally run off of a belt and is a multiple of engine speed regardless of how much pumping power is needed to cool the engine. There were six studies found that measured parasitic losses associated with the water pump on an engine. One measured the fuel consumption of a 2011 Mercedes Sprinter van with a 3.0 L V6 diesel engine that was driven on a chassis dyno with a dual mode (electrical/mechanical) water pump; this study showed a 2.3% relative fuel efficiency improvement [5]. Two additional studies demonstrated the potential to improve fuel economy by 5% by electrifying the water pump and cooling fan [6] [7]. However, one of these studies shows that 95.5% of this efficiency gain is achieved by electrifying the cooling fan, while only 4.5% is attributed to electrifying the water pump; this would equate to a 0.4% relative fuel efficiency improvement from the electric water pump [6]. Another study measured the water pump parasitic losses on a 280kW diesel bus engine to be 0.4% by measuring the torque and speed on the water pump shaft during the normal bus drive cycle [8]. Finally, one paper demonstrated a method for measuring parasitic losses of the water pump by driving the pump shaft with an external motor and measuring pump speed and torque; this study shows a 0.3-1.3% relative brake thermal efficiency improvement for a 15 L Cummins Engine [9].

The range of parasitic loss results displayed by these papers is large; obtaining more parasitic loss data will help narrow down this wide range of results. Three of these papers used methods of measuring fuel consumption or brake torque on a vehicle in order to quantify parasitic losses [5] [6] [7]. The problem with this method is that parasitic losses are very small

compared to total engine output power. It is very difficult to accurately measure a small change by measuring the difference between two relatively large numbers.

Two of these studies directly measured the torque on the water pump shaft [9] [8] using the methods shown in Figure 2-1. Method A [8] modifies the shaft of the water pump by adding a strain gage and slip ring, which allows for the direct measurement of the pump torque while the engine is powering the pump. Method B runs the water pump [9] with an external electric motor and an inline torque transducer. Both of these methods produce a direct measure of the water pump power exerted on the shaft and are therefore expected to have a higher fidelity than the other literature methods.
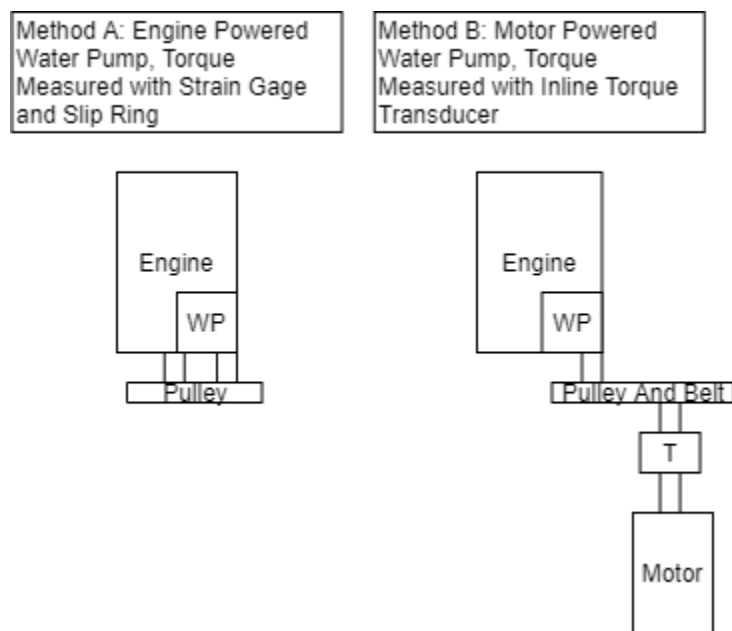
Figure 2-1: Methods used in the literature to measure water pump parasitic losses using pump shaft torque.

Method A requires significant changes to the water pump shaft; as a result, Method B was selected as the best method to measure pump parasitic losses. More details of the selected method are shared in chapter 4.

Findings from the six studies suggest that the parasitic losses of the water pump will be between 0.4% – 2.3 % relative fuel efficiency improvement. It is important to note that a small efficiency improvement (0.4% - 2.3%) holds the potential to save hundreds of millions of gallons of fuel in the United States alone, if this improvement was applied to every vehicle. This simple illustration shows why even a 1% improvement in fuel efficiency is of interest.

2.2   Measurements of Vacuum Pump Parasitic Losses

The vacuum pump supplies vacuum to a reservoir that is used to actuate the brakes on vehicles and perform other functions; it is normally run off the camshaft at half the engine speed regardless of how much vacuum is needed. Two studies were found that quantify the parasitic power losses of a mechanical vacuum pump. One of these simply tested the fuel economy over a typical drive cycle for a car and a larger utility vehicle respectively with a mechanical and electric vacuum pump. The data were then generalized to a yearly distance of 20,000 km and showed the potential to save 14 L of diesel fuel in a year. The results of this study showed a fuel efficiency improvement with an electrified vacuum pump, but it did not quantify the total parasitic load of the vacuum pump [10].

The second study removed the vacuum pump from the engine and powered it with an electric motor as it filled a 10 L container with vacuum. The torque on the vacuum pump shaft was measured with an inline torque transducer. These results showed the potential for a 1.5% relative fuel efficiency improvement [11].

The lack of published research in this area suggests additional data could be impactful by providing further quantification of vacuum pump parasitic losses.

2.3   Anticipated Contributions

The purpose of this thesis is to make a contribution in the area of fuel efficiency of internal combustion engines. This purpose will be met in multiple ways.

The first objective is to set up an operational engine test lab (outfitted with all necessary auxiliary systems), while not exceeding a hardware budget of $20,000. This lab will be capable of being used for ICE class labs, capstone projects, and future research. Each of these uses will provide students with a way to familiarize themselves with engine operation, efficiency, and emissions. Education is a critical step for improving efficiency and reducing emissions in the future.

The second objective is to create experimental labs for students in the ICE class to run and learn about fuel efficiency and emissions of a diesel engine. Deliverables will include instructions on how to run the engine and take data for the respective labs. This will further enhance the ability of students to learn about ICEs.

The third and final objective is to measure the total parasitic losses of the water pump and vacuum pump on the Cummins 2.8 L engine. The deliverable will be a report outlining these findings. (See section 5.11) The parasitic losses of these pumps represent the total potential for fuel efficiency improvements by removing the pumps from the engine and powering them with regenerative energy sources. This testing will provide additional insights into parasitic losses as few studies are publicly available. It also has the potential to provide automotive manufacturers with key information needed to take a system level approach to improve vehicle fuel efficiency.

9

3   BACKGROUND

This chapter provides information useful for understanding how an AC dynamometer (an apparatus used to test an engine) works when connected to an engine to achieve the torque, speed, and power data that is required for the engine laboratory experiments.

3.1   AC Dynamometer Capabilities

Equation (3-1) shows the relationship between the forces acting on the engine crankshaft from combustion, friction, and the dynamometer.

The first term on the left side is the power generated by the engine, $\dot{W}_{eng}$, on the crankshaft. The engine produces work in each cycle (two rotations) dependent on the amount of fuel injected and burned. The work produced in a cycle and the torque produced on the connecting rod are proportional and differ only by a constant. Thus, an operator may produce more work or torque by increasing the amount of fuel injected per cycle up to the point that there is no longer enough air to burn the fuel. At this point the engine is at 100% of its rated load. The pedal position can represent the amount of fuel injected per cycle. When the engine is at idle, the pedal position is somewhere near 5-10% of the full load or full pedal position. The engine power produced within the cylinder is proportional to the product of the fuel injected per cycle (or work per cycle) and engine speed (cycles/second) and is called the indicated power.

The second term in the equation, $\dot{W}_{fric}$, represents the losses in power from the crankshaft due to friction, pumps, compressors, and the alternator. These are termed parasitic losses or friction power. The loss in a given cycle tends to be proportional to engine speed. As engine speed increases, the friction loss per cycle increases. The friction power is the product of the

10

engine speed and the friction work per cycle and is therefore proportional to the engine speed squared.

The third term, $\dot{W}_{dyno}$, is the power applied to the crankshaft by the dynamometer. Normally a dynamometer adds resistance to the motion of the engine, slowing it down and causing it to decelerate. The sign of the dynamometer power in the equation is such that a positive dynamometer work is slowing the engine, similar to the friction power.

Other variables acting on the crank shaft are: $\dot{\omega}_{shaft}$ (acceleration), I (moment of inertia), N (engine speed), T (torque), and $\dot{m}_f$ (fuel flow rate).

$$\dot{W}_{eng}(N, \dot{m}_f) - \dot{W}_{fric}(N, \dot{m}_f) - \dot{W}_{dyno}(N, T) = I\dot{\omega}_{shaft} \tag{3-1}$$

When all the three of the terms on the left side of the equation sum to zero, the engine will no longer accelerate and will remain at a fixed speed. The engine control unit (ECU) does not allow an engine speed to be specified. The input to the engine is the fuel injected per cycle, or pedal position. The speed is an output and is dependent on the amount of negative power produced by friction and the dynamometer.

An engine at idle without a dynamometer connected will increase in speed at a fixed pedal position (fuel injected per cycle) until the friction power equals the engine power. This works because the engine power is increasing with engine speed but the friction power increases with engine speed squared until the two match. A balance is naturally obtained. If pedal position is increased above a certain point, the engine speed at equilibrium becomes too high and a dynamometer is needed.

The custom built AC motoring dynamometer, purchased from Dyne Systems (formerly known as Taylor Dynamometer), has two modes of operation. A "motoring mode" which allows the dynamometer power to be added or subtracted to the system ($\dot{W}_{dyno}$ can be positive or negative) and "absorb only" mode where the dynamometer power is always working opposite the engine. Either of these modes can be selected from the "Dyno Control" menu where the engine speed is also selected.

When the engine is in absorb only mode, it can be controlled in one of two ways. First, the user specifies the desired output speed of the system and the pedal position of fuel injected per cycle. The dynamometer controller then adjusts the amount of torque, or braking force, required to make the brake power produce a net power of zero. Second, the user specifies the desired engine output speed and fixes the braking force (torque) desired and the dynamometer controller adjusts the pedal position until the power is at a net of zero for the specified speed. Note that for both cases, speed is an input to the dynamometer, not the engine.

To use the first control method, the user selects "throttle position" on the Dyne systems control menu and specifies a number between 0 and 100%. The term throttle position applies to spark ignition engines which use a throttle to control the fuel added per cycle. Diesel engines do not have throttles and so the user should think of this command as pedal position. To use the second method of control, the user should select "torque control" and specify the output torque desired.

For purposes of relating a dynamometer to every day experience, consider the dynamometer as a hill. If you desire to run a car at 2000 RPM, you can adjust the pedal position while driving down the road until the car is at 2000 RPM. This allows the engine to be studied at a fixed engine speed. Going up a hill requires an increase in pedal position to reach the same speed. The

dynamometer is like a variable hill allowing different pedal positions (fuel flows) to be studied. The Dyne Systems controls allow the user to specify the steepness of the hill (both uphill or downhill are possible) and adjusts the pedal position to produce the desired speed for that hill; or it allows the user to specify the pedal position and adjusts the hill steepness to produce the desired speed.

4 METHODS

This chapter first outlines the methods used to design the engine auxiliary systems with the $20,000 hardware budget. Second, it outlines the methods used to create the instructional laboratories for the ICE class. Finally, it outlines the methods used to test the parasitic losses of the water pump and vacuum pump.

4.1 Engine Auxiliary Facilities Design Method

An engine test cell is a laboratory used for testing an engine; it is outfitted with an engine connected to a dynamometer and all auxiliary systems necessary to run the engine The method for designing the engine auxiliary systems was to first identify the design requirements and constraints; second, produce potential system designs; third, analyze and evaluate designs; and finally, select and test the design. Installation of the engine into the test cell will require the design of the following auxiliary systems:

- Coupling system – driveline to connect the engine to the dynamometer

- Coolant system – A heat exchanger or radiator

- Intake and exhaust system – An air supply, intercooler, and a means of expelling exhaust from the room

- Fuel system – A fuel tank and means of supplying and measuring fuel to the engine

- Controls and data acquisition system – At a minimum, a means of controlling pedal or throttle position. Ideally, a system to measure and control a large number of engine parameters

These room systems were supplied with the test facility. They were not part of the thesis design, but were considered as design constraints.

- An intake air supply and variable frequency drive (VFD) exhaust fan duct system

- A motoring AC dynamometer

- A slotted floor for engine mounting, control room, and observation window

- A chilled water system with specified flow rates

Design of the auxiliary systems required that the room and engine capabilities be considered. The room systems included the dynamometer, chilled water cooling system, exhaust vent, and room air supply. The room specifications are summarized in Table 4-1 along with the respective power capacities of each system.

Table 4-1: Capacity of Engine Facility Dynamometer, Cooling, and Air Intake/Exhaust Systems

System	Maximum Capacity	Power Capacity
AC Dynamometer	1100 N-m 3200 RPM	342 kW
Chilled Water Cooling Capacity	15 gpm $T_{in} = 18°C$ $\Delta T = 40°C$	157 kW
Air Intake/Exhaust System (Supply) With 10:1 air to exhaust ratio	2000 SCFM (supplied) 200 SCFM (for combustion)	58 kW

The following section outlines the design constraints created by the laboratory then the engine design requirements will be outlined.

4.1.1 Design Constraints by the Room

The room contained the AC dynamometer, air intake and exhaust fans, and chilled water cooling systems. Each of these subsystems was evaluated to understand the engine power that could be enabled based on the respective system specifications.

AC Dynamometer Capabilities

The torque and power curves for the dyno, as provided by Dyne Systems, are shown in Figure 4-1. The two curves for each parameter represent the normal rating for the dynamometer and the de-rated values applicable at the elevation in Provo, Utah. Any value of speed, torque and power that are below the de-rated curves can be achieved while values above the curves are beyond the capacity of the dynamometer. This dynamometer is optimal for high-torque low-speed engines as is normally the case for turbocharged diesel engines. The peak engine power at 3200 RPM is 342 kW, or 460 hp. Because the Cummins 2.8 L engine is rated at 110 kW, and has only been tested up to 50 kW, current testing has all occurred in the 'Constant Torque Range,' below 2000 RPM and well below 1757 Nm.
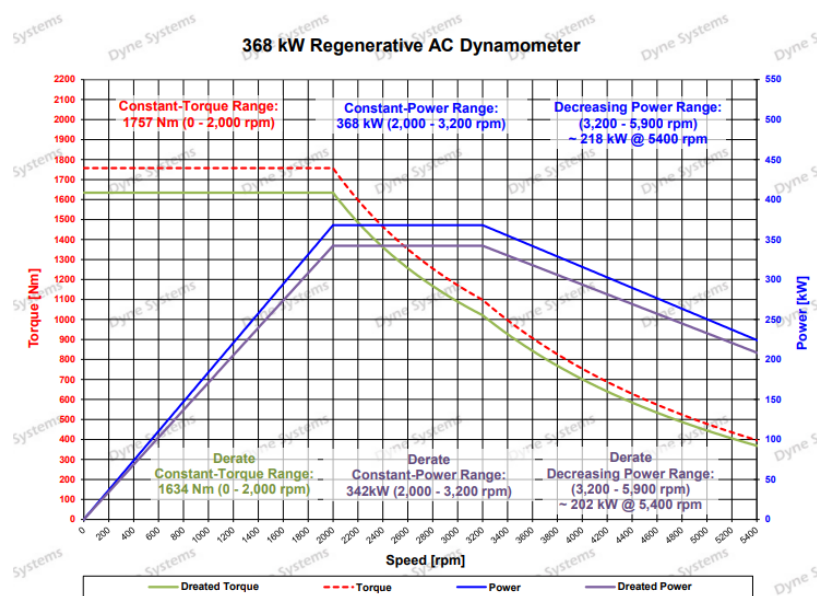
Figure 4-1: Dyne Systems AC Dynamometer Torque and Power Curves

Chilled Water Cooling System

The test cell room is supplied with chilled cooling water that is returned to a building heat exchanger and cooled by the universities central heating and cooling plant. The water flow capacity for the current regulator in the room is 56.85 L/min (15 gpm). Assuming a maximum allowable temperature rise of 40 oC, the heating capacity for the average temperature of water, and the mass flow, the maximum cooling capacity of the heat exchanger was calculated to be 157 kW. Detailed engine lab power capacity calculations can be found in Appendix E.

Air and Exhaust Fan Capacity

The air capacity for the room was specified to be 2000 SCFM, which is large enough to supply a 570 kW diesel engine running at max load. This was the power originally thought capable for the room.

After running the installed engine, it was discovered that the exhaust duct work required the air be diluted with additional air in order to keep the exhaust temperature below 70 $^{\circ}$C. An assumption was made that the exhaust would need to be diluted at a ratio of 10:1 parts air to exhaust. This leaves the air flow available for combustion use in the engine to be 200 SCFM. Diesel engines are never run at a stoichiometric (14.7:1) air to fuel ratio, so a conservative value just over two times larger than the stoichiometric mass flow of air to mass flow of fuel ratio of 30:1 was used to calculate the amount of fuel that could be burned with the 200 SCFM supply. This calculation showed the power capacity of the intake/exhaust system to be 58 kW. If the room rollup-door is opened, the supply is increased and higher powers are enabled. Detailed calculations of engine lab power capacity as a result of intake and exhaust system components can be found in Appendix E.

4.1.2 Design Requirements

Two engines were considered as engine donations, a Cummins 2.8 L and a Cummins 5.0 L engine. The torque, speed, and power at peak torque and maximum power conditions for each engine are shown in Table 4-2. The power requirements of the 5.0L engine are seen to more completely utilize the capabilities of the dynamometer. The auxiliary systems were specified to work for the Cummins 5.0 L engine as the upper design requirement and for the Cummins 2.8 L engine for the minimum design requirement. Appendix F. demonstrates the data sheets for the Cummins 2.8 L and 5.0 L engines.

Table 4-2: Ratings of Cummins 2.8 L/5.0 L Engines at
Peak Torque and Maximum Power Conditions

Engine	Parameter	Peak Torque	Maximum Power
Cummins 2.8 L Engine	Torque	360 N-m	360 N-m
	Speed	1500 RPM	2900 RPM
	Power	56 kW	110 kW
Cummins 5.0 L Engine	Torque	759 N-m	613 N-m
	Speed	2000 RPM	3200 RPM
	Power	159 kW	205 kW

Design for the engine coupling, cooling, fuel, and intake/exhaust systems were designed to meet the power requirements of the larger 5.0 L engine to maximize the utilization of the room capacity. Once the engine was known, many system components required modifications in order to connect to the 2.8 L engine. The systems are designed to meet the power requirements of both engines, but interface modifications will be necessary if installing the Cummins 5.0 L, or another engine in the future. A summary of power requirements is given in Table 4-3.

Table 4-3: Design Requirement Targets for Engine Auxiliary Systems

Engine Auxiliary System	Engine	Peak Torque Values	Maximum Power Values
Coupling	5.0 L	759 N-m 2000 RPM 159 kW	613 N-m 3200 RPM 205 kW
Coolant	5.0 L	105.5 kW	142.4 kW
Fuel	5.0 L	34.3 kg/hr (9.53 g/s)	49.6 kg/hr (13.7 g/s)
Intercooler and Exhaust (Engine Output)	5.0 L	159 kW	205 kW

4.1.3   Design Options, Analysis, and Selection

This section outlines the options considered for the engine coupling, cooling, and fuel systems. The intake/exhaust system and controls systems are not discussed here because the system design was simple and most components were readily available through automotive suppliers. For each option discussed, the engineering calculations used to evaluate the option are presented followed by the option selected.

Engine Driveline and Coupling

A functional engine coupling system required the design of the engine coupling, driveline, engine mounts, and driveline guard.

In the previous engine test facility, the diesel engine was coupled to a dynamometer using a Dodge PH-131 flexible coupling. This coupling worked well and was considered in comparison to three additional options. Table 4-4 compares these options using the following criteria: 1) Cummins 5.0 L engine compatibility (upper design requirement), 2) vibration damping capability, 3) coupling assembly length, 4) complexity of modifications required to install the coupling, and 5) cost.

Table 4-4: Coupling Options Considered

Option	Meet Cummins 5.0L engine requirements	Vibration Damping	Coupling Length (in)	Complexity (1 Least complex 5 Most complex)	Parts Cost ($)
Dodge PH-131 Coupling	No	Yes	12	3	800
JCGMI_221 Periflex	Yes	Yes	24	1	6500
Dyne Systems SAE 1550 Assembly	Yes	No	24	1	5000
LoveJoy LF-Series	No	Yes	12	4	1000

Both the Periflex and Dyne Systems couplings could be connected to the engine without engine modifications; however, both of them would utilize a driveline, similar to those found in vehicles, with U-joints on each end. These drivelines would have made the system over 24 inches in length. This length was weighted heavily because the dynamometer is dual-sided, meaning that separate engines can be installed on either end of the dynamometer. Utilizing a 24-inch shaft in the confined space of the engine test facility would limit the dynamometer to connection to one engine. As a result, these couplings were not selected, even though the cost was within budget.

The remaining couplings were similar in length, price, and installation complexity, and met the peak torque values for both engines. However, neither coupling met the maximum power value for the 5.0 L engine. This was deemed an acceptable tradeoff in order to maintain the dynamometer capacity to use engines on either side. Both couplings were rated to handle ~90% of the maximum power for the 5.0 L engine. This led to a decision based on installation complexity. The Dodge PH-131 coupling could be attached to the engine flywheel without an adapter, while the LoveJoy coupling would require the design of an adapter. As a result, the Dodge PH-131 coupling was selected to simplify design.

Some design modifications were needed in order to connect the engine to the dynamometer with the PH-131 coupling. 1) The existing flywheel had to be drilled and tapped with an SAE 11.5 bolt pattern to attach the flexible element. 2) A shaft was designed to transmit power between the engine and dynamometer. 3) Engine mounts needed to be adjustable to align the engine and dynamometer shafts, and 4) Finally, a driveline guard needed to be designed and fabricated for safety.

Driveline Shaft Design

A simple keyed shaft was designed to connect the PH-131 Flexible coupling to the HBM T40B adapter. Calculations were performed to obtain a minimum diameter for a mild steel shaft to sustain the maximum torque of 759 N-m. The equation for maximum torque on a solid shaft was solved for minimum shaft diameter and is shown in Equation (4-1), where D is diameter, T is torque, and τ is shear stress of the shaft material.

$$D_{min} = \left(\frac{16\tau_{max}}{\pi T_{max}}\right)^{1/3} \tag{4-1}$$

These calculations showed a minimum shaft diameter of 1.20-inches to support 759 N-m. A larger 2.5-inch shaft was selected to achieve a single diameter shaft that could connect to the flexible element on one side, and the HBM T40 B adapter on the other.

Engine Mount Design

The flexible rubber coupling was specified to support up to 1° of angular misalignment between the engine crankshaft and the dynamometer; Equation (4-2) shows the allowable misalignment as a function of the shaft length. For the selected shaft length of 12.5-inch, the total allowable misalignment is 0.21-inches.

$$y = L * Tan(1°) \tag{4-2}$$

In order to keep engine vibrations from causing excess shaft misalignment, the motor mounts were designed to be solid, rather than absorptive. This will minimize the stress transmitted to the dynamometer. The engine stands and mounts must allow for adjustment to ensure that the engine can be aligned with the dynamometer.

Driveline Guard Design

The requirement for the driveline guard was to surround the length of the driveshaft from the engine to the dynamometer in order to reduce the possibility of items contacting, or being caught in the driveshaft. The driveshaft guard will also shield bolts or small parts that might come loose or be dispelled from the driveshaft from a free trajectory across the room. The shield should remove energy from the driveshaft should it come loose from the coupling, but it is not intended to completely contain the shaft.

Engine Cooling System Design

Two options were considered for the engine cooling system. A radiator (water to air heat exchanger) or a water to water heat exchanger. A radiator would reject heat from the coolant into the test lab further increasing the temperature in the exhaust duct. The water to water heat exchanger was considered a better option because the building provides chilled water that would remove the heat from the room.

The engine cooling system design was centered around the purchase of a heat exchanger capable of removing the maximum heat load from the Cummins 5.0 L engine of 142.4 kW. Approximate thermodynamic calculations were performed to verify supplier quotes and a commercial heat exchanger was identified by working with the Thermal Transfer Systems

(TTS), a supplier that was used for the previous diesel engine heat exchanger. Quotes for both a shell and tube heat exchanger and a plate heat exchanger were received. Both heat exchangers were similar in cost, but the plate heat exchanger was selected because of its lower pressure drop.

4.1.4   Final Options Selected

Table 4-5 describes the options selected for the engine systems and a brief comment for justification.

Table 4-5: Auxiliary Systems Selected Options

System	Option Selected	Justification
Engine Coupling	Re-use: PH -131 Coupling Modify: Engine flywheel Design: shaft, engine mounts, and driveline guard	Minimize driveline length and simplify installation Rated for 675 N-m @ 3750 RPM. 265 kW
Engine Cooling	Plate heat exchanger will be purchased A standard thermostat will be used.	Will cool 142.4 kW of heat Plate heat exchanger has a lower pressure drop than shell and tube. Simplicity: no controls required
Air Intake/Exhaust System	Aftermarket intake components will be purchased Exhaust pipe will be built at a local shop	Purchasing automotive components will save time and engineering design
Fuel System	Fuel pump will be purchased Fuel cooler will be purchased	To overcome flow meter restriction To allow for the use of flow meter
Controls and Data Acquisition	Dyno will be used to control engine startup, speed, and fueling National Instrument cRIO data acquisition system and LabView will be used	Will yield a simple but functional controls and data acquisition system. Record fuel flow rate.

4.2 Lab Testing Methods

The objectives of the instructional laboratories for the ICE class are to measure engine brake torque, power, fuel flow, and emissions as a function of fuel flow rate, or pedal position, at a constant engine speed. This was accomplished by running the engine at 1500 RPM, taking fuel flow, torque, and speed data at increasing fuel loads and calculating brake fuel conversion efficiency. See Appendix G. for the diesel engine operating instructions.

4.3 Measuring Parasitic Losses of the Water Pump

A method was developed to test the power input and output of the Cummins 2.8 L water pump corresponding to an engine speed range of 300 - 3000 RPM. A torque transducer and speed encoder were used to quantify power input; a flow meter and three individual pressure transducers were used to quantify the water pump power output. The ratio of power output to power input was used to calculate a pump efficiency. Both open and closed thermostat cases were simulated.

Figure 4-2 is a schematic diagram of the water pump test setup. The left side of the figure shows the water flow route used to simulate open and closed thermostat cases while the right side shows how data were recorded. The heat exchanger normally used to cool the coolant exiting the engine was replaced with a radiator to simulate the pressure drop of a functioning engine. The open thermostat test case was simulated by removing the thermostat and plugging the bypass tube, which forced the entire water flow to return through the radiator. There was no pressure drop across the thermostat, because it was removed, so reported values represent the minimum pumping work required to push a fluid across the radiator. The closed thermostat test

case was simulated by inserting the thermostat, which stopped flow to the radiator and returned

all flow through the engine bypass.
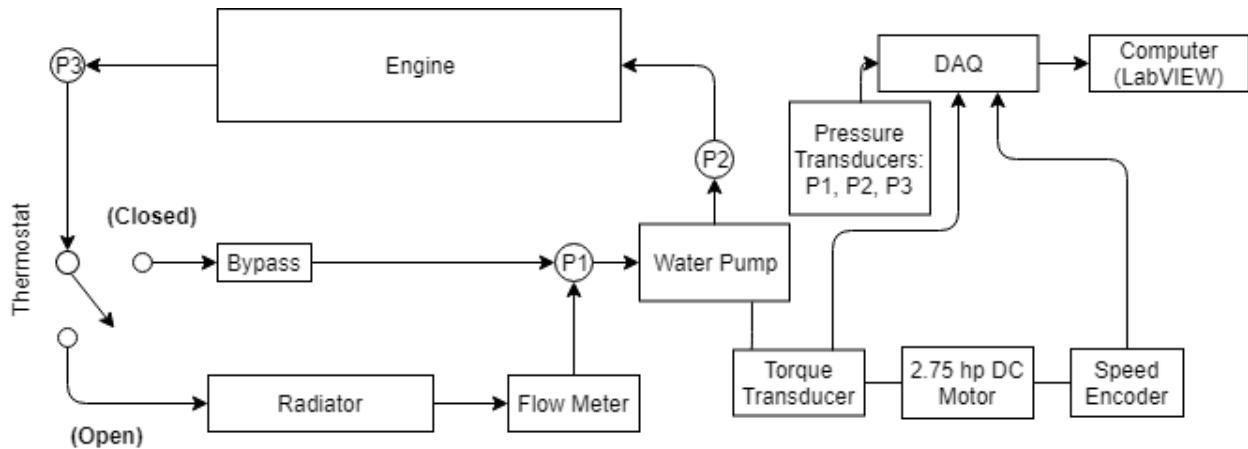
Figure 4-2: Diagram of the Water Pump Test Setup

The water pump was powered independent of the engine by a 2.75 hp DC motor. The

engine was not running or hot during testing. Room temperature tap water was used for testing in

place of an antifreeze mixture to clearly define the fluid properties. It was assumed that the

power required to pump the water through the engine would demonstrate a similar trend as a

heated antifreeze mix, however, the values will not be exactly the same. While the engine may

not require the full flow rate produced by the water pump, there was no attempt made to evaluate

the minimum flow needed to produce the required cooling.

When changing between an open and closed test, water had to be drained to remove or

install the thermostat; this introduced air bubbles into the system. It was noted that air bubbles in

the line reduced average torque to the pump and produced inconsistent flow. It was therefore

important to remove the air bubbles before beginning a test. This was accomplished by running

the water pump at an intermediate speed for approximately 10 minutes, without the radiator cap,

and simultaneously adding additional water. This was especially important for the closed

thermostat scenarios. The radiator cap was opened between tests to ensure a consistent starting pressure.

As seen in the right side of Figure 4-2, pressure, torque, and speed data were sent to a DAQ system and recorded. See Table 4-6 for DAQ and sensor details. Data were taken at a frequency of 100 Hz and averaged for 2 seconds (200 sampled points); the average and standard deviation were displayed on a monitor. When standard deviation of the water pump speed for the 200 sampled points was less than 2 RPM, the system was assumed to be at steady state and the average pressures were recorded. A sweep of pump speeds was performed with one averaged point recorded at each speed. Multiple sweeps were then collected for the open and closed conditions on multiple days for a range of speeds that varied from below the engine idle speed to the speed at maximum power.

A table of sensors and transducers used for the measurements along with the measurement range and resolution is given in Table 4-6. The measurement equipment was borrowed from the Department of Mechanical Engineering.

Table 4-6: Specifications for Sensors Used to Test Parasitic Losses

Component	Range	Resolution
Schlenker Ent. Torque Transducer	0-20 N-m	±0.2% FS (0.04 N-m)
Quadrature Speed Encoder TRD-SH1000BD	0-6000 RPM	1000 PPR, 200 kHz response
National Instruments DAQ cRIO-9074	8-Slot	100 MHz CPU, 128 MB DRAM
Absolute Pressure Transducer (S/N 12506)	0-50 psi	±0.2% FS (0.1 psi) @ 500 Hz
Copal Electronics PA-500-502G Pressure Transducers (2)	0-490 kPa	±0.5% FS (2.5 kPa) @ 1000 Hz
Digiten Water Flow Sensor Model: FL-1608	10-200 L/min	±0.2% FS (4 L/min) @ 40 Hz

Figure 4-3 shows an image of the actual test setup. The torque transducer can be seen between the water pump and the electric motor. The positions of the pressure transducers, are indicated by P1, P2, and P3.
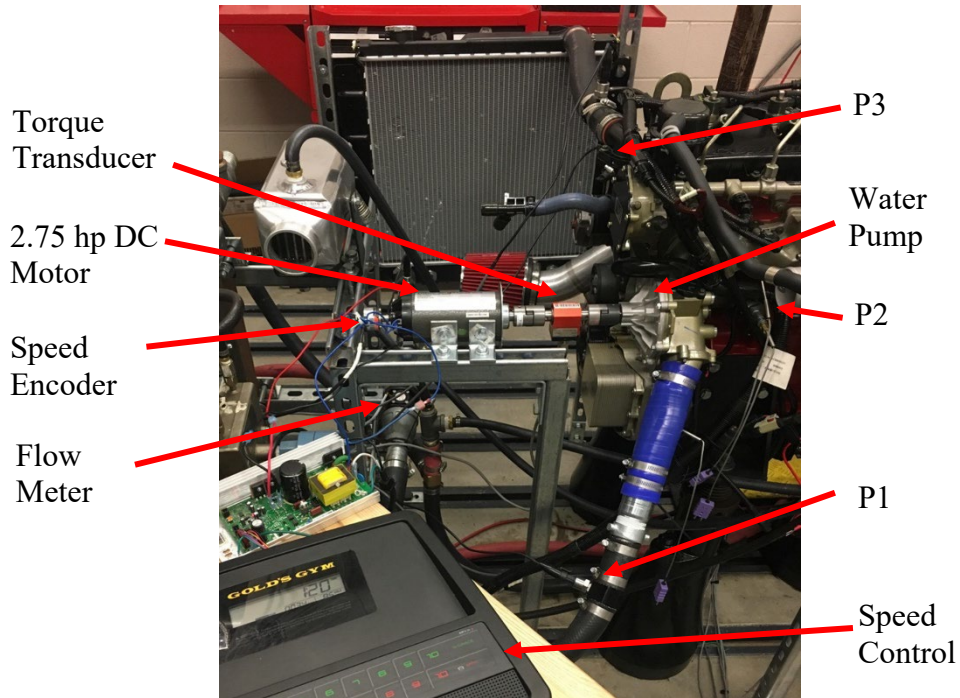
Figure 4-3: Actual Water Pump Parasitic Loss Test Setup

4.4 Measuring Parasitic Losses of the Vacuum Pump

A method was developed to test the shaft power input on the Cummins 2.8 L vacuum pump for an engine speed range of 400 – 2400 RPM. The pump was powered with a 2.75 hp DC motor or an electric drill motor. Power input was quantified using measurements from a torque transducer and speed encoder set up as shown in Figure 4-4. The torque transducer was located in line with the vacuum pump and motor shafts.

A.	Vacuum Pump
B.	Oil Pump
C.	Torque Transducer
D.	Speed Encoder
E.	Absolute Pressure Gauge
F.	Driving Motor
G.	2 L Tank (not shown)
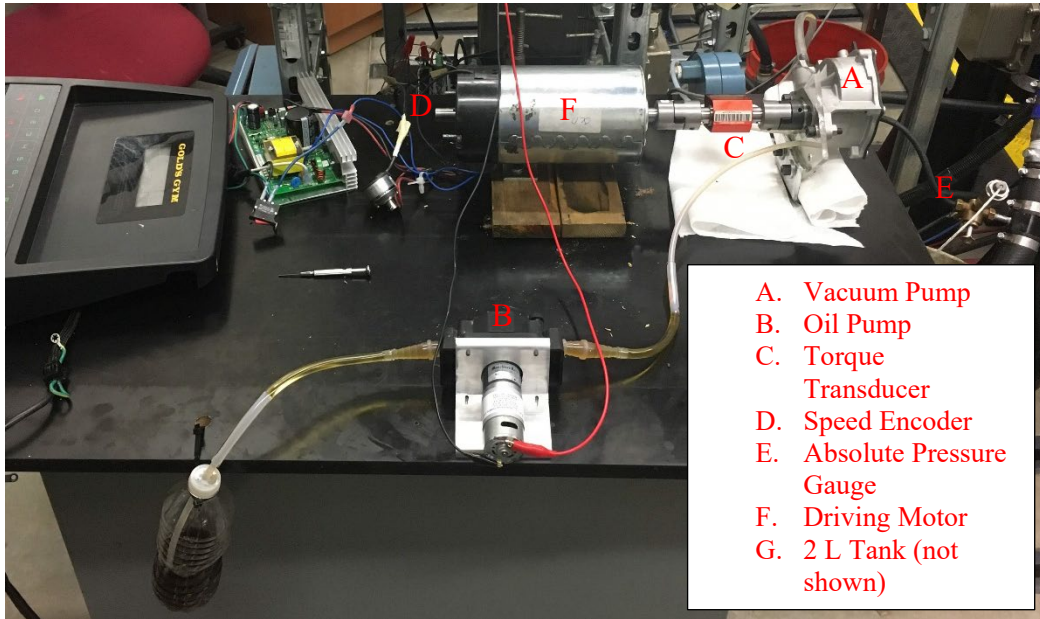
Figure 4-4: Actual Vacuum Pump Parasitic Loss Test Setup

Absolute pressure, torque, and speed data were collected by a data acquisition system (DAQ), which recorded input signals a frequency of 100 Hz (every 10 ms). 150 samples were averaged over the course of 1.5 seconds and recorded as a single data point. Tests were conducted on three different days. Each respective test demonstrated less than 10% variation from tests on previous days; this established a strong testing repeatability.

The vacuum pump required high torque at low speeds and often stalled the electric motor; this led to subsequent testing with a drill motor. Testing with the drill motor did not include speed data. Torque measurements for both electric motors were similar in magnitude. The power for the pump was obtained at 1) various oil supply pressures; 2) while the pump was pulling a vacuum pressure in a tank (closed tank); and 3) while the pump was only pumping air from atmospheric pressure at the inlet to atmospheric pressure at the outlet (open tank). Table 4-7 explains the oil pressure and tank variations that were tested.

It is important to note that the valve on the vacuum tank was small so it still built a vacuum pressure inside, rather than pulling from completely atmospheric air.

Table 4-7: Vacuum Pump Test Variations

Test Name	Vacuum Container (2L)	Oil Supply	Motor
1	Open	None	1
2	Open	Drip	1
3	Closed	Drip	1
4	Open	Pressurized	2
5	Closed	Pressurized	1, 2

The pump required oil lubrication, which is normally delivered within a closed compartment surrounding the pump. For the measurements, the pump was removed from inside the engine head and a spinning shaft had to pass through the back of the test fixture. The fixture was not well sealed and oil leaked out of the back at an increasing rate with an increase in oil supply pressure. For this reason, oil was only supplied at very low pressures. The test fixture was altered to remove the seal on the backside of the vacuum pump by creating an air gap. The pump torque was then tested to determine if the back pressure on the pump would alter the shaft torque. Results indicated that back pressure had minimal impact on measured torque.

5   RESULTS AND DISCUSSION

This chapter presents results for the major objectives of this work. First, the resulting engine test cell auxiliary system setup is presented; total hardware costs for these systems totaled $8,100 of the $20,000 budget. A system schematic of the implemented systems, provides a description of each system, shows rated performance of individual systems components, and ends with measured performance results demonstrating a working setup. Second, the capacity of the system to take fuel flow, torque, power, and speed data for the engine labs is demonstrated with sample plots. Finally, the results for parasitic losses for the water and vacuum pumps are presented and compared to vehicle drive cycles to explore the overall efficiency improvements possible by removing the pumps.

5.1   Engine Lab Setup

A schematic diagram of the test cell setup is shown in Figure 5-1. The setup is divided into five systems: 1) a driveline coupling system (which includes the guard and motor mounts), 2) an engine cooling system, 3) an air intake and exhaust system, 4) a fuel system, and 5) a controls and data acquisition system. The schematic of the setup is a view of the engine from above, with the top of the figure being the east side of the room; the building coolant system is closest to the control room. The fuel system is located on the bottom of the figure, or the west side of the room. The diagram shows the general location of auxiliary system components and the direction of flow for coolant, air, exhaust, and fuel.
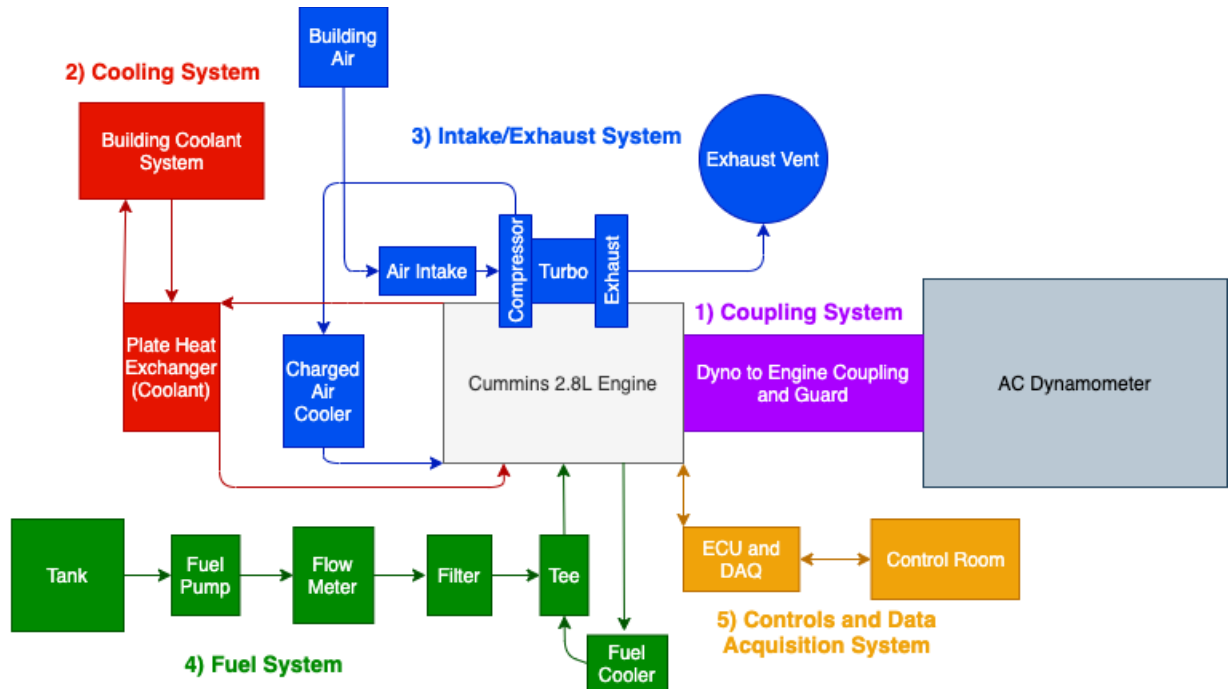
Figure 5-1: Schematic of Engine Test Cell Setup with Auxiliary Systems

Figure 5-2 shows a digital image of the engine lab setup. This image is taken from the west, or fuel system side of the room looking east at the engine. The dynamometer is the grey object that is cut off on the right side of the image. The engine is red and is mostly hidden by the intake manifold, tubing, and wires. The Unistrut structure to the left, or north end of the room, holds the fuel tank, fuel flow meter, coolant heat exchanger, data acquisition hardware, and other system components that required a mounting location. This structure also allows for future modifications or the installation of components that might be used for other engines.

An overview of each of the five systems will be given in the following sections; for details about the specific auxiliary system components see the bill of materials in Appendix A.

31
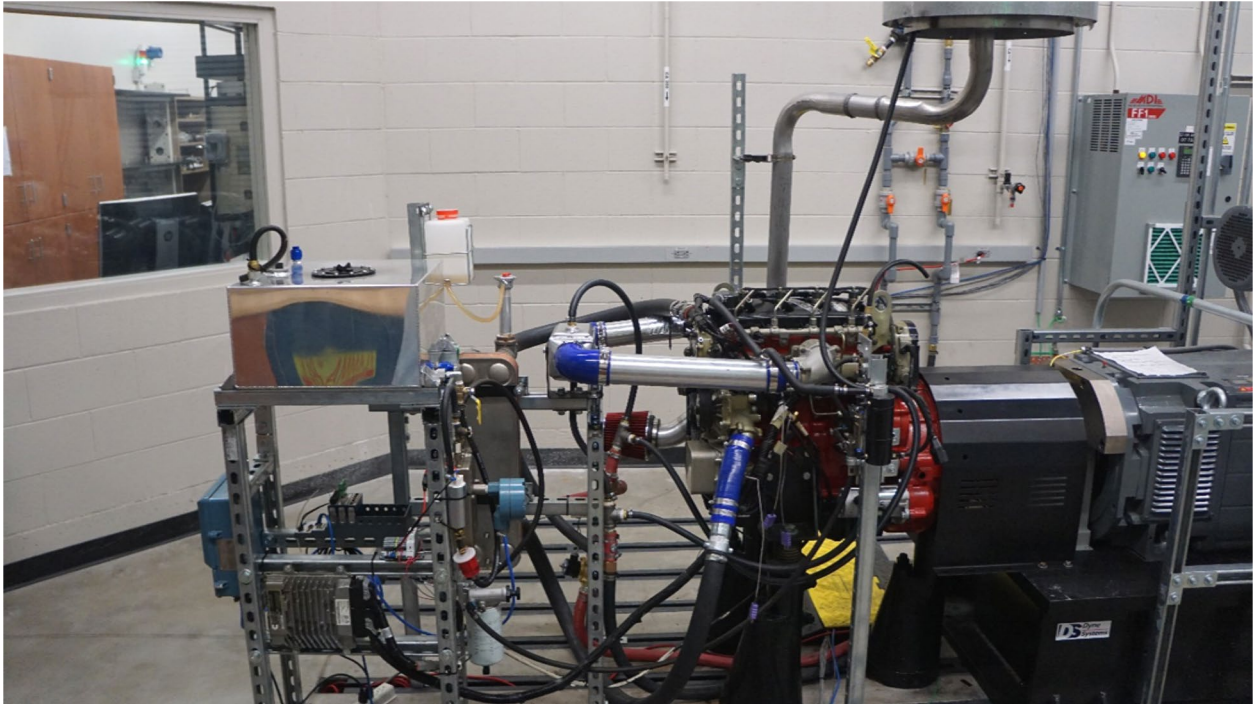
Figure 5-2: Final Engine Lab Setup with Installed Auxiliary Systems

5.2   Driveline Coupling System

The driveline coupling system will be described followed by a description of the rated performance based on component specifications and the actual system performance based on a limited set of measurements.

5.2.1   Driveline Coupling Description

The driveline coupling system required a mixture of custom designed and fabricated parts integrated with commercially available purchased components. A CAD model of the system is shown in Figure 5-3 with an accompanying table identifying parts. The guard that was fabricated as a safety shield and installed around the coupling is not shown. The coupling assembly and drawings can be found in Appendix B.
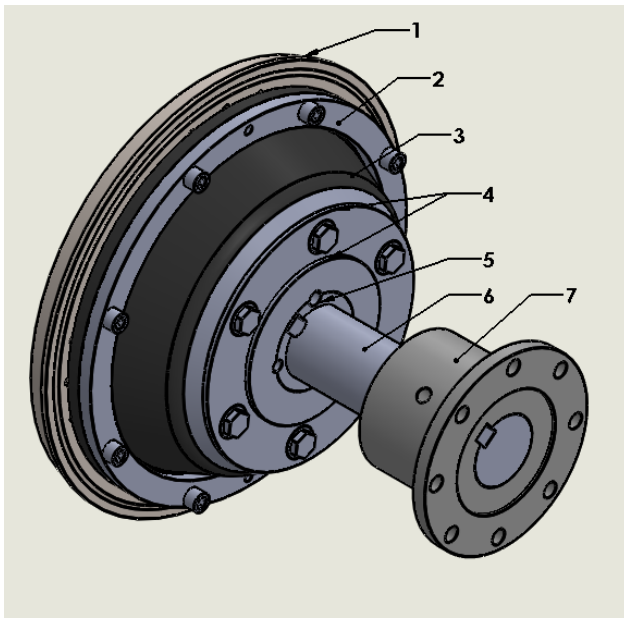
Part #	Part Description	P or D*
1	Cummins 2.8 L Flywheel SAE 11.5 Modified	P&D
2	PH-131 Bolt Ring	P
3	PH-131 Paraflex Element	P
4	PX-110 Flange Assembly	P
5	Taperlok Bushing 2517 (2.5" Bore)	P
6	2.5" Shaft	D
7	MSI 2.5" to HBM T40B Adapter	P
8	HBM T40B (5 kN-m) Torque Transducer	P

*P = Specified and Purchased
D = Designed and Manufactured

Figure 5-3: Final Engine to Dynamometer Coupling Components

The stock Cummins flywheel (Part #1) was drilled and tapped to match the bolt pattern for the Dodge bolt ring (Part #2). The Dodge PH-131 Paraflex element (Part #3) absorbs vibrations and allows for 1 degree of misalignment between the respective engine and dynamometer drive shafts; this equates to 0.21-inches of allowable misalignment for the 12.5-inch shaft length. To achieve this small misalignment, the engine mounting brackets were designed to be rigid and prevent excessive misalignment between the engine and dynamometer during engine operation.

The Dodge PX 110 flange assembly (Part #4) and Taperlock bushing 2517 (Part #5) were selected to connect the Paraflex element to a custom made 2.5-inch shaft (Part #6). While a shaft diameter of 1.2-inches was determined to be large enough to handle the expected maximum torque of the 5.0 L diesel engine (759 N-m), the size was increased to 2.5-inch in order to achieve a common shaft diameter to connect the bushing (engine side) to the shaft flange adapter (dynamometer side). The shaft-flange adapter (Part #7) purchased from Machine Services

Incorporated (MSI) was used to connect the shaft to the dynamometer. This resulted in a coupling that is just under 12.5-inches in length; this assembly is shown in Figure 5-4.

Dodge Flexible Coupling Element
(265 kW or 675 N-m @ 3750 RPM)

Custom Designed 2 in. Shaft

MSI Flange to Shaft Adapter
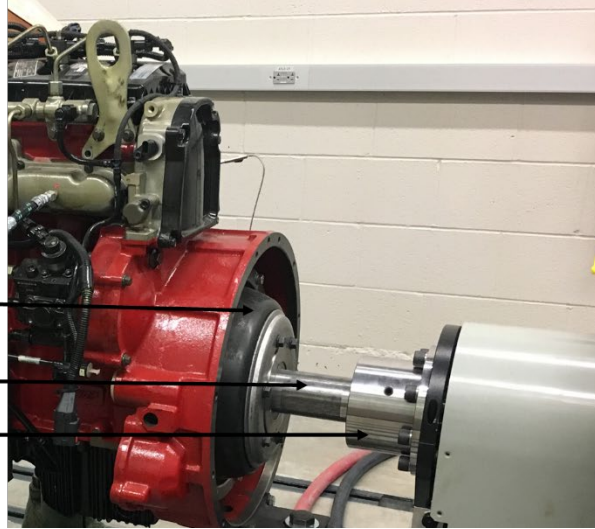
Figure 5-4: Installed Engine to Dynamometer Coupling Assembly

Other components critical to connecting the engine to the dynamometer were the engine mounting brackets (2 front and 1 rear) and a driveline guard. The mounts bolt to the sides and rear of the engine and sit on the engine stands that were taken from the previous engine testing facility. The engine stand height can be adjusted to achieve the vertical alignment with the dynamometer. Mounts were formed by water jet cutting a sheet of 5/16" steel and welding the resulting pieces.

The driveline, or shield, was designed to bolt down to the dynamometer table and cover the driveline. The guard was made by water jet cutting 1/8-inch steel in the projects lab and bending it in the precision machining lab (PML). 1/8-inch steel was selected because it was the maximum thickness that could be bent on the press.

5.2.2 Driveline Coupling Rated Performance

The engine coupling assembly is limited by thePH-131 flexible element, which is rated for 265 kW, or 675 N-m at 3750 RPM. This flexible element is anticipated to be the first component to fail in the case of a coupling failure, based on component ratings; element pieces should be contained within the shield and people are not allowed in the room during operation so safety should be maintained. It is recommended that the element cracks be checked routinely and the coupling be replaced if necessary.

5.2.3 Driveline Coupling Measured Performance

The installed driveline coupling has been used to run the engine up to 325 N-m @ 1500 RPM (50 kW). The flexible element showed a series of cracks even though the torque and speed were below the rated capacity. These cracks are attributed to excessive torque on the coupling bolts during installation. These bolts were backed off to the correct torque and further testing showed no lengthening of the cracks. However, due to the need to run the engine labs for the internal combustion engine class without risk of failure it was decided to not test the maximum torque and speed of the engine coupling. These cracks should be monitored regularly to know if the coupling should be replaced.

5.3 Coolant System

5.3.1 Coolant System Description

Building coolant passes through a plate heat exchanger and cools the engine water when the engine thermostat is open. The building coolant and engine coolant enter adjoining, but separate, channels of the heat exchanger and cools the engine coolant; the two fluids are not mixed. This

heat exchanger is displayed in Figure 5-5, with the engine and building coolant entrance and exit locations labelled. A solenoid valve was placed in the building coolant line, and connected to the key switch, to ensure coolant flow starts before the engine is started.
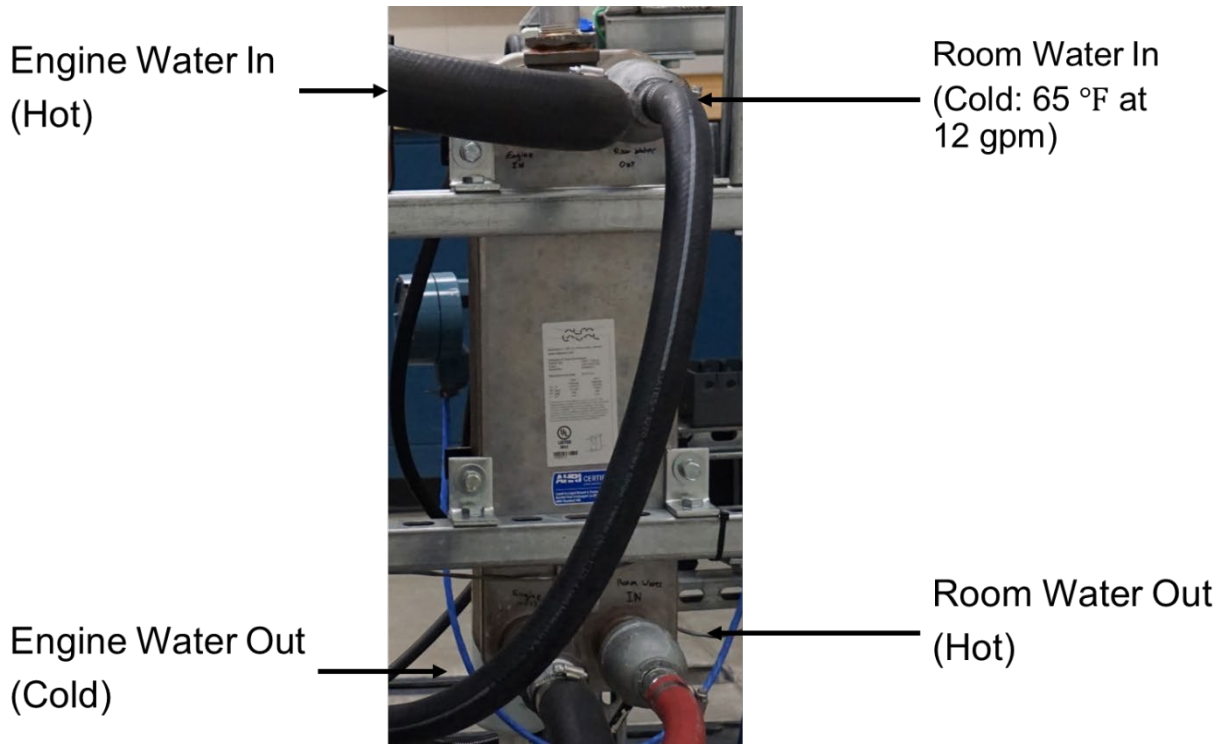
Figure 5-5: Installed Plate Heat Exchanger with Coolant Lines Labelled

5.3.2   Coolant System Rated Performance

The plate heat exchanger from Thermal Transfer Systems (TTS) is rated to remove up to 142.4 kW of heat from the engine. See supplier documents and drawing in Appendix C. Building coolant has a flow rate of 12 GPM and a temperature of 18 °C (65 °F) entering the engine test cell and would exit at 53.4 °C (128 °F) in order to remove heat at the rated capacity of the heat exchanger. Thus, the flow rate of water is high enough to support the current heat exchanger. Engine operating temperature is approximately 80 °C (176 °F).

5.3.3　Coolant System Measured Performance

At peak torque (360 N-m @ 1500 RPM [56 kW]), the cooling requirement of the engine is rated at 32.9 kW, or 58% of the engine power output. The engine was tested up to 325 N-m @ 1500 RPM [51 kW], or 91% of total power at peak torque. Because it was operated so close to the power at peak torque, a conservative assumption was made that the heat rejected by the heat exchanger was 91% of the 32.9 kW, or 30 kW. The systems cooling capacity could be observed by monitoring the engine coolant temperature on the Cummins Calterm software; the coolant temperature fluctuated between 77-86 ℃ as the thermostat opened and closed. It appears that the thermostat opens completely and closes completely because the temperature can be seen to increase slowly then decrease rapidly in a matter of approximately 10-15 seconds as the thermostat opens and the water is cooled in the heat exchanger.

5.4　Intake/Exhaust System

5.4.1　Intake/Exhaust System Description

Figure 5-6 displays a picture of the installed intake and exhaust system components. The exhaust fan and building air supply were specified prior to engine installation and were not part of the auxiliary design. The exhaust fan, labelled at the top of the figure, removes exhaust from the room and speeds up as exhaust temperature increases. The building air supply comes from the vent in the ceiling and is not shown.

The rest of the components were part of the design. The intake system consists of an air filter, which routes air to the front of the turbo, or compressor. As the compressed air leaves the turbo, it is cooled in an aftermarket Frozenboost Type 19 water-to-air charged-air cooler. The coolant provided to the charged-air cooler comes from the building coolant system. The cooled

and charged air then enters the engine at a higher density. The actual temperature of the air before and after the cooler was not measured, but was checked by touching the hot side and the cool side after running the engine; the charged air-line upstream of the cooler could only be touched briefly because of the high temperature while the charged air-line downstream of the cooler was cool to the touch.

After the fuel/air mixture combusts, it is exhausted through a custom/locally built exhaust pipe into the overhead exhaust vent.
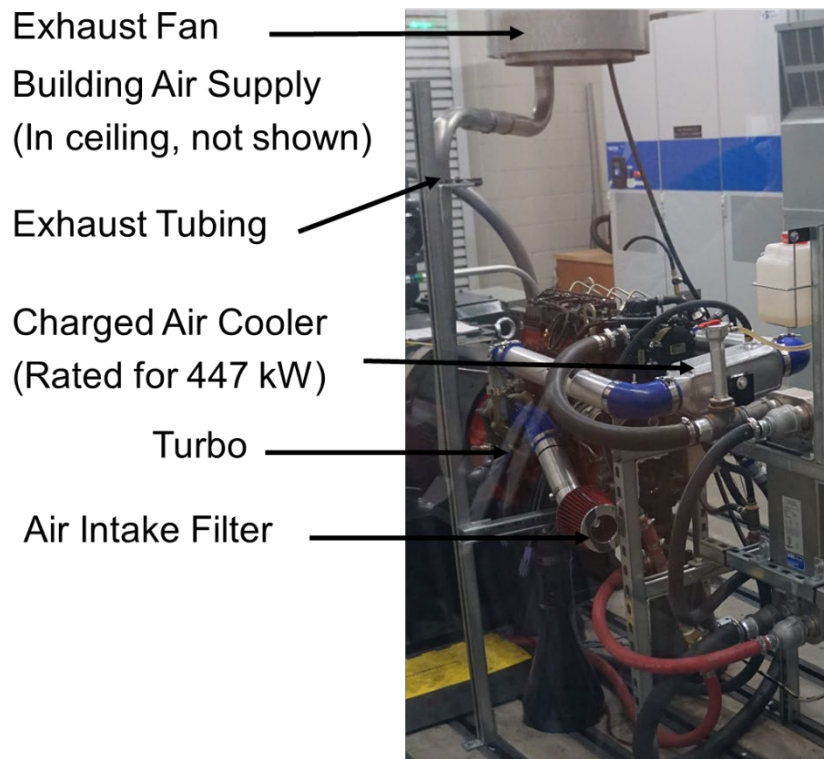
Figure 5-6: Intake and Exhaust System Components

5.4.2 Intake/Exhaust System Rated Performance

The intake/exhaust system is not limited by the auxiliary components, but by the building systems that provide and remove air. During the building design, a flow of 2000 SCFM was

specified for the test cell. Assuming that the lab is built to specifications and that 10 parts of air are used to cool one part of exhaust in the exhaust vent, the maximum theoretical power of the engine with this flow, and the rollup door closed, would be 58.3 kW. The building air supply and amount needed for dilution is the limiting factor for engine operation currently.

5.4.3   Intake/Exhaust System Measured Performance

It was observed that during engine operation that loads above 2.6 g/s of fuel flow could not be maintained without opening the roll-up door and allowing outside air to enter the test cell. This corresponds to a tested engine power limitation of 40 kW. With the roll-up door open, a higher performance of the test cell design could be evaluated and the Cummins 2.8 L engine was tested up to a value of 50 kW. (The engine was not tested above 50 kW during development of the laboratory experiments) These test results demonstrate that the exhaust fan is removing more air ($\dot{m}_{Ex\,Vent}$) than is supplied to the room ($\dot{m}_{Building\,Supply}$) as shown in Equation (5-1).

$$\dot{m}_{Ex\,Vent} > \dot{m}_{Building\,Supply} \tag{5-1}$$

A portion of the mass air flow delivered to the room enters the engine through the intake, while the remaining portion exits the room through the exhaust vent and helps dilute, or cool, the exhaust in the duct; this relationship can be seen in Equation (5-2). The current workaround to this problem is to increase $\dot{m}_{Intake}$ by opening the roll-up door. In the future, $\dot{m}_{Dilution}$ could be decreased by reducing the exhaust speed, or cooling the exhaust with an additional heat exchanger.

$$\dot{m}_{Ex\,Vent} > \dot{m}_{Intake} + \dot{m}_{Dilution} \tag{5-2}$$

The exhaust vent fan has a temperature feedback system which increases the exhaust fan speed to maintain a low temperature in the exhaust duct. The exhaust flow can clearly exceed the intake flow for the room creating a negative pressure. The observed problem was not a result of the test cell components built for this project and was therefore beyond the scope of work. Future investigations should be completed to understand the exact limitations of the building air supply system and verify whether the air supply to the room can be increased, or if the exhaust flow can be lowered.

5.5   Fuel System

5.5.1   Fuel System Description

The components of the fuel system are shown in Figure 5-7. The fuel moves from the fuel tank through an inline fuel pump, which increases the fuel line pressure upstream of the Coriolis flow meter. After the flow meter, the fuel passes through a filter, which removes debris and water from the fuel, before it enters the engine.
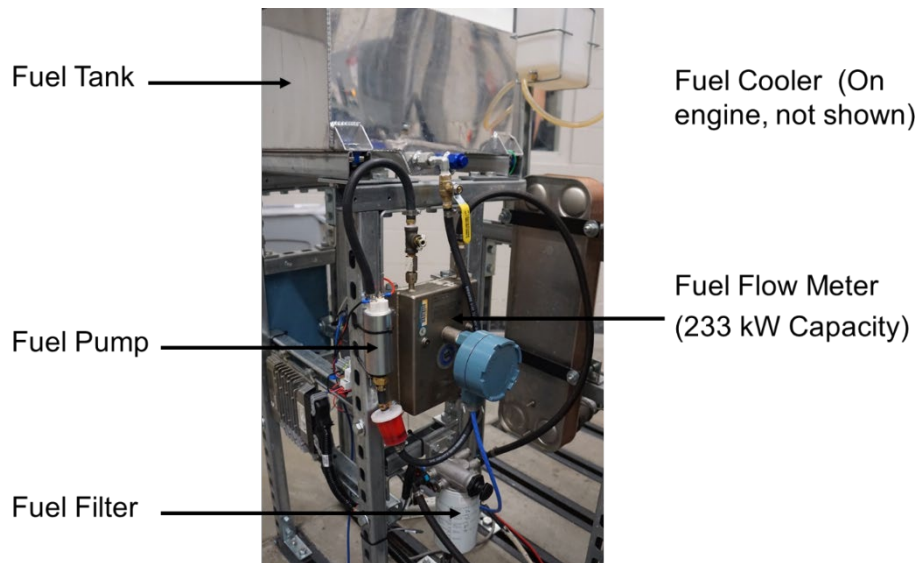
Figure 5-7: Installed Fuel System Components

The engine also has a high pressure fuel pump (not shown in the diagram) driven off the crankshaft which is pulling fuel from the tank to the engine and pressurizing the fuel rail. Normally, this high pressure fuel pump on the engine is sufficient to pull fuel from the tank to the engine, but the Coriolis flow meter poses a large restriction. The large pressure drop caused from this restriction required the addition of an inline fuel pump in order to prevent vaporization of fuel in the lines.

Diesel engines normally pump a much larger flow of fuel through the injectors and rail than is actually injected in order to keep the injectors cool. The excess fuel is normally cooled by returning it to the tank and letting it mix with the stored fuel. In order to utilize a single flow meter, fuel was not returned to the tank but instead routed through a small heat exchanger where it is cooled and returned directly to the high pressure injection pump.

5.5.2   Fuel System Rated Performance

The fuel system has multiple installed components that can limit flow. The Coriolis flow meter poses the largest restriction to fuel flow of all the components limiting the maximum fuel flow rate to 15.1 g/s. At 35% brake efficiency, this flow rate could accommodate a 233 kW engine. This is a higher capacity than the current 2.8 L engine but smaller than the capacity of the dynamometer. This is the second most limiting component in the engine auxiliary systems after the air discrepancy that requires the bay door to be opened. This means that a different engine (rated up to 233 kW) could be installed on the dyno without changing major auxiliary system components.

5.5.3   Fuel System Measured Performance

Initially, the fuel system was installed without the inline fuel pump. This allowed the engine to run, but the response time for the Coriolis flow meter was approximately three minutes. With the pump installed, response times decreased to approximately 30 seconds. It is clear that the fuel pump has an effect on the dynamic response of the fuel system. It is not clear what portion of the slow response can be attributed to the flow meter and what is now attributed to the fuel system dynamics. The maximum fuel flow tested on the engine was 3.06 g/s; higher flows can be tested in the future.

5.6   Controls/DAQ System

5.6.1   Controls/DAQ System Description

Figure 5-8 shows various components contributing to the controls and data acquisition system. The picture on the left displays the components in the test cell. First, there is the Cummins engine control unit (ECU), which is the primary control for the engine. Second, Fuel flow data is currently collected from the Coriolis flow meter via a National Instruments cRIO 9074 data acquisition module and read with a LabVIEW program on the computer in the control room.

The Control room is shown on the right in the figure and contains the computer and dynamometer control box. The dynamometer has a control box that is connected to the ECU; this control box receives torque and speed feedback data from the torque transducer on the dynamometer and varies the commands to the ECU based on the torque or pedal position specified by the user. This allows for simple control of the engine with the dynamometer control box (located in the control room). Brake torque and engine speed are displayed on the control

box. Emissions data was taken using a stand-alone gas analyzer. See Appendix D. for the wiring

diagram to connect sensors, data acquisition system, and controls.
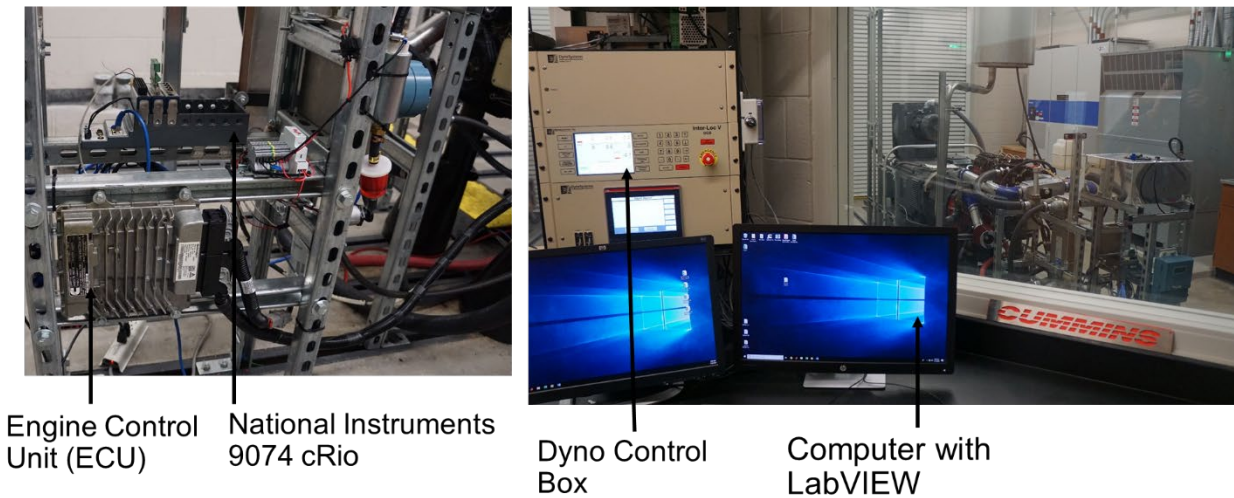
Figure 5-8: Left: Engine bay - Engine control unit and data acquisition system. Right: Control room - dynamometer control box, computer with LabVIEW data recording software.

5.6.2 Controls/DAQ System Rated Performance

The HBM T40B torque transducer mounted on the dynamometer is rated to measure torque

up to 5000 N-m, which is much larger than the max rating of 1750 N-m of the dynamometer.

The torque transducer was selected by the dynamometer supplier without appropriate oversight

by BYU before delivery. It was not changed after dynamometer delivery due to cost

considerations.

5.6.3 Controls/DAQ System Measured Performance

Torque and engine speed were successfully measured, displayed, and recorded by hand from

the dynamometer control box. A torque uncertainty of ±3.5 N-m was measured by checking the

standard deviation of torque measurements during testing; this uncertainty is due to the torque transducer's large measuring range.

Fuel flow rate was collected through the LabVIEW program; in the future, additional sensor data can be collected through the National Instruments cRIO 9074 expansion slots. Currently engine torque and speed are shown on the dyno control box and fuel data are read into LabVIEW.

The Cummins Calterm software limited license allows for the reading of engine data such as engine temperature and diagnostic codes. Some variables, such as fueling, can be temporarily altered in the Calterm software, but any long-term calibration changes must be conducted by Cummins. Using the Calterm software for more than simple monitoring of engine sensors requires a learning curve as it is Cummins specific and not designed for third parties. For this reason, Calterm is currently used only to monitor the engine coolant temperature while engine control is conducted with the dynamometer control box.

5.7   Summary of Engine Auxiliary Setup Ratings and Measured Performance

This section summarizes the rated and measured performance of the auxiliary systems (See Table 5-1) to enable readers to understand necessary changes that would be required to install a different engine in the test cell. All of the current components are shown to function above the operating range of the current 2.8 L engine except for the flexible element in the coupling assembly, which is rated for the engine but was potentially damaged during installation. The current system has been demonstrated to work for the ICE class laboratory experiments and capstone design projects. Some power ratings are taken from applicable supplier documents, and others are calculated in Appendix E.

Table 5-1: Rated and Demonstrated Results for Key Component Parameters.

System	Performance Parameter	Rated Performance	Demonstrated	Comment
AC Dynamometer	Torque Speed Power	1750 N-m 2000 RPM 342 kW	325 N-m 1500 RPM 50 kW	Dynamometer has much higher capability than current engine.
Driveline Coupling	Torque Speed Power	675 N-m 3750 RPM 265 kW	325 N-m 1500 RPM 50 kW	Flexible coupling demonstrates cracks from excessive torque on the bolts during installation.
Engine Cooling	Heat removal	142.4 kW	30 kW	Cooled without problems.
Lab Intake and Exhaust System (Door Closed) (Door Open)	Amount of exhaust in room Max fuel flow Max Power Max fuel flow Max power	None 3.7 g/s 58.3 kW No Limit No Limit	None 2.16 g/s 40 kW 3.06 g/s 50 kW	No exhaust in room. *Exhaust vent removes more air than is supplied to room
Intercooler	Maximum Flow Rate Rated engine power	0.28 kg/s (500 SCFM) 444 kW	0.066 kg/s 50 kW	Temperatures were not measured but line downstream of the intercooler is cool to the touch
Fuel	Max flow Max Power Response time	15.1 g/s 233 kW	3.06 g/s 50 kW ~ 30 s	Testing was limited by coupling cracks from incorrect installation
Torque Transducer on Dyno	Max Torque Resolution	5000 N-m ± 3.5 N-m	325 N-m ± 3.5 N-m	Torque resolution is limited by HBM T40B 5 KN-m
Engine 2.8 L Cummins	Torque (Peak) Speed (Max) Power (Governed)	360 N-m 2900 RPM 110 kW	325 N-m 2000 RPM 50 kW	None

Each auxiliary system has a limiting component; these components are listed here in order of decreasing limitations:

1. Building air supply and exhaust vent discrepancies currently limit power with the roll-up door closed to 40 kW. This is currently overcome by opening the door.

2. The current setup is limited by the fuel flow meter to 68% of the dynamometer capacity. If an engine rated for more than 233 kW (312 hp) is to be used, the flow meter would need to be replaced.

3. The coolant heat exchanger has a capacity for 142.4 kW of cooling. Assuming this removes 58% of the fuel energy delivered to the engine, as is the case for the current Cummins specification, this would allow an engine output power of 245 kW.

4. The coupling assembly is rated for 265 kW. Cracks formed during operation due to incorrect installation. The coupling has been tested up to 50 kW, but not to failure.

Power capacity ratings of individual systems are summarized on the lab schematic for easy visualization in Figure 5-9. Note that, the only system that was tested to failure wat that of the intake/exhaust system, which was limited by the air supply to the room; this system displays a rated and tested value. The rest of the values shown here are rated values as laboratory experimental setup did not require testing to failure.
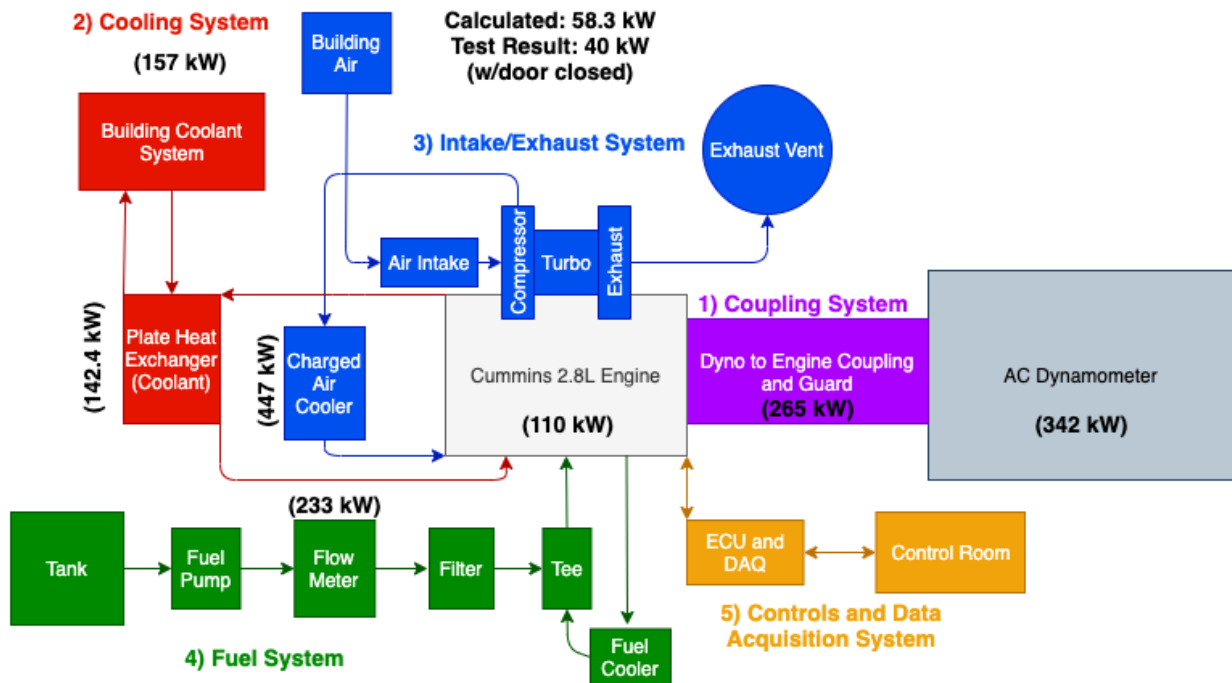
Figure 5-9: Schematic of engine test cell set-up with rated power capacity limitations.

5.8   Example Coursework Engine Lab Testing

This section demonstrates that the engine test cell has been used to record brake engine torque, power, speed, fuel flow, and emissions data for the ICE class laboratory experiments. Engine operating instructions can be found in Appendix G. The student laboratory instructions can be referenced in Appendix H. and are complete with sample data taken during the lab. This data can be used to educate the students in the ICE class in the case that anything prevents the students from being able to physically run the lab and take the data. It also provides a baseline to benchmark future engine performance against initial engine performance.

A sample plot of engine brake torque and engine brake power at constant engine speed (1500 RPM) as a function of fuel flow rate are shown in Figure 5-10 and Figure 5-11 respectively with error bars representing 1 standard deviation of 4 measured data points. These plots demonstrate the capacity of the lab to measure torque, fuel flow, and power data.
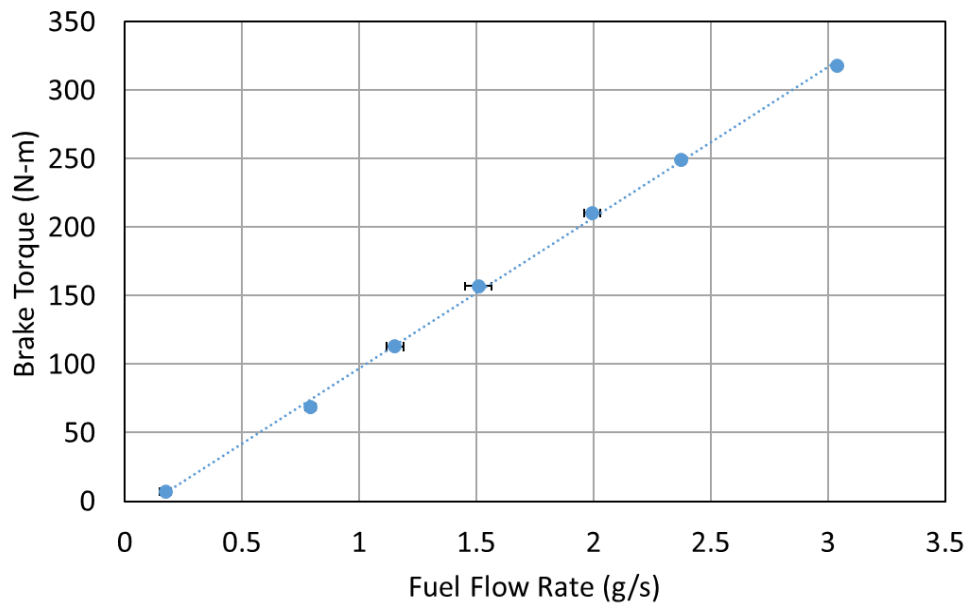
Figure 5-10: Sample data set for brake torque as a function of fuel flow rate at a constant speed of 1500 RPM. Error bars represent 1 standard deviation of 4 data points.

Data were collected at 7 points between idle (5.5% load) up to a maximum of 96% load at a constant speed of 1500 RPM. The data show a maximum torque of 325 N-m and power of 50kW. The increase in torque and power as a function of fuel flow is seen to be almost linear with a negative intercept. The negative intercept indicates the power consumed by parasitic losses in the engine.
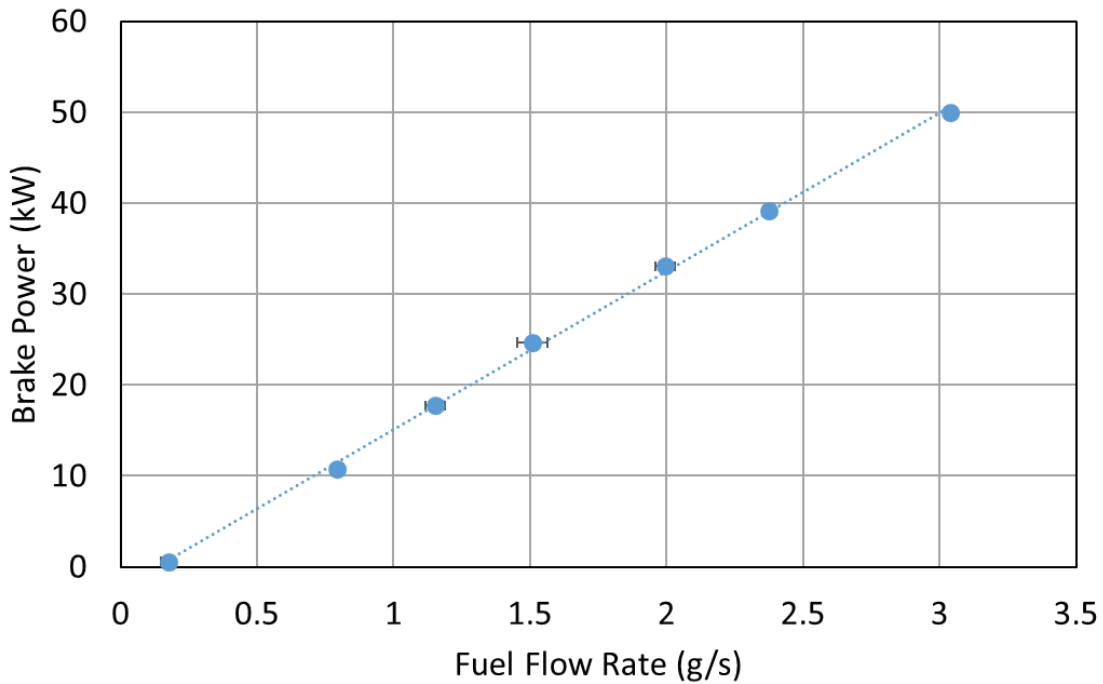
Figure 5-11: Sample data set for brake power as a function of fuel flow rate at a constant speed of 1500 RPM. Error bars represent 1 standard deviation of 4 data points.

Using the measured data, fuel conversion efficiency was calculated. The calculated efficiency shown in Figure 5-12 was found to increase to a maximum of 37% at 1.5 g/s fuel flow and remain nearly constant for increasing fuel flows. The increase in efficiency is caused by a decrease in the fraction of total power required to overcome parasitic losses. The data are as expected and can be used to help students understand the interactions of fuel energy, energy to work conversion, and losses.
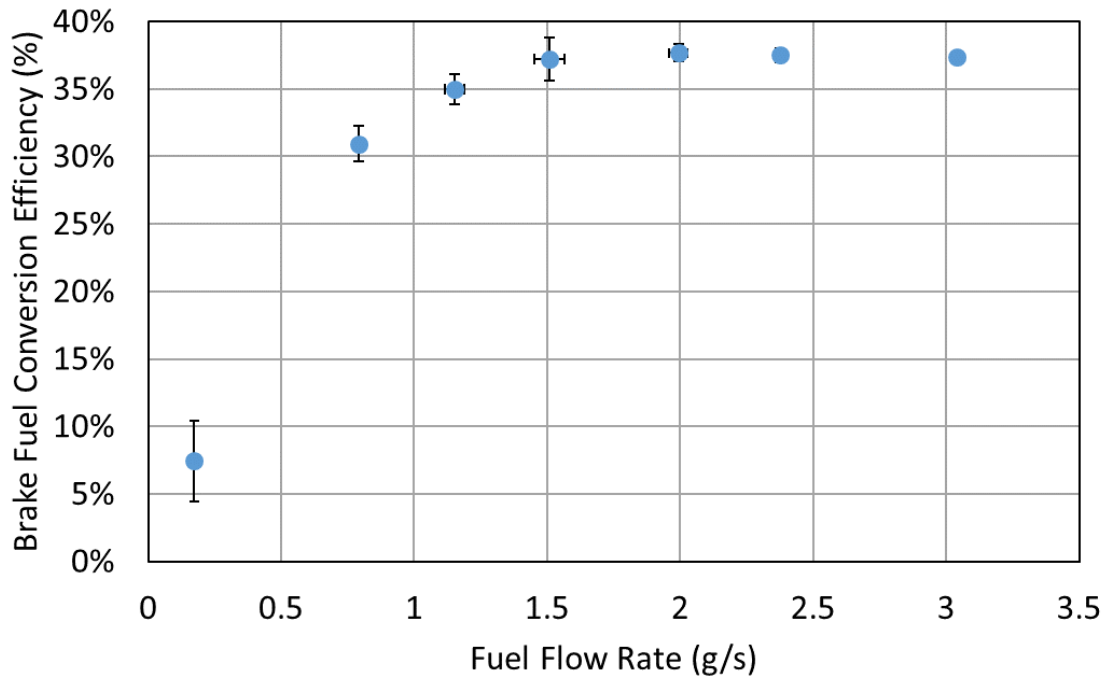
Figure 5-12: Sample data set for brake fuel conversion efficiency as a function of fuel flow rate at a constant speed of 1500 RPM. Error bars represent 1 standard deviation for 4 data points.

Figure 5-13 shows the sample results of emissions tests illustrating capabilities of the system to measure Nitrogen Oxides (NOx), Carbon Monoxide (CO), Carbon Dioxide (CO_2), and Oxygen (O_2). These sample data points were measured for the same data points where the torque and power were measured. Note that the concentrations of NO_X and CO are given in PPM, and the concentrations of CO_2 and O_2 in percentages (1% = 10,000 PPM). Although the values and trends will not be explained, they are consistent with expectations discussed in the BYU ICE class and can be used to support theories presented that affect emissions. Note that the trends for the emissions are simply rough trend lines added to help students to follow the respective emissions as fuel flow rate increases.
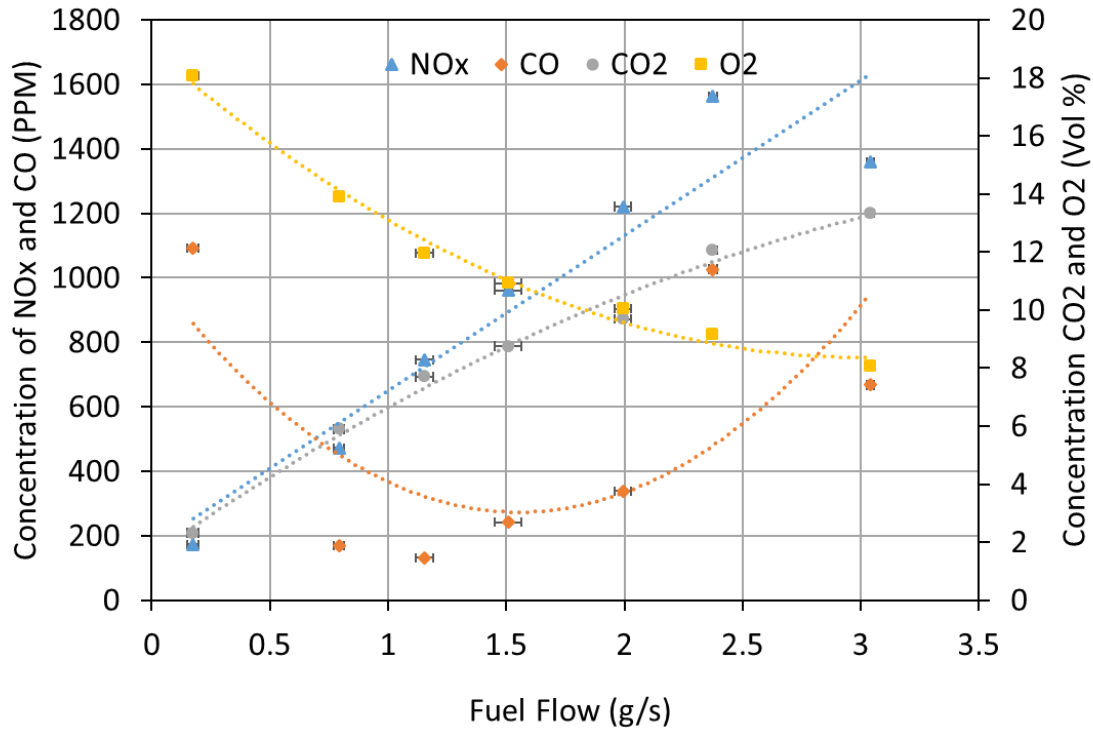
Figure 5-13: Sample data set and rough trend lines for emissions concentrations as a function of fuel flow for Cummins 2.8 L engine running at 1500 RPM. Error bars represent 1 standard deviation for 4 data points.

5.9   Measuring Parasitic Losses of the Water Pump

This section outlines key findings such as pump power input, output, and efficiency. Results are separated between open thermostat and closed thermostat findings. Uncertainties were calculated from the standard deviations of the test data for maximum engine speeds; all of these uncertainties were below 4.6%, demonstrating a high repeatability for the tests.

5.9.1   Open Thermostat

With the thermostat open, water flows through the engine and radiator before returning to the pump. The volume flow rate as a function of water pump speed is shown in Figure 5-14.

Flow measurement uncertainty was estimated from the standard deviation of the four runs to be 0.9% at maximum engine speed. The results show an almost linear relationship between flow rate and water pump speed (N); this demonstrates that flow rate is proportional to engine speed as represented by Equation (5-3).
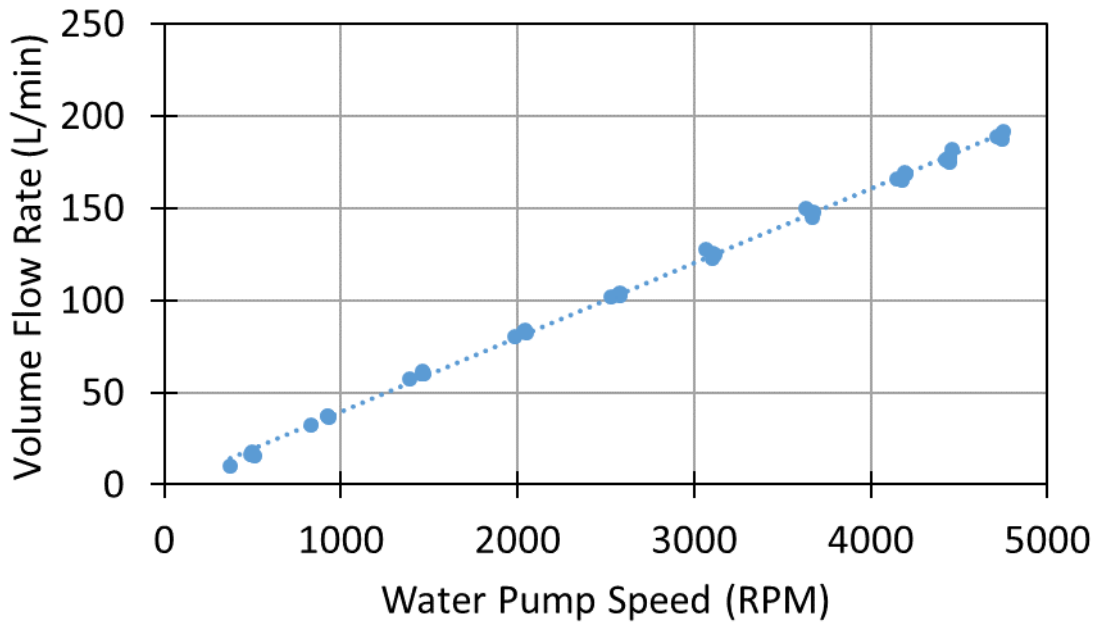
Figure 5-14: Volume flow rate of the water pump as a function of engine speed for an open thermostat condition.

$$\dot{V} \propto N \qquad\qquad (5\text{-}3)$$

Figure 5-15 shows the absolute pressure changes measured across the pump, engine, and radiator respectively. The pressure increased over the pump and decreased across the engine and return (radiator). Volumetric flow was measured between the radiator and pump as shown in Figure 4-2. Pressure measurement P1 was located approximately 1.5 feet in elevation below the water pump, as shown in Figure 4-3, and therefore the effective pressure (ΔP_{pump}) added by the pump and the pressure drop in the return were calculated as the sum of hydrostatic and static

pressure as shown in Equation (5-4). The elevation difference between P2 and P3 was small, so hydrostatic pressure was neglected in ΔP_{engine} but used again in ΔP_{return}. Pressure measurement uncertainty estimated from the standard deviation of the four runs was 3.8% at maximum engine speed.

$$\Delta P_{pump} = (P_2 - P_1) + \rho g h_{H_2O}$$
$$\Delta P_{engine} = (P_2 - P_3)$$
$$\Delta P_{return} = (P_3 - P_1) + \rho g h_{H_2O}$$

(5-4)
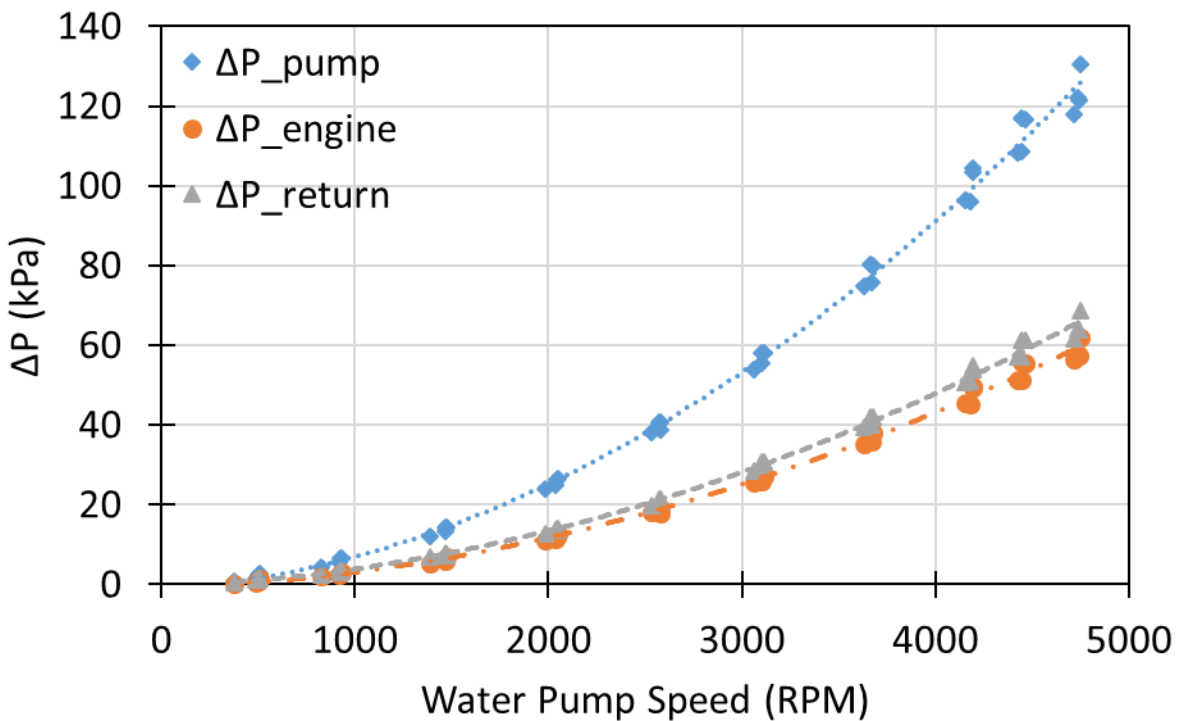
Figure 5-15: Pressure changes across water pump, engine, and return (radiator) for open thermostat tests.

The data in Figure 5-15 show that the pressure drops through the engine and the radiator were similar and that these pressure changes were proportional to the water pump speed squared. Combining this with Equation (5-3) it can also be seen that the pressure change is proportional to the volume flow rate squared as shown in Equation (5-5).

$$\Delta P \propto N^2 \propto \dot{V}^2 \tag{5-5}$$

This result is consistent with classical internal fluid flow. Flow through the engine can be modeled as major losses through a pipe by Equation (5-6) where f is the friction factor, l and d are the length and diameter of the pipe, V is velocity, and ρ is the fluid density. Since volume flow rate is proportional to the velocity, this equation suggest that pressure drop should be proportional to volume flow rate squared, as observed.

$$\Delta P_{major\ losses} = f\left[\frac{l}{d}\right]\left[\frac{\rho V^2}{2}\right] \tag{5-6}$$

The minor losses expression in Equation (5-7) also shows a velocity squared dependence, along with a new variable K_L, which represents a total engine minor loss friction factor. Again, since volume flow rate is proportional to the velocity, pressure drop should be proportional to volume flow rate squared and engine speed squared, which serves to validate experimental results.

$$\Delta P_{minor\ losses} = K_L\left[\frac{\rho V^2}{2}\right] \tag{5-7}$$

Calculations showed that the Reynolds numbers for each test condition was in the transitional flow range, where the major losses friction factor (f) is decreasing. This decrease reduces the effect of the velocity squared term in the major losses equation. This finding suggests that fluid flow through the engine and radiator can be modelled as minor losses of fluid flowing around restrictions in a pipe, or major losses under turbulent flow conditions in a pipe.

Figure 5-16 shows the measured torque as a function of water pump rotational speed. Torque measurement uncertainty was estimated from the standard deviation of the four runs to be a maximum of 2.9% at maximum water pump speed.
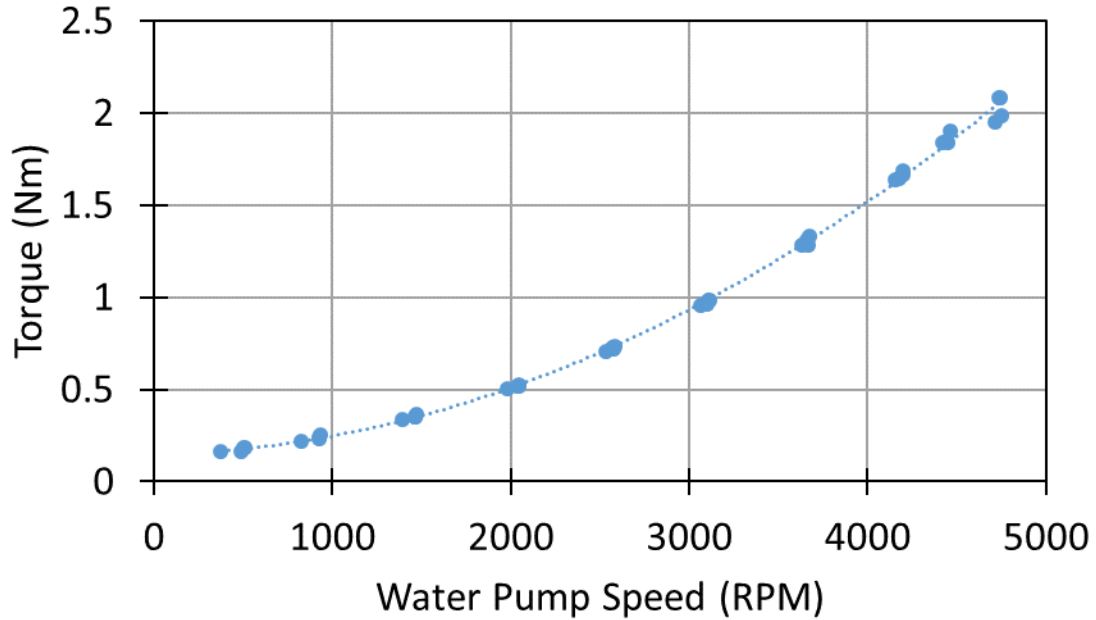
Figure 5-16: Torque required by water pump shaft to pump water through open thermostat loop as a function of water pump speed.

Torque is seen to increase proportional to the water pump speed squared. This can be understood by equating the power input as shown in Equation (5-8) and the power output of the pump shown by Equation (5-9) to obtain Equation (5-10); where N is the pump speed, T is the torque, $\dot{W}$ is power and $\dot{V}$ is the volume flow rate. Replacing the dependencies of $\dot{V}$ which is proportional to engine speed, N, and ΔP_{pump} which is proportional to engine speed squared as shown in Equation. (5-10); this equation also shows that torque is proportional to pump speed squared.

$$\dot{W}_{in} = 2\pi NT \tag{5-8}$$

$$\dot{W}_{out} = \dot{V}\Delta P_{pump} \tag{5-9}$$

54

$$2\pi NT = \dot{V}\Delta P_{pump} \propto N * N^2$$

$$T \propto N^2$$

(5-10)

From the previously stated power equations, pump power input and outputs were calculated and are shown in Figure 5-17. Power input and output uncertainties were estimated from the standard deviation of the four runs to be 3.0% and 4.6% respectively.
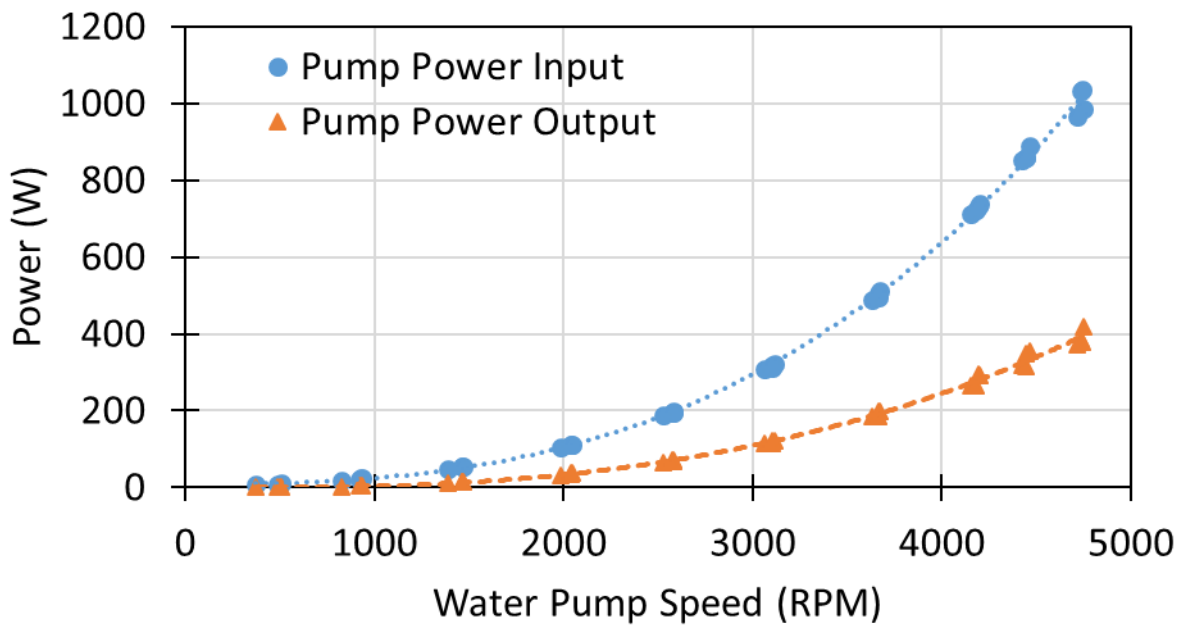
Figure 5-17: Water pump power input and output for the open thermostat speed sweeps as a function of water pump speed.

The power curves support the trends predicted by major losses in fluid dynamics. Substituting the correlation from Equation (5-10) into Equation (5-8) for torque, gives Equation (5-11):

$$\dot{W}_{in} \propto N^3$$

(5-11)

These findings suggest that for the setup used, fluid flow through the engine and radiator can be modelled as fluid flowing through a pipe.

The pump efficiency was calculated with Equation (5-12), and a plot of efficiency as a function of pump speed is shown in Figure 5-18. The pump efficiency is near zero at low speeds and increases until it asymptotes at 38% above pump speeds of 3500 RPM. This shows that the pump spins at low speed without flowing any fluid, perhaps due to the need to overcome hydrostatic forces. Once water is flowing, the mechanical friction and hydrostatic forces become a smaller fraction of the total force required, and the pump losses become a constant fraction of the total power at high speed.

$$\eta = \frac{\dot{W}_{out}}{\dot{W}_{in}} \hspace{4cm} (5\text{-}12)$$
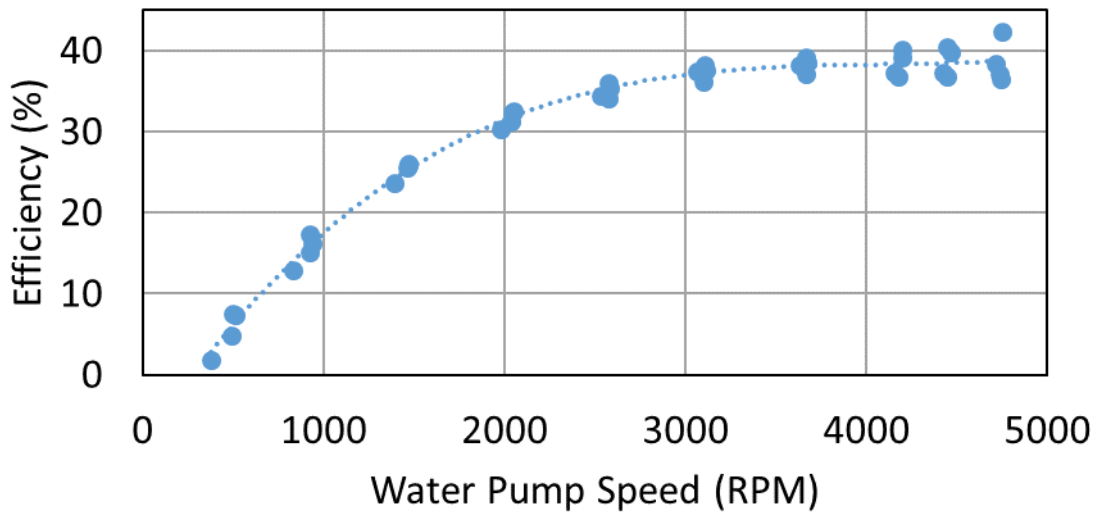
Figure 5-18: Water pump efficiency as a function of water pump speed for the open thermostat water pump speed sweeps.

5.9.2 Closed Thermostat

The pressure changes as a function of pump speed for the closed thermostat sweeps are shown in Figure 5-19. In comparison to the open thermostat, the pressure increase is larger for the closed thermostat as a result of the pressure drop through the return bypass tube being larger than the pressure drop through the radiator. This is due to the smaller diameter of the tube exiting the closed thermostat in comparison to the larger diameter tube and passage through the radiator.
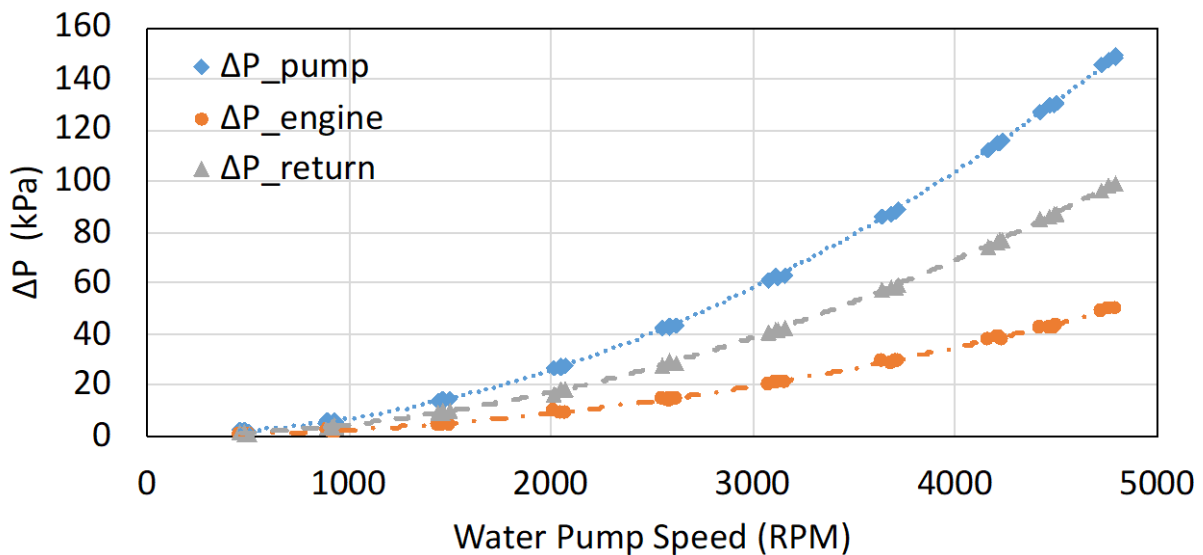
Figure 5-19: Pressure changes across water pump, engine, and return (bypass) for closed thermostat tests.

The torque required for the sweep through water pump speeds is shown in Figure 5-20. The torque for the closed thermostat shows less than 1% relative difference from the open thermostat torque for a given speed. Due to the small variability in torque and power between the two cases, only the open thermostat trend fit equation was used in later calculations that compare the water pump power to the engine power.
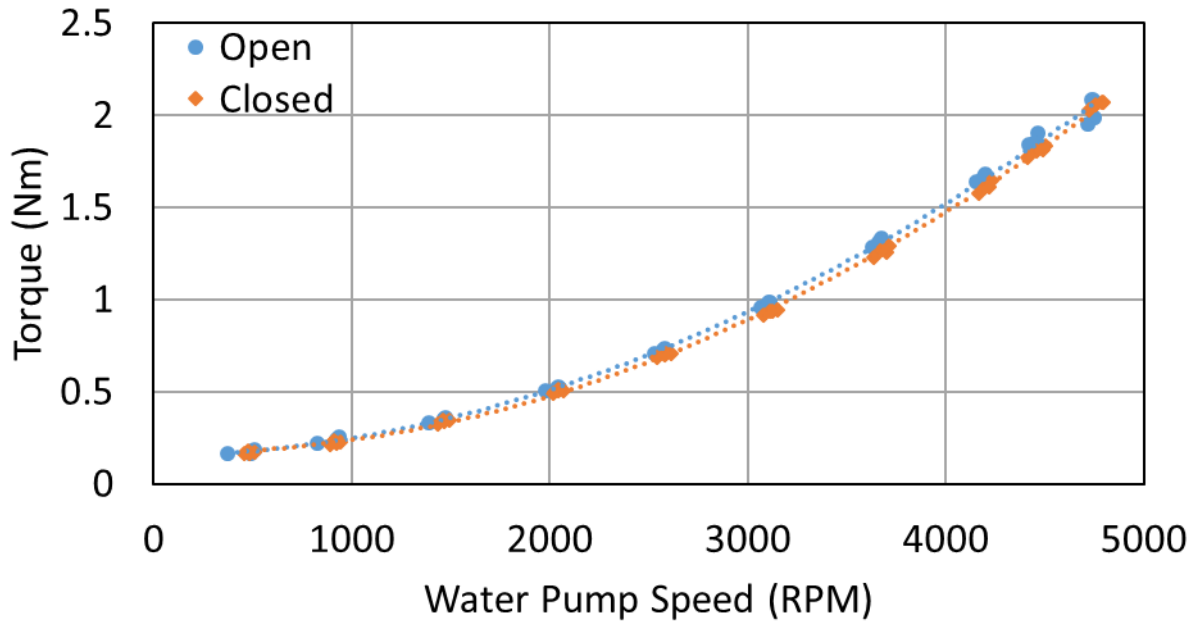
Figure 5-20: Water pump shaft torque as a function of water pump speed for open and closed thermostat test sweeps.

The flow meter was installed between the radiator and the pump but there was no flow through this section of flow circuit when the radiator was closed, nor was there a location that provided a ready access for a flow meter to be inserted into the engine bypass tube. In order to estimate the flow rate through the circuit when the thermostat was closed, a correlation between flow rate and pressure drop across the engine was determined from the open thermostat data. This correlation is shown in Figure 5-21. Equation (5-13) enabled the calculation of the predicted volume flow rate for the closed thermostat sweeps; as shown in Figure 5-22. Note that the y-axis ($\dot{V}$) represents the volume flow rate and the x-axis (ΔP) represents the pressure drop across the engine.

$$\dot{V}\left(\frac{m^3}{s}\right) = -0.0356(\Delta P)^2 + 4.8154(\Delta P) + 23.467 \tag{5-13}$$
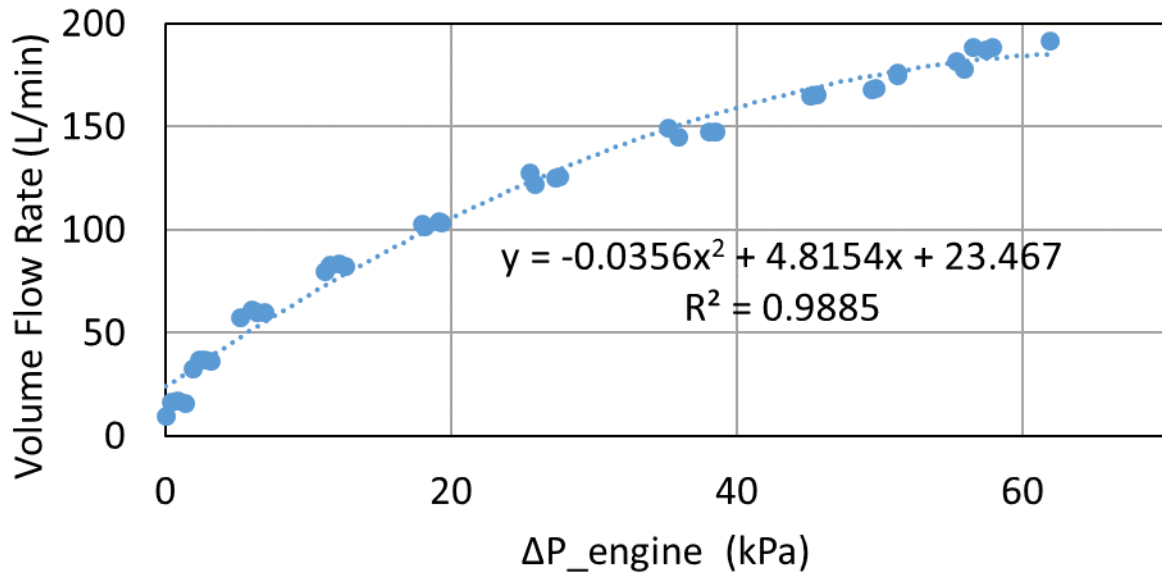
Figure 5-21: Correlation of volume flow rate as a function of pressure drop across the engine.
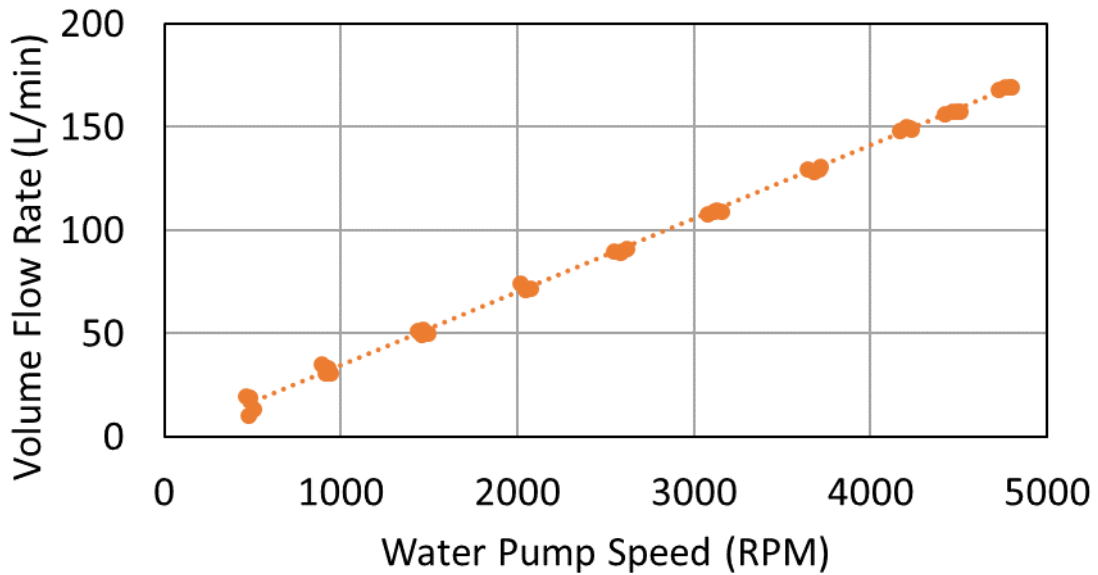
Figure 5-22: Predicted volume flow rate as a function of water pump speed for the closed thermostat.

Using the predicted volume flow rate, measured pressure increase across the pump,

measured torques, and measured pump speeds, the total power input and output for both the open

and closed thermostat cases was calculated and is shown in Figure 5-23. The data show that the

power input and output required is less than 2% relative difference between open and closed thermostat cases. While the closed thermostat has a higher pressure drop, the flow rate is proportionally lower such that the product of the flow rate and pressure drop, or power output, remains nearly constant for both the open and closed thermostat sweeps, for the conditions tested. Note that powers are for a 'new' engine and radiator with little restrictions. Power requirements will be larger with more restrictions or fouling in the engine.
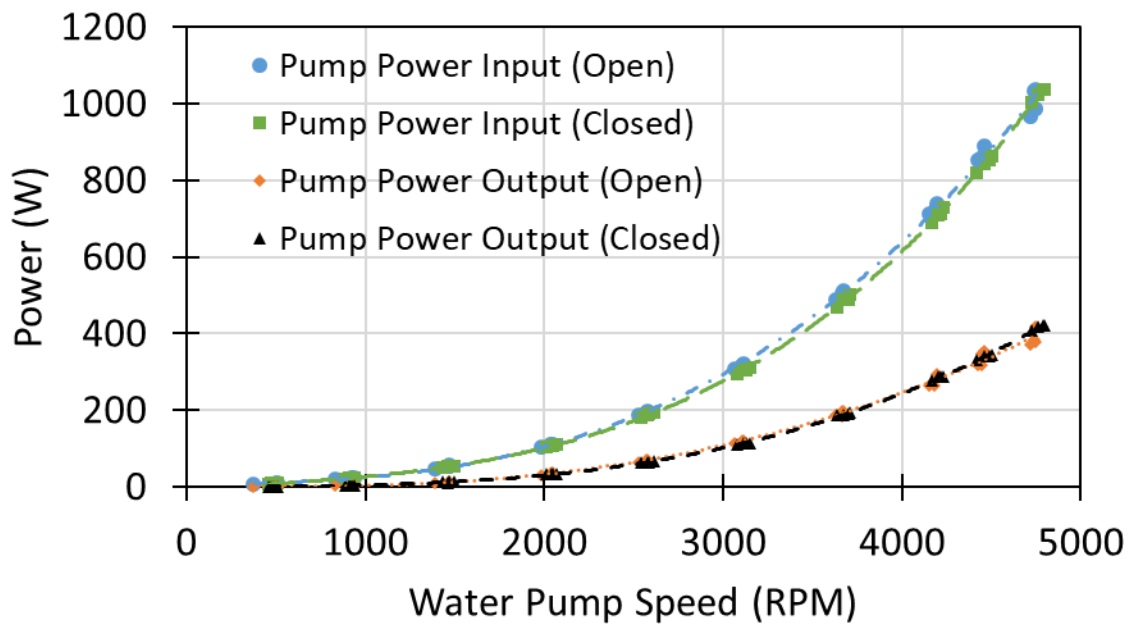
Figure 5-23: Water pump power input and output for the open and closed thermostat sweeps as a function of water pump speed. Powers are for a 'new' engine and radiator with little restrictions. Power requirements will be larger with more restrictions or fouling in the engine.

The similar power input and output curves for the open and closed thermostat motor speed sweeps produce the similar efficiency curves shown in Figure 5-24. Since the same pump was used for both the open and closed thermostat sweeps, it makes sense that the pump would have almost the same efficiency for both test cases.
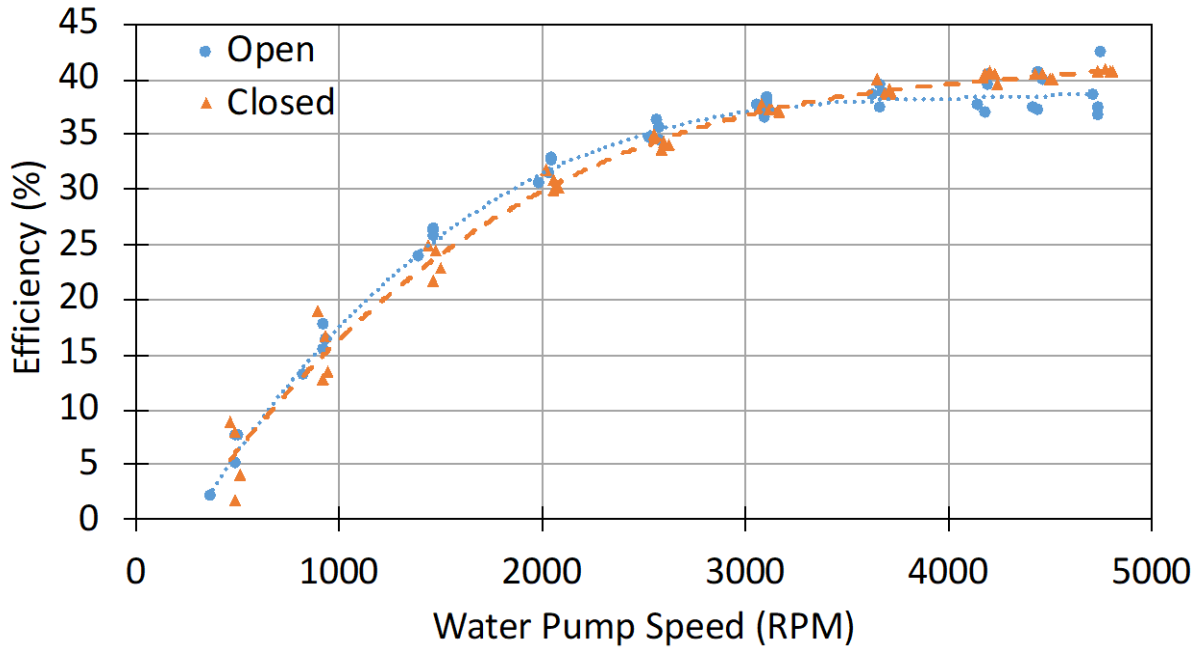
Figure 5-24: Water pump efficiency as a function of water pump speed for the open and closed thermostat cases.

5.10 Measuring Parasitic Losses of the Vacuum Pump

Figure 5-25 shows the recorded torque as a function of motor speed for all of the test cases; these tests are outlined as follows: 1) oil supplied with an oil drip and the vacuum reservoir closed; 2-3) a pressurized oil supply and the vacuum reservoir closed; 4) oil supplied with an oil drip and the vacuum reservoir open to atmosphere. The average torque was nearly constant at 4 N-m for all oil supply and tank conditions tested. Vacuum pump speed also had a minimal effect on the results; the only two points below 4 N-m were recorded while the driving motor was speeding up. Once the vacuum pump speed exceeded 200 RPM, the torque was consistently around 4 N-m regardless of whether the vacuum tank was closed or open to atmosphere and independent of the lubrication condition. Torque measurement uncertainty calculated from taking the standard deviation of points above 200 RPM was estimated to be 2.9%.
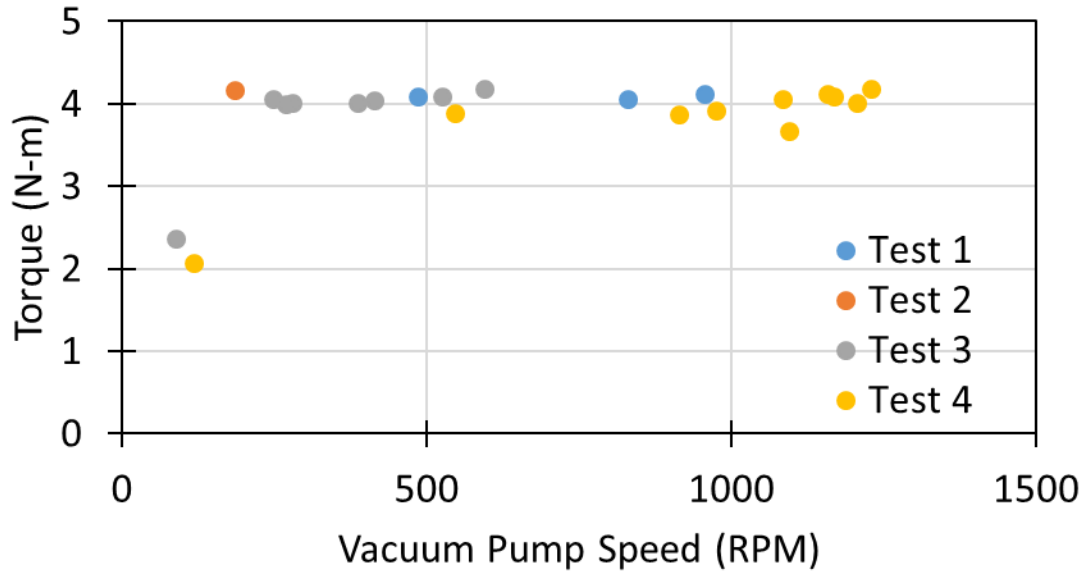
Figure 5-25: Torque input required as a function of vacuum pump speed

Because the vacuum pump required such high torque at low speeds, the first motor stalled. Further tests were run with a high torque drill; however, this test setup did not allow for the measurement of speed. This was deemed acceptable because the torque measurements showed no measurable difference at different speeds. The vacuum pump torque is shown in Figure 5-26. Torque values remained around 4 N-m except when the pump was open to the atmosphere. For these cases, the torque was reduced to approximately 3.6 N-m.

Test cases were conducted, as described in Table 4-7, with: 1) no oil supplied to the pump; 2) an oil drip supply and the vacuum reservoir open to atmosphere; 3) an oil drip supply and the vacuum reservoir closed; 4) a pressurized oil supply and the vacuum reservoir open; 5) a pressurized oil supply and vacuum reservoir closed. Figure 5-27 shows the vacuum pump input power as a function of vacuum pump speed. The power is seen to increase linearly as expected for a constant torque pump.
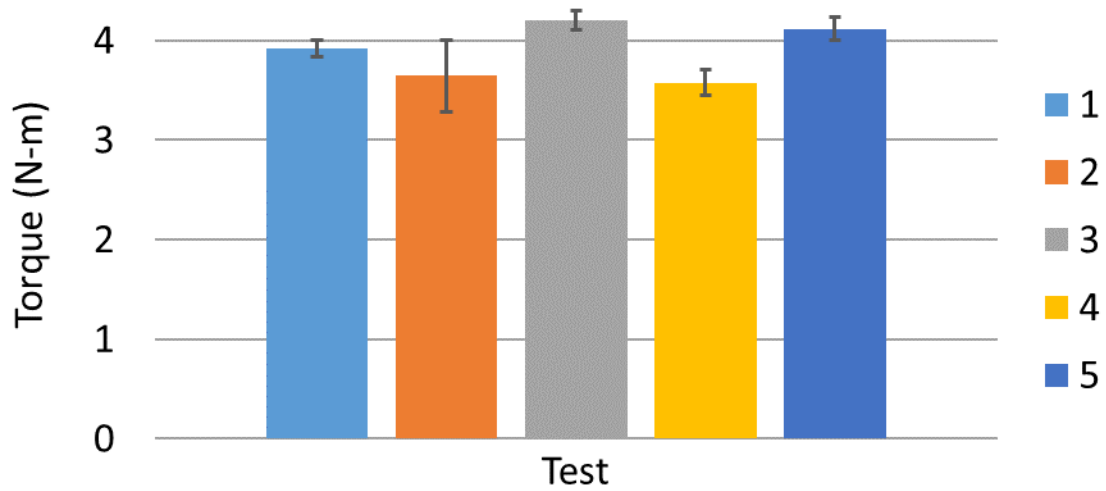
Figure 5-26: Average torque required to power vacuum pump for various test cases.
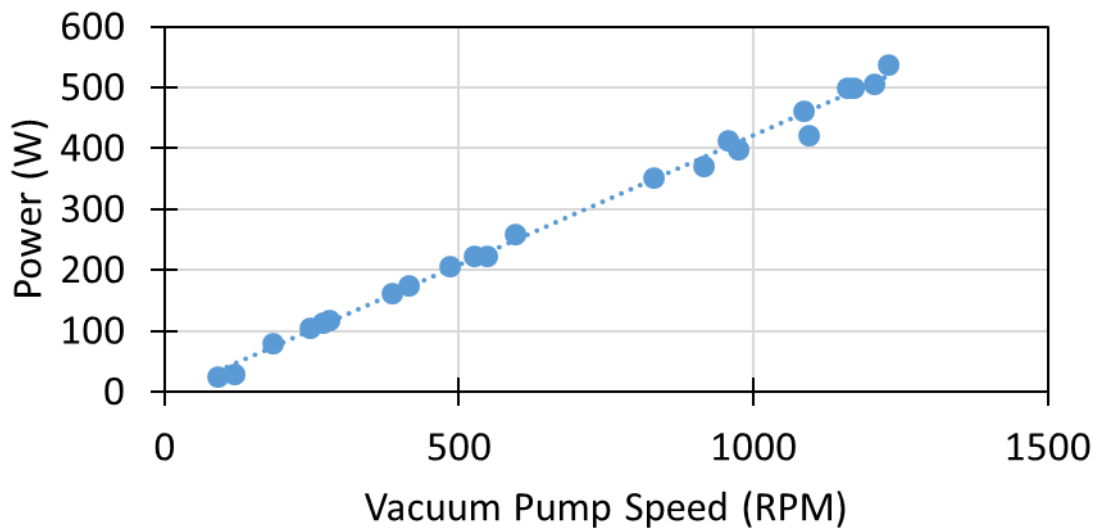
Figure 5-27: Vacuum pump power input as a function of vacuum pump speed.

Figure 5-28 shows the pressure drop of the vacuum pump as it reaches a maximum vacuum pressure for a 2 L container open and closed to atmosphere. Measurement uncertainty of the vacuum pressure was 2.25%. The vacuum pump is seen to reach an equilibrium vacuum pressure within 5 seconds for a closed vacuum container. A larger vacuum container would change this time, but the trend would be similar. Pumping the vacuum with the tank open represents an 11%

savings relative to a closed tank; it is important to note that the valve on the tank was small so

the open tank still displayed a vacuum pressure of -4 psi in the vacuum tank.
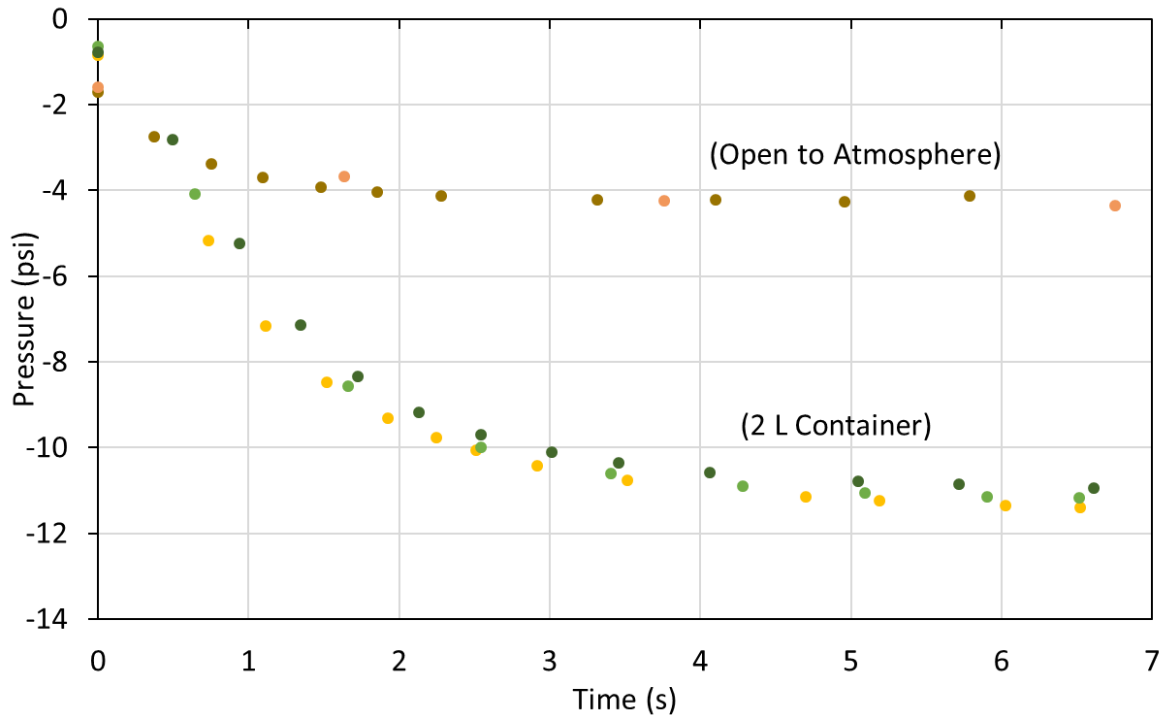
Figure 5-28: Vacuum pressure as a function of time required to reduce the pressure in a 2 L container open to atmosphere and closed.

5.11 Combined Parasitic Losses

Torque values for both pumps are shown as a function of engine speed in Figure 5-29. Water

pump torque starts low and increases as a function of engine speed squared to a maximum value

of 2 N-m at 3000 RPM while the vacuum pump torque raises very rapidly to 4 N-m and remains

constant over the entire range of engine speeds.

Note that Figure 5-29, and all following figures, use engine speed, rather than pump speed

so that the pumps values can be compared against the engine. These engine speed equivalents

were calculated as follows: 1) The vacuum pump is driven by the camshaft and runs at half of the

engine speed, 2) The water pump is driven by the serpentine belt and a pulley that is smaller than the crankshaft pulley; this causes the pump to run at 1.6 times the engine speed.
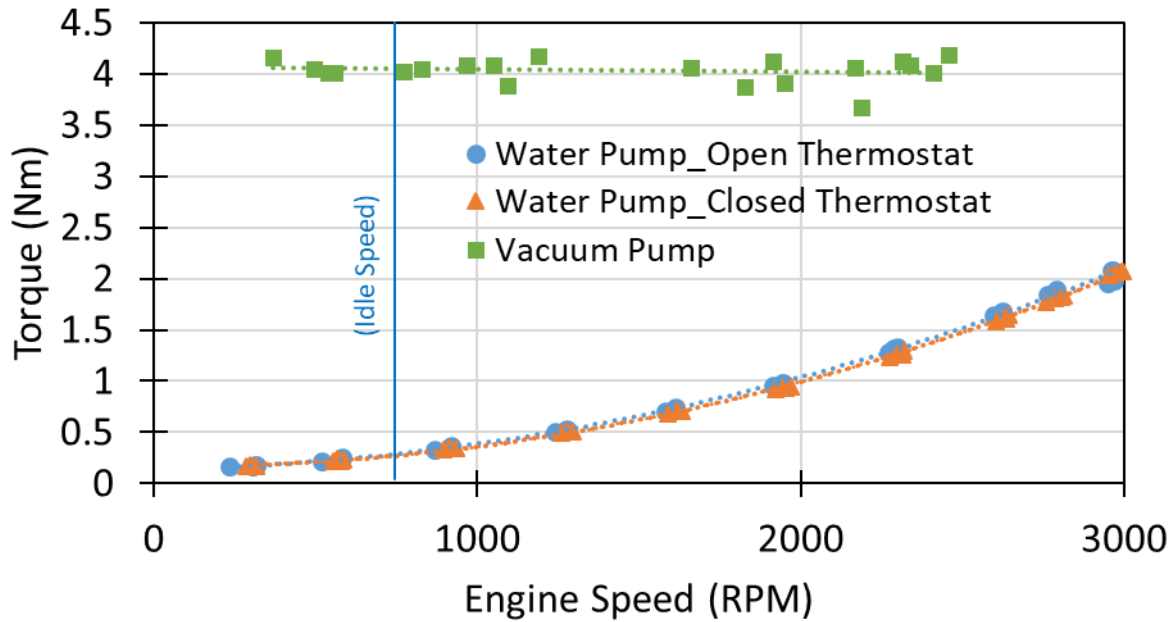
Figure 5-29: Shaft torque required by the vacuum and water pumps as a function of engine speed.

Figure 5-30 displays the power requirements of the pumps as a function of engine speed. The vacuum pump power is seen to increase linearly with the engine speed while the water pump power increases with engine speed cubed. The vacuum pump draws more power off the engine than the water pump at speeds below 2300 RPM. Extrapolating the vacuum pump power to higher speeds, and summing the pump power requirements for the maximum engine speed of 2900 RPM shows the maximum power consumed by the pumps to be 1675 W.

The data collected here does not indicate the flow rate required to cool the engine or the pumping capacity needed by the vacuum pump; therefore, the minimum power required to operate the engine has not been determined, only the amount of power currently being used by the two pumps.
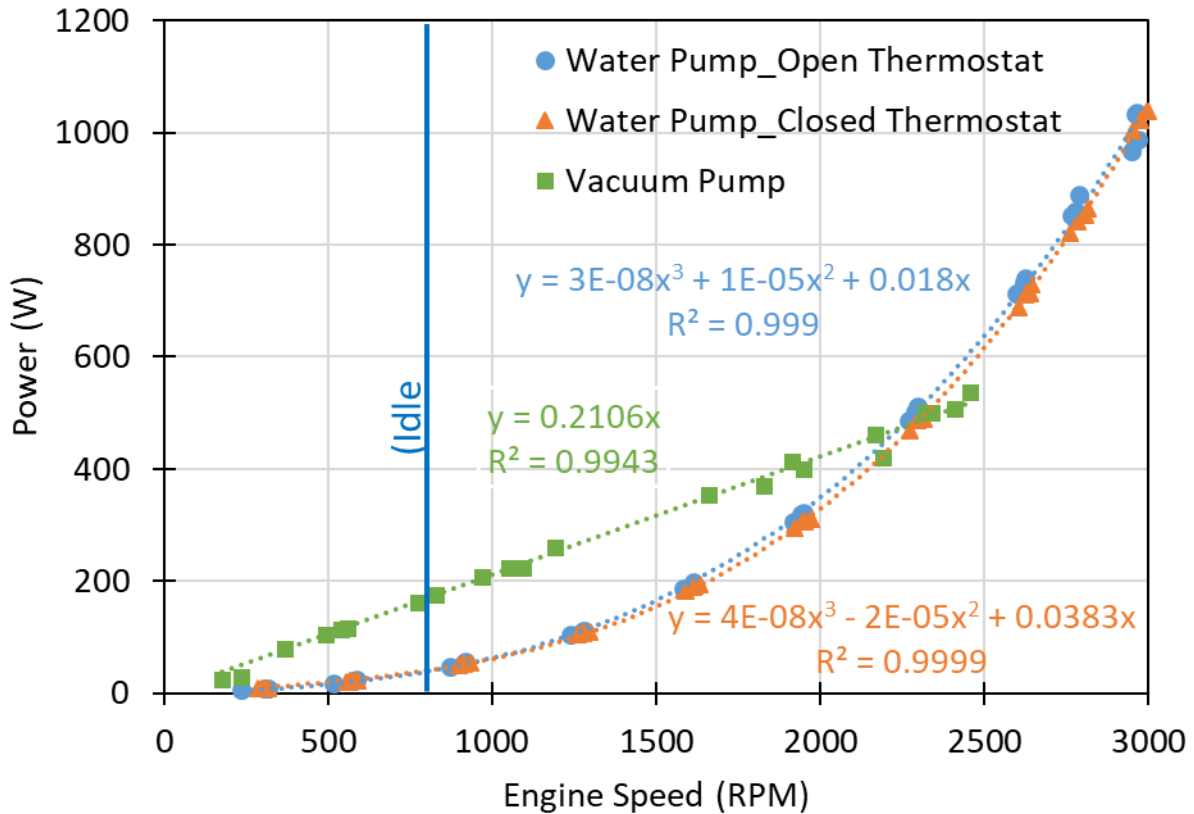
Figure 5-30: Shaft power required by the vacuum and water pumps as a function of engine speed.

The curve fit for the vacuum pump power from Figure 5-30 was compared against the power of the power ratings for the Cummins 2.8 L engine for 25%, 50%, 75%, and 100% of the maximum engine load conditions (See Cummins data sheet in Appendix F.). Figure 5-31 shows the percent of engine power consumed by the vacuum pump as a function of engine speed; individual curves represent the percent of engine power consumed at the stated engine loads.

For example, if the engine is run at 2000 rpm and 100% load (maximum fuel flow rate), 0.50% of the engine power is consumed by the vacuum pump. If the engine is run at the same engine speed and 25% load (25% of maximum fuel flow rate at 2000 RPM), then 2.25% of the engine power is consumed by the vacuum pump.
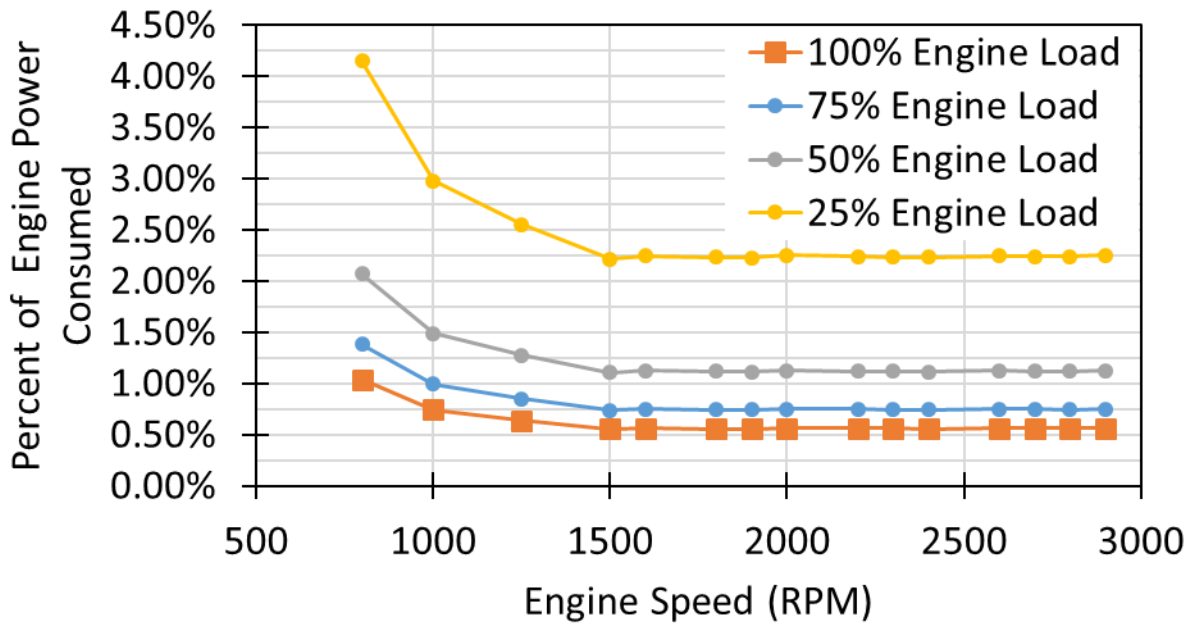
Figure 5-31: Percent of engine power consumed by the vacuum pump as a function of engine speed. Different curves represent different engine fuel load conditions.

The vacuum pump consumes the largest percentage of power from the engine at low engine speed and low load. This percentage decreases then remains constant after 1500 RPM (which is where the 2.8 L engine reaches peak, and constant torque for the rest of the engine speed range). This trend is explained by the fact that the vacuum pump torque is nearly constant at 4 N-m, which constitutes a large portion of the engine power at low speeds, but a constant percentage once the engine hits peak/constant torque.

The curve fit for the water pump power from Figure 5-30 was compared against the power of the 2.8 L engine for 25%, 50%, 75%, and 100% of the maximum engine load conditions (See Cummins data sheet in Appendix F.) to yield values for the percent of engine power consumed at varying speeds and loads. These percentages of pump power to engine power are shown as a function of engine speed in Figure 5-32. The different curves show the percent of engine power consumed by the pump compared to the engine power at the stated loads.
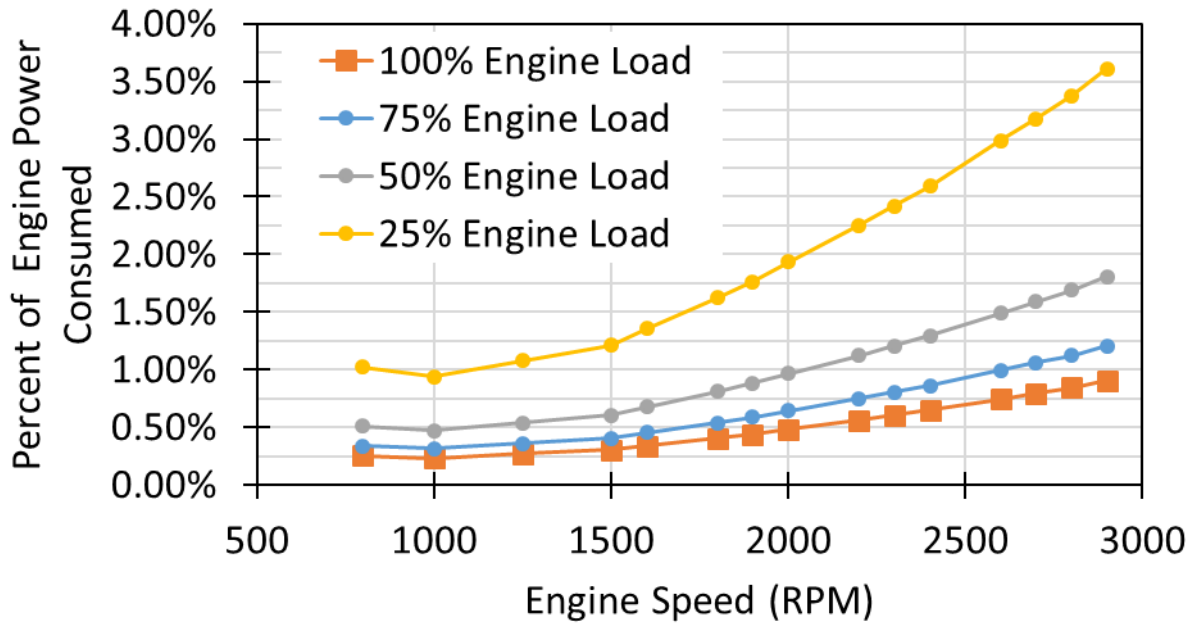
Figure 5-32: Percent of engine power consumed by the water pump as a function of engine speed. Different curves represent different engine fuel load conditions.

The percentage of engine power consumed by the water pump increases slowly until the engine hits 1500 RPM then it increases more quickly. The water pump consumes the largest percentage of power from the engine at high engine speeds and low loads.

A common trend between both pumps is that running the engine at a low load dramatically increases the fraction of power consumed by the pumps compared to the engine power. This means that the most power can be saved by removing the pumps if the vehicle is predominantly used in a low-load drive cycle. Most vehicles operate at different loads and speeds continuously during operation. To evaluate the total fuel improvement that could be realized during a real drive event, the pump power curves were compared to four independent drive cycles [12]:

1. FTP Transient: Simulates both urban and freeway driving, and it is used for emissions certifications in the United States.

68

2. AVL 8-Mode Heavy Duty Cycle: Steady state test designed to mirror the FTP test.

3. Low Load Cycle: Represents real-world urban tractor and vocational vehicle operations characterized by low engine loads.

4. Constant Speed, Variable Load (CSVL): Transient test cycle developed by the EPA for constant-speed engines. (Not used in emissions regulations)

Heavy duty engine tests cycles were chosen for analysis because they are performed with an engine dynamometer and specify % speed and % load data that could easily be applied to the 2.8 L engine. Efficiency improvements were calculated for each cycle; only the FTP cycle is shown for visualization.

Figure 5-33 demonstrates the engine power as a function of time for the FTP test. Total engine power for the 2.8 L engine is shown in black and corresponds to the axis on the left side of the plot. The orange and red data displayed on the plot represent the vacuum pump power and water pump power at the same points in the FTP test; these data correlate to the right axis, which was altered to be 10 times smaller than the left axis, in order to highlight the pump power trends.

Integrating under the curves and summing the values yields the total work produced by the engine and consumed by the pumps. Using Equation (2-1), an increase in the relative brake fuel conversion efficiency for the engine was calculated to be 2.9% for the FTP Transient cycle with the pumps removed. This relative efficiency improvement compares the increase in power of the engine without pumps to the original engine power with the pumps.
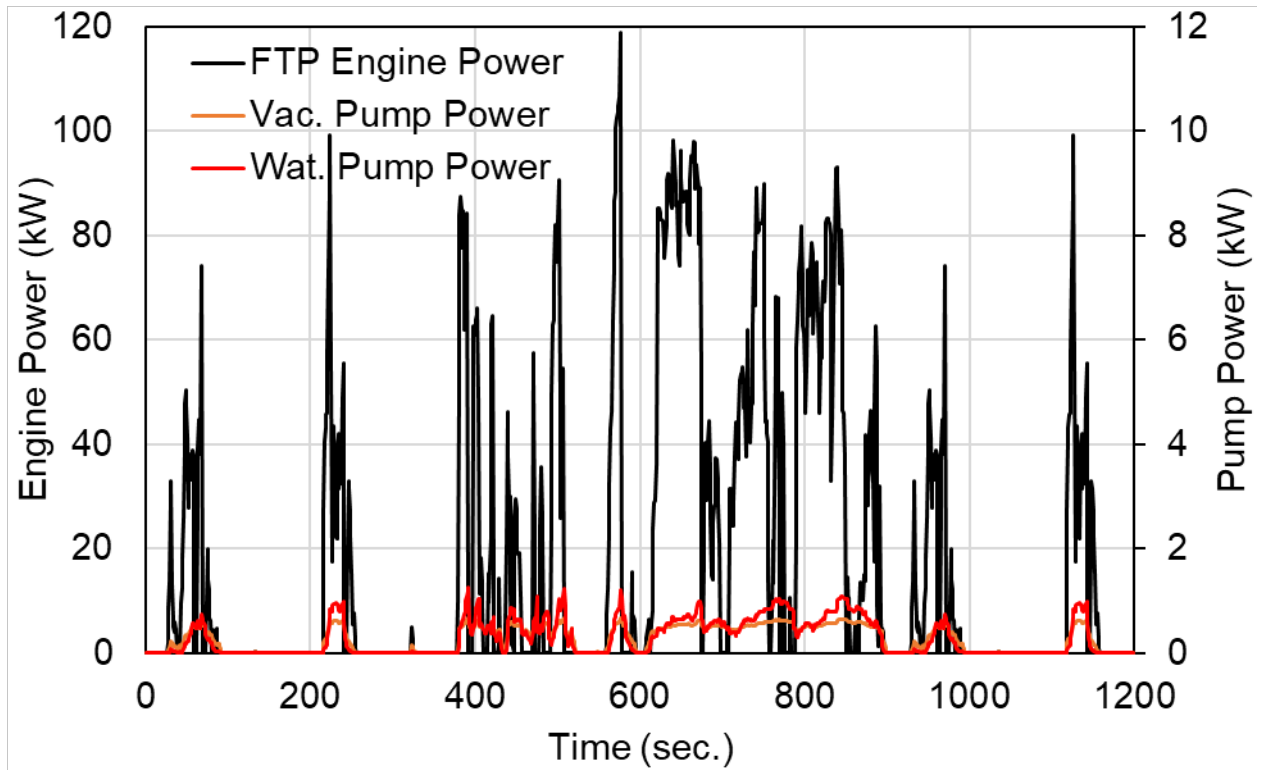
Figure 5-33: Engine power load for the FTP cycle and corresponding power consumption of the water pump and vacuum pump. (Note that pump power is shown on a scale 10 times smaller than engine power in order to display trends)

These findings can be further refined by calculating the absolute brake fuel conversion efficiency improvement, η_{abs}, by comparing the work consumed by the pumps, W_{pumps}, to the total theoretical fuel work, $W_{fuel,total}$, using Equation (5-14).

$$\eta_{abs} = \frac{W_{pumps}}{W_{fuel,total}}$$

(5-14)

This calculation demonstrated a 1.0% absolute fuel efficiency improvement; this means that an engine with a brake fuel conversion efficiency of 35% would be increased to 36%, when operating under the FTP cycle.

Three other cycles were analyzed to determine the range of potential efficiency improvements based on other drive cycles. The first two cycles test higher loads, while the latter two test lower loads. A brake fuel conversion efficiency of 35% was selected as a baseline to demonstrate the improvements of the engine without the water pump and vacuum pumps. These data are shown in Table 5-2.

Table 5-2: Relative and absolute brake fuel conversion efficiency improvements possible for various drive cycles by removing the vacuum and water pumps from the Cummins 2.8 L engine.

Drive Cycle	Brake Engine Efficiency with Pumps (η_{b,w_p})	Brake Engine Efficiency without Pumps (η_{b,wo_p})	Relative Fuel Efficiency Improvement (η_{rel})	Absolute Fuel Efficiency Improvement (η_{abs})
AVL 8-Mode	35.0%	35.8%	2.4%	0.8%
FTP	35.0%	36.0%	2.9%	1.0%
Low Load Cycle	35.0%	36.6%	4.5%	1.6%
CSVL	35.0%	36.7%	4.9%	1.7%

A range of 0.8% to 1.7% absolute efficiency improvement can be achieved by removing the pumps from the engine and powering them with a regenerative source. The AVL 8-Mode and FTP cycles show smaller pump parasitic losses because the cycles utilize higher average engine loads. A conservative estimate shows that removing the pumps would save 1.0% of the fuel, except in rare cases when operating at very high loads for extended portions of time. While 1% is a small number for one vehicle, normalizing this across the vast number of vehicles and corresponding 142 billion gallons of fuel consumed in the United States each year [13], shows the potential to reduce fuel consumption by 1.42 billion gallons annually.

Both the Low Load Cycle and CSVL are characterized by high engine speeds and low loads; This type of a drive cycle would be seen more in cases when a vehicle is travelling at a constant

speed and low load the majority of the time as opposed to the more stop-and-go FTP and AVL 8-Mode drive cycles. Lower load cycles showed the potential to increase absolute brake fuel conversion efficiency by up to 1.7%. This is more than a 0.5% increase over the other drive cycles. This demonstrates that removing the pumps will make a larger difference for vehicles that normally operate at low loads. One optimal application might be long-haul semi-tractor trailer trucks that travel large distances each year on the freeway.

The real world implications of these results can be demonstrated by applying the FTP 2.9% relative efficiency improvement (which correlates to a 1% absolute efficiency improvement) to a car that currently achieves 33 mpg. The resulting fuel economy with the vacuum pump and water pump removed (powered by a regenerative source such as exhaust or braking) would be 34 mpg. Repeating this calculation for the same vehicle on the Low Load Cycle would yield a 34.5 mpg vehicle.

6 SUMMARY AND CONCLUSIONS

A diesel engine test cell has been commissioned with a Cummins 2.8 L diesel engine connected to an AC motoring dynamometer. The auxiliary coupling, cooling, intake and exhaust, fuel, and controls/data acquisitions systems are fully operational. Power ratings of key components are outlined in Figure 5-9 and Table 5-1; the test cell has been demonstrated on the 2.8 L diesel engine up to a brake power of 50 kW, and is designed to run the current engine at 110 kW. The bill of materials, applicable drawings, and wiring diagrams can be referenced in the Appendices.

The test cell has been used for ICE class instructional labs that measure brake engine speed, torque, power, fuel consumption, and emissions. Diesel engine operating instructions have been developed, tested, and are included in Appendix G. Additionally, laboratory instructions have been developed and used to run two separate lab experiments for 40 students. The laboratory instructions are included in Appendix H. and are complete with sample data taken from the labs. This data can be used in the future in the case that the lab cannot be physically run; it can also be used to benchmark future engine performance against initial operating performance.

The parasitic losses of the vacuum pump and water pump have been measured. These results have been analyzed to reveal power trends for the respective pumps. The respective pump parasitic power requirements have been compared against various drive cycles to understand the overall potential improvement in brake fuel conversion efficiency of the engine by removing the pumps. Conclusions from the parasitic loss results are as follows:

1. The water pump torque increases proportional to engine speed squared. This finding suggests that fluid flow through the engine and radiator can be modelled as minor losses

of fluid flowing around restrictions in a pipe, or major losses under turbulent flow conditions in a pipe. Water pump power consumption increases proportional to engine speed cubed.

2. Vacuum pump torque was measured and found to be nearly constant at 4 N-m for all vacuum pump conditions tested. The vacuum pump power consumption increases linearly with engine speed.

3. The percent power consumed by the pumps with regards to engine power has been demonstrated for various engine loads and speeds. (See Figure 5-31 and Figure 5-32)

4. Finally, pump power consumption has been applied to 4 heavy duty engine drive cycles and relative and absolute fuel conversion efficiencies have been calculated. Relative brake fuel conversion efficiency improvements possible by removing both pumps range from 2.4% to 4.9%. Absolute brake fuel conversion efficiency improvements possible by removing both pumps range from 0.8% to 1.7%. Efficiency improvements are maximized for vehicles operating at low engine loads and high engine speeds.

REFERENCES

[1] EPA, NHTSA, "2017 and Later Model Year Light-Duty Vehicle Greenhouse Gas
     Emissions and Corporate Average Fuel Economy Standards"," Federal Register, 2010.

[2] Government, "Federal Register 06576," 2017.

[3] CNBC, "Trump Administration rolls back plans to raise fuel economy standards," 02 08
     2018. [Online]. Available: https://www.cnbc.com/2018/08/02/trump-administration-rolls-
     back-plans-to-raise-fuel-economy-standards.html .

[4] F. Economy.gov, "fueleconomy.gov," [Online]. Available:
     https://www.fueleconomy.gov/feg/atv.shtml. [Accessed 2020].

[5] J. P. R. Shutty, "Advanced Thermal Management Strategies," *SAE,* vol. 36, no. Fig 19, p.
     542, 2013.

[6] R. A. D. Chalgren, "Light Duty Diesel Advanced Thermal Management," *SAE Intl.,* vol.
     01, p. 2020, 2005.

[7] R. M. S. N. R. Babu, "Electrical Operated Fan for Cooling System on Agricultural
     Tractors," *SAE International,* vol. 26, p. 0079, 2019.

[8] M. D. B. K. Y. Lyu, "A Study of Vehicle Fuel Economy Improvement Potential by
     Optimization of the Cooling and Ancillary Systems of a Heavy Duty Engine," *SAE
     International,* vol. 01, p. 1772, 2007.

[9] D. M. J. Bitsis, "Optimization of Heavy Duty Diesel Engine Lubricant and Coolant Pumps
     for Parasitic Loss Reduction," *SAE International,* vol. 01, p. 0980, 2018.

[10] N. Anandakumaran, "Development of an Electrcally Operated Vacuum Pump," *SAE
     International,* vol. 28, p. 1772, 2007.

[11] D. Scopacasa, "Effects of Supplemental Vacuum Production to Support Pump," *SAE
     International,* vol. 01, p. 2528, 2014.

[12] DieselNet, "Dieselnet.com," [Online]. Available:
     https://dieselnet.com/standards/cycles/index.php#us-hden. [Accessed 2020].

[13] E. I. Administration, "eia.gov," [Online]. Available:
     https://www.eia.gov/tools/faqs/faq.php?id=23&t=10.

APPENDIX A. BILL OF MATERIALS FOR ENGINE SETUP

The following tables outline the parts purchased, or designed in order to furnish the engine

with all auxiliary systems necessary to run. Each system is displayed in a separate table for

clarity.

Table A-1: Bill of Materials for Engine Coupling System

Category	Part Name	Qnty	Supplier	Supplier P/N	Cost ($)
Coupling	SAE 11.5 Modified Flywheel	1	PML	N/A	200
Coupling	PH-131 Bolt Ring	1	Kaman Ind.	0-11251	568.06
Coupling	Paraflex Element (PH131)	1	MROSupply.com	PH131	235.78
Coupling	Px110 Para-Flex Flange	1	Kaman Ind.	0-10607	338.57
Coupling	2.5" Taperlok Bushing (2517)	1	Kaman Ind.	0-3479	30.82
Coupling	2.5" Keyed Shaft	1	PML	N/A	130
Coupling	HBM to 2.5" shaft adapter	1	Machine Service Inc (MSI)	669026-58	277.43
Coupling	HBM T40B Torque Transducer	1	HBM		w/ Dyno
Coupling	3/8x16x2" Bolts/washers	1 (8 pack)	Projects Lab	N/A	5.52
Coupling	M14x2mm Socket Head Screws	1 (8 pack)	McMaster Carr	91290A720	7.8
Coupling	M14 Socket Head Lock Washer	1 (8 pack)	Mcmaster Carr	94241A580	4.5
Coupling	5/8" Keyway (foot)	1	Mcmaster Carr	98491A206	15.45
Coupling	Rear Motor Mount (5/16" Steel)	1	Student Built	N/A	135
Coupling	Front Engine Mount (5/16" Steel)	2	Student Built	N/A	189
Coupling	Driveline Guard (1/8" Steel)	1	Student Built/PML Bent	N/A	150

Table A-2: Bill of Materials for Engine Coolant System

Category	Part Name	Qnty	Supplier	Supplier P/N	Cost ($)
Coolant System	Plate Heat Exchanger	1	Thermal Transfer Systems	CB110AQ-20L	1473.76
Coolant System	1" Solenoid Valve	1	US Solid	JFSV00003	45.99
Coolant System	Cummins Thermostat (stock)	1	Included w/Engine	N/A	0
Coolant System	1" M-NPT Nipple (6 in long/Aluminum)	1	Etsy: Metal Craft Supplies	None	22.25
Coolant System	1" Weld-on, Aluminum Radiator Cap	1	Speedway Motors	91015708	19.98
Coolant System	Radiator Cap 16 psi	1	Autozone	7016	5.99
Coolant System	Universal Coolant Overflow kit	1	Autozone	BVR-4	9.99
Coolant System	1.625" to 1.5" Silicon Reducer	1	Amazon: HPS	HTSRNBLK-039	19.64
Coolant System	1" Water Hammer Arrester	1	Sioux Chief	1010	20
Coolant System	(3) 2.5" Channel Cable Protector (2)	1	Discount Ramps		199.98
Coolant System	1" Radiator Hose (30 ft)	1	Hose and Rubber		$366.10
Coolant System	1" F-NPT to Hose Barb	5	Hose and Rubber		$366.10
Coolant System	1" F-NPT Tee	1			
Coolant System	3/4" F-NPT Tee	2			
Coolant System	1/2" M-NPT to 1/2" Hose Barb	10			
Coolant System	1" Hose Barb Tee	2			
Coolant System	1/2" Heater Hose (12 ft)	1			
Coolant System	1.5" Radiator Hose (12 ft)	1			
Coolant System	2" F-NPT to 1" F-NPT Reducer	2			
Coolant System	1" M-NPT to 1" Hose Barb	1			
Coolant System	2" F-NPT to 1.5" F-NPT Reducer	2			
Coolant System	1.5" M-NPT to 1.5" Hose Barb	2			
Coolant System	1.5" F-NPT Tee	1			
Coolant System	1.5" M-NPT to 1" F-NPT	1			
Coolant System	2" Hose to 2" Hose adapter	1			
Coolant System	2" Silicon Hose (1ft)	1			
Coolant System	Pipe Thread Sealant (PTFE)	1			

Table A-3: Bill of Materials for Engine Intake and Exhaust System

Category	Part Name	Qnty	Supplier	Supplier P/N	Cost ($)
Intake/Exhaust	Spectre Air Filter	1	Autozone	8132	25.39
Intake/Exhaust	Charged Air Lines Kit	1	DNA Motor Inc	DNA-FMICPPU3ST	126.33
Intake/Exhaust	Charged Air Cooler Type 19	1	FozenBoost	INT000219	188.98
Intake/Exhaust	Exhaust Pipe*	1	Taysom Tire and Auto	None	129.84
Intake/Exhaust	Exhaust Outlet Elbow/V-band clamp	1	Cummins Rocky Mtn	3910993	178.28
Intake/Exhaust	Silicone 3" 45 Degree Elbow	1	DNA Motor Inc	SH-3-45-BL	11.22
Intake/Exhaust	Silicone 3" to 2.5" Reducer	2	Amazon: AC Performance	SP00-200-250_BL	12.99
Intake/Exhaust	Universal Rubbber Exhaust Bracket	1	Autozone or other auto shop	N/A	10

Table A-4: Bill of Materials for Engine Fuel System

Category	Part Name	Qnty	Supplier	Supplier P/N	Cost ($)
Fuel System	10 Gal Fuel Tank	1	Amazon: Super Fast Racing	SU38829	99.69
Fuel System	Fuel Pump 49.4gph	1	O'Reilly Auto Parts	E16116	120.75
Fuel System	Coriolis Flow Meter	1	BYU Engr	RFT9712	0
Fuel System	2.8L Water Separator/Priming Assm	1	Cummins Rocky Mt	5317657	72.99
Fuel System	Springflow 250 Fuel Cooler	1	Utah BioDiesel	Springflow 250	208
Fuel System	9.49 mm Priming Assm Fuel Fittings	2	Araymond: Michael Desrochers	130719	0
Fuel System	7.89 mm Cond Fuel Fitting	1	Araymond: Michael Desrochers	205146	0
Fuel System	7.89 mm NC Male End Form Fitting	1	Araymond: Michael Desrochers	0-19868	0
Fuel System	Inline Fuel Filter (5/16 Inlet/Outlet)	1	O'Reilly Auto Parts	33002	2.7
Fuel System	5/16" Fuel Hose (4')	1	BYU Hardware	N/A	4
Fuel System	3/8" Fuel Hose (8')	1	BYU Hardware	N/A	10
Fuel System	1/4" Fuel Hose (4')	1	BYU Hardware	N/A	4
Fuel System	Non-NPT Fittings and Hose Clamps	3	Hose and Rubber	N/A	15
Fuel System	Various NPT Fittings	10	Hose and Rubber/Checkout room	N/A	15
Fuel System	1/4" Check Valve	1	Amazon	MI1PN8XP2	8.8

Table A-5: Bill of Materials for Engine Controls and Data Acquisition System

Category	Part Name	Qnty	Supplier	Supplier P/N	Cost ($)
Controls/DAQ	NI CRio	1	BYU	NI cRIO-9074	0
Controls/DAQ	Key Switch	1	McMaster-Carr	*Ask Kevin Cole	104.34
Controls/DAQ	Ethernet Cable (75 feet)	1	Amazon: Ultra Clarity Cables	UC075	19.99
Controls/DAQ	16 AWG 2 Cond. Shield Wire (500 ft)	1	Belden	19C3712	182
Controls/DAQ	AC-DC Converter, DIN Rail	1		1254964	0

Table A-6: Bill of Materials for Miscellaneous Lab Components

Category	Part Name	Qnty	Supplier	Supplier P/N	Cost ($)
Controls/DAQ	Fuel Setting Connector USB to RS485	1	JBtek	MH9KB3G52	6.99
Exhaust Overpressure Oil	Oil Catch Can	1	Amazon	MA71P3IW0	18.9
Parasitic Loss Test	LoveJoy L070 0.626 in coupling	1	Wideopendes	N/A	20
Parasitic Loss Test	200L/min Flowmeter	1	Epic Solution	N/A	37.68
Parasitic Loss Test	Jeep Radiator	1	Rocky Mountain Radiator	N/A	130
Testing	1x Transcuder Adapter/Plug, 2-3 Washers	1	Rapid Prototyping and Engr (IN)	CD0416-007	175
Testing	SS rod to make transducer plug	1	Online metals	N/A	30.23
Commissioning	Cummins Starter	1	Cummins	5363153	243.52
Installation	T-slots for floor	1	Grainger	N/A	27
Installation	Metal and Fasteners	1	Hardware Store	N/A	?
Maintenance	Cummins Serpentine Belt	1	1stRock 4x4	3288656	32.99
Maintenance	Oil 15W-40	1	Walmart	N/A	77.32
Maintenance	Antifreeze (least expensive) battery	1	Walmart	N/A	211.85

APPENDIX B. COUPLING ASSEMBLY DRAWINGS

This appendix outlines the coupling components purchased or designed.

- The flexible coupling and flange to shaft adapter were both purchased and supplier documents are included.

- The flywheel was modified to enable connection to the flexible element; a drawing outlining these modifications is included.

- Drawings for designed components (2.5-inch shaft, motor mounts, and driveline guard) are included.

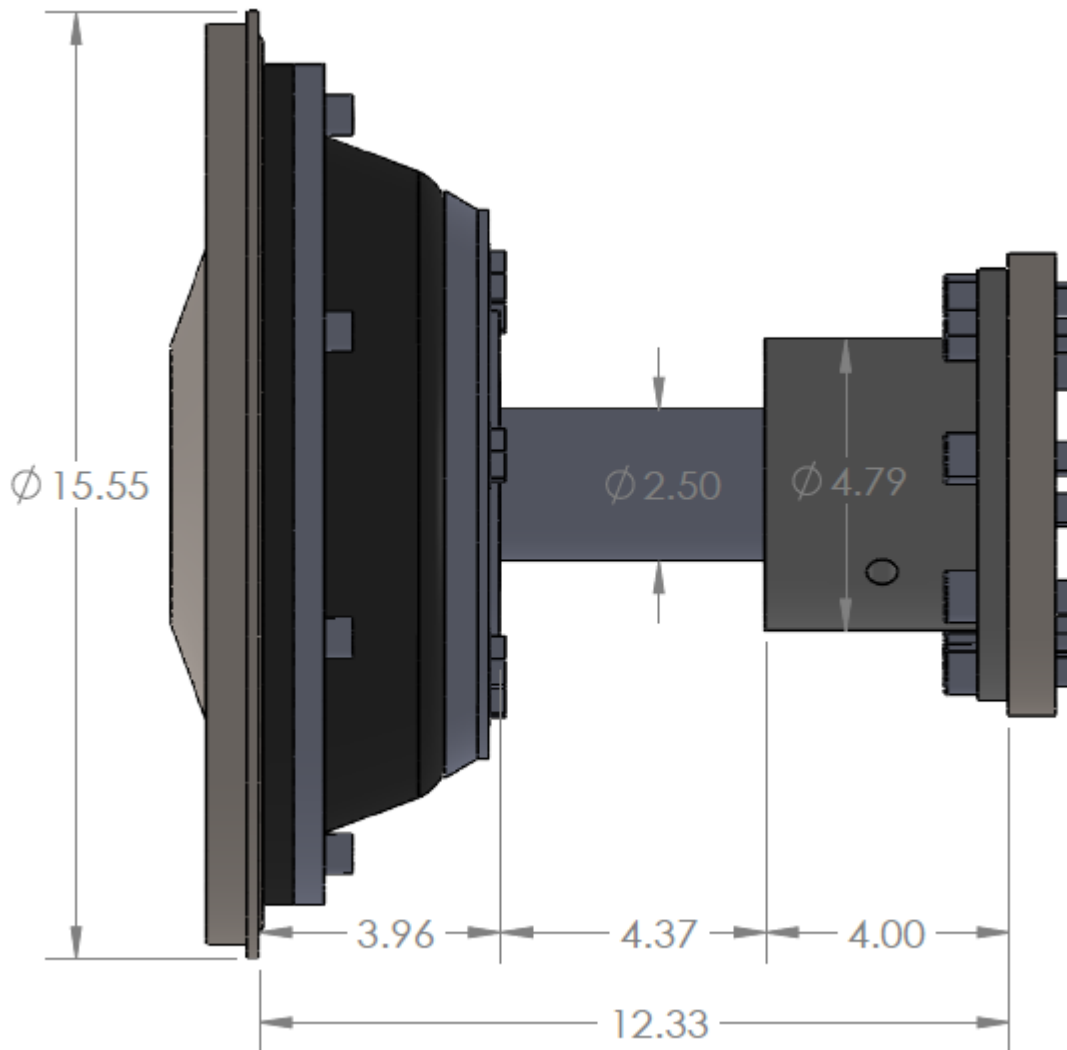**Engine Coupling Assembly: Side-View and Dimensions**

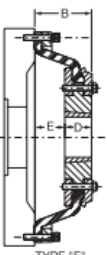Figure B1: Side View of Driveline Coupling Assembly

Flexible Element: Dodge PH-131 (Same as PF-131)

The flexible element is rubber and absorbs vibrations from the engine. It was purchased. Dodge specifications are shown below. Allowable misalignment: 1° angular, 1/16" parallel, 3/16" end float. (See Dodge PT Components Engineering Catalog)
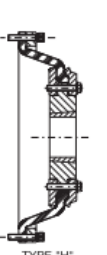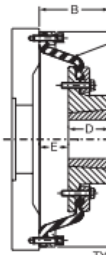
SELECTION/DIMENSIONS
Flywheel, TAPER-LOCK

DODGE®

TYPE "F"   TYPE "H"
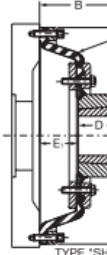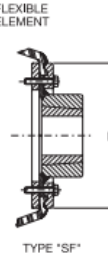SIZES PF87-PF131

TYPE "H"   TYPE "F"
IRON FLANGE AND CLAMP RING   SIZES PF172-PF192

TYPE "SH"   TYPE "SF"
STEEL FLANGE AND CLAMP RING   SIZES PF172-PF252

Coupling Size	Bushing Size	Min. Bore	Max. Bore	HP/100	Torque (In-Lbs)	Max. RPM Gray Iron Flange	Max. RPM Steel Flange	A	B Iron Flg.	B Steel Flg.
PF87	1610	1/2	1-11/16	3.00	1890	6000	6000	9.44	2.69	.....
PF96	2012	1/2	2-1/8	4.50	2835	5230	5230	10.31	2.83	.....
PF116	2517	1/2	2-11/16	7.10	4470	4050	4050	12.31	3.14	.....
PF131	2517	1/2	2-11/16	9.50	5985	3750	3750	13.81	3.70	.....
PF172	3535	1-3/16	3-15/16	23.00	14490	1860	2800	18.31	5.81	6.72
PF192	4040	1-7/16	4-7/16	47.00	29610	1620	2430	20.31	6.56	7.50
PF213	4545	1-15/16	4-15/16	90.00	56700	.....	2130	22.50	.....	9.00
PF252	5050	2-7/16	5-5/16	135.00	85050	.....	1945	26.50	.....	10.81

Coupling Size	Bushing Size	C Iron Flg.	C Steel Flg.	D	E	E1	Weight (Lbs) Less Bushing Iron Figs	Weight (Lbs) Less Bushing Steel Figs	Inertia (Lb-Ft²) Iron Figs	Inertia (Lb-Ft²) Steel Figs
PF87	1610	.....	.....	1.00	1.34	....	9.9	.....	0.6	.....
PF96	2012	.....	.....	1.25	1.58	....	13.5	.....	1.05	.....
PF116	2517	.....	.....	1.75	1.39	....	22.3	.....	2.35	.....
PF131	2517	.....	.....	1.75	1.95	....	33.3	.....	4.35	.....
PF172	3535	7.50	7.00	3.50	2.31	3.12	87.2	77.5	17.49	15.73
PF192	4040	8.63	8.50	4.00	2.56	3.50	128.6	128.6	28.84	28.12
PF213	4545	.....	8.75	4.50	-	4.50	221.2	190.2	74.47	64.36
PF252	5050	.....	9.50	5.00	-	5.81	297.9	260.9	121.79	111.38

PF87 THRU PF252 Part Numbers

| Coupling Size	TAPER-LOCK Flange Std Flange	Iron Flange Type H	Iron Flange Type F	Steel Flange Type SH	Steel Flange Type SF	Bolt Ring Assembly	High Speed Element	T-L Bushing Size
PF87	010603	.....	.....	.....	.....	011247	011227	1610
PF96	010604	.....	.....	.....	.....	011248	011228	2012
PF116	010606	.....	.....	.....	.....	011250	011230	2517
PF131	010607	.....	.....	.....	.....	011251	011231	2517
PF172	.....	011134	011154	010290	010294	011254	011234	3535
PF192	.....	011137	011157	010291	010295	011256	011236	4040
PF213	.....	.....	.....	010292	010296	011259	011239	4545
PF252	.....	.....	.....	010293	010297	011262	011242	5050

Complete coupling consists of: (1) TAPER-LOCK Flange Assembly (as selected), (1) Bolt Ring Assembly, (1) High Speed Element, and (1) TAPER-LOCK Bushing. TAPER-LOCK Bushings must be ordered separately.
See page PT1-34 for Flywheel & Power Take Off housing information. Refer to bushing section PT6-16.

FEATURES/BENEFITS PAGE PT1-17	SELECTION/DIMENSION PAGE PT1-18	MODIFICATION/ACCESSORIES PAGE PT1-79	ENGINEERING/TECHNICAL PAGE PT1-81

PT1-21

84

PT Component
Reference Guide

Couplings

Clutches and Brakes

FLEXIDYNE

Fluid Couplings

TORQUE-TAMER

SELECTION/DIMENSIONS
Flywheel, Bored to Size

DODGE®
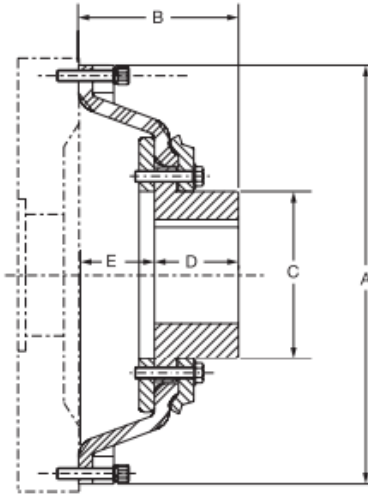
PF87B THRU PF252B Bored-To-Size Flywheel Couplings

Coupling Size	Min. Bore	Max. Bore	HP/100	Torque (In-Lbs)	Max. RPM Steel Flg	A	B	C	D	E	Weight (Lbs)	Inertia (Lb-Ft^2)
PF87B	none	2-1/8	3.0	1890	6000	9.44	3.38	2.94	1.75	1.63	10.5	0.61
PF96B	none	2-9/16	4.5	2835	5230	10.31	3.94	3.69	2.00	1.94	14.3	1.08
PF116B	none	3-1/4	7.1	4470	4050	12.31	4.68	4.94	2.63	2.00	24.3	2.47
PF131B	none	3-15/16	9.5	5980	3750	13.81	5.50	5.44	3.00	2.50	33.7	4.56
PF172B	2-1/4	4-1/2	23.0	14490	2800	18.31	6.81	7.00	3.88	3.13	84.2	16.73
PF192B	2-1/2	6	47.0	29610	2430	20.31	8.44	8.50	5.13	3.50	129.6	32.02
PF213B	2-1/2	6-1/4	90.0	56700	2130	22.50	9.00	8.75	4.69	4.50	188.2	65.76
PF252B	2-7/8	6-7/8	135.0	85050	1945	26.50	10.81	9.50	5.19	5.81	250.9	113.58

PF87 - PF252B Part Numbers

Coupling Size	BS Flange Assembly	Bolt Ring Assembly	High Speed Element
PF87B	010301	011247	011227
PF96B	010302	011248	011228
PF116B	010304	011250	011230
PF131B	010305	011251	011231
PF172B	010530	011254	011234
PF192B	010531	011256	011236
PF213B	010508	011259	011239
PF252B	010509	011262	011242

Complete coupling consists of: (1) BS Flange Assembly, (1) Bolt Ring Assembly, and (1) High Speed Element.

Unless otherwise specified, Size 60-120 BS flanges are clearance fit per

SAE Power Take Off & Flywheel Info.

Coupling Size	Fits Within These SAE Power Take-Off Housings	SAE Flywheel		
		Bolt Circle Diam.	Tapped Holes	
			No.	Size
PF87	6,5	8-3/4	8	5/16-18
PF96	4,3	9-5/8	6	3/8-16
PF116	4,3,2,1	11-5/8	8	3/8-16
PF131	3,2,1,0	13-1/8	8	3/8-16
PF172	0	17-1/4	8	1/2-13
PF192	0	19-1/4	8	1/2-13
PF213	0	21-3/8	6	5/8-11
PF252	0	25-1/4	12	5/8-11

Figure B2: Dodge PH-131 Flexible Element Specifications
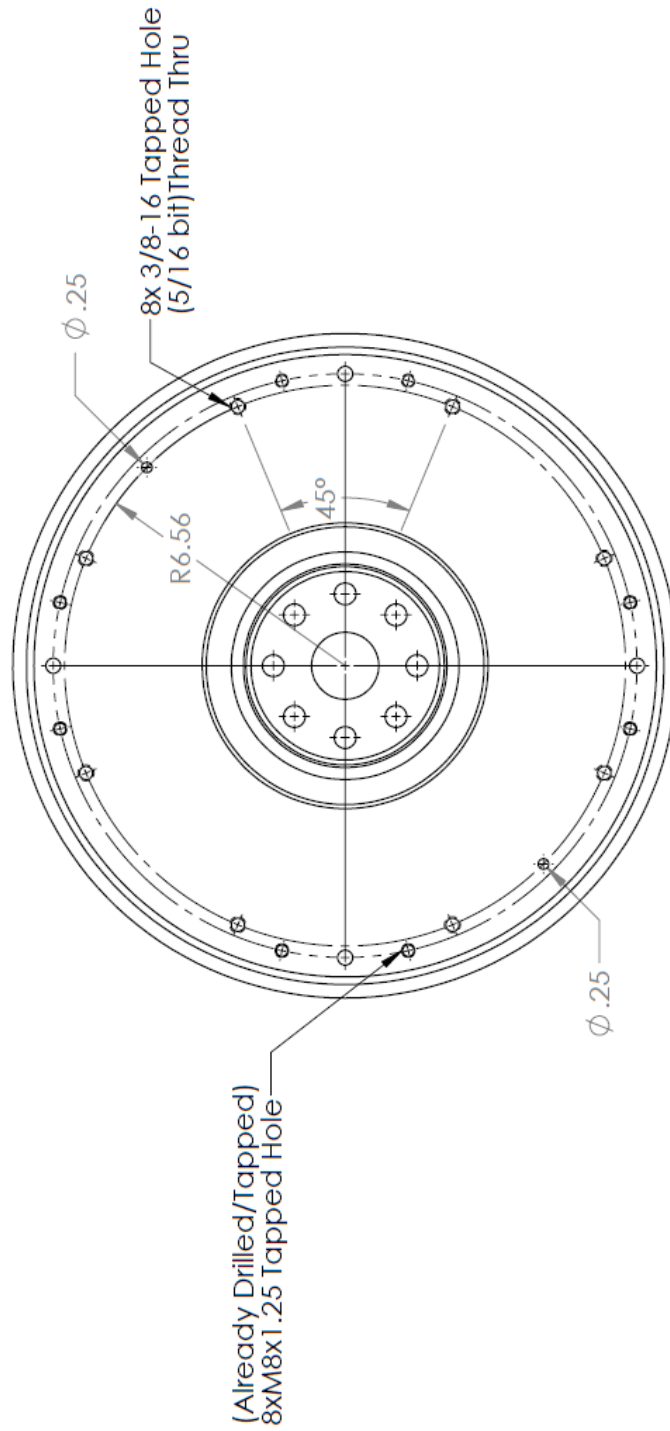
Flywheel Modifications Drawing

Figure B3: Drawing for Flywheel Modifications (SAE 11.5 Modified)

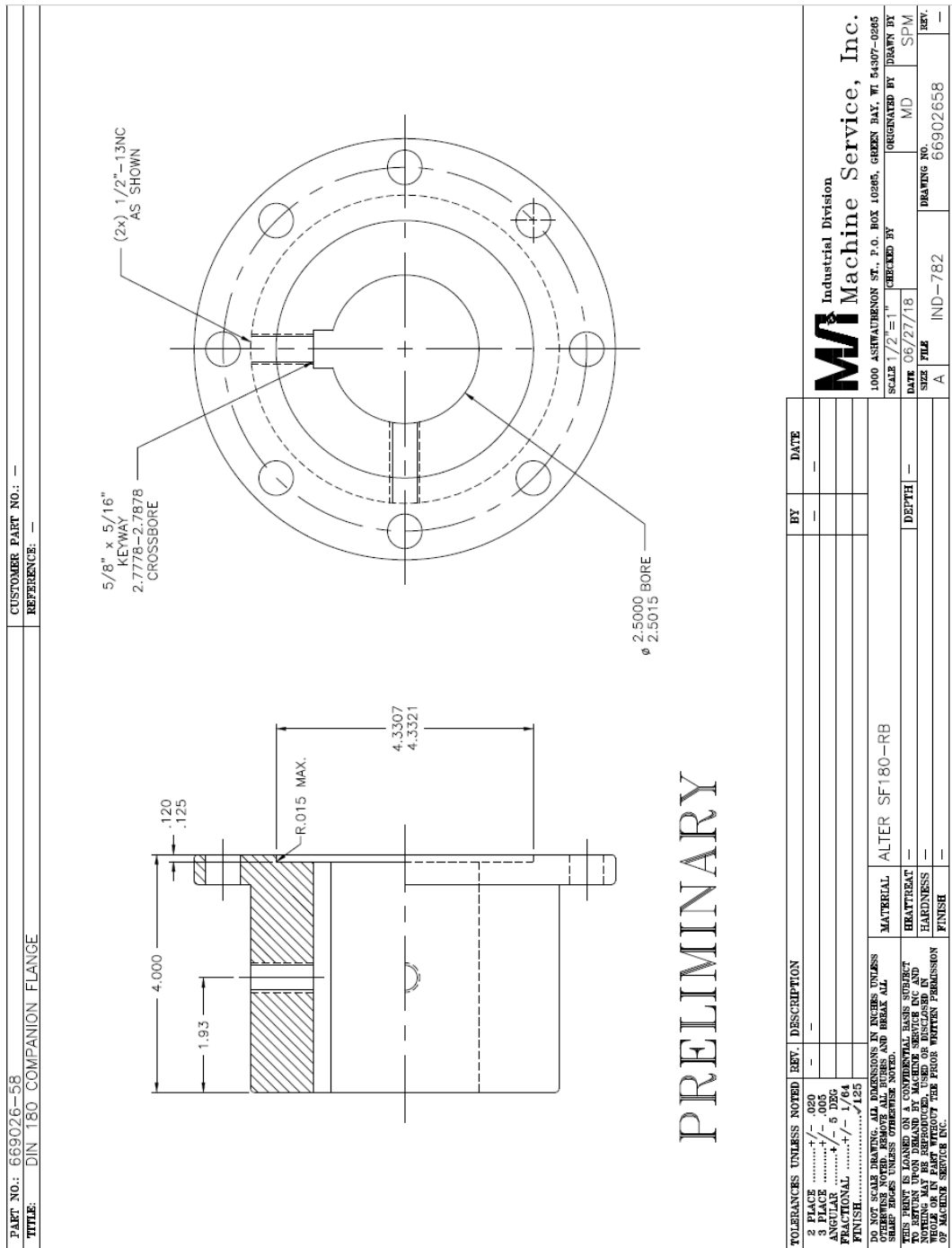**Machine Services Inc. (MSI) Shaft to Flange Adapter**

Figure B4: MSI Shaft to Flange Adapter
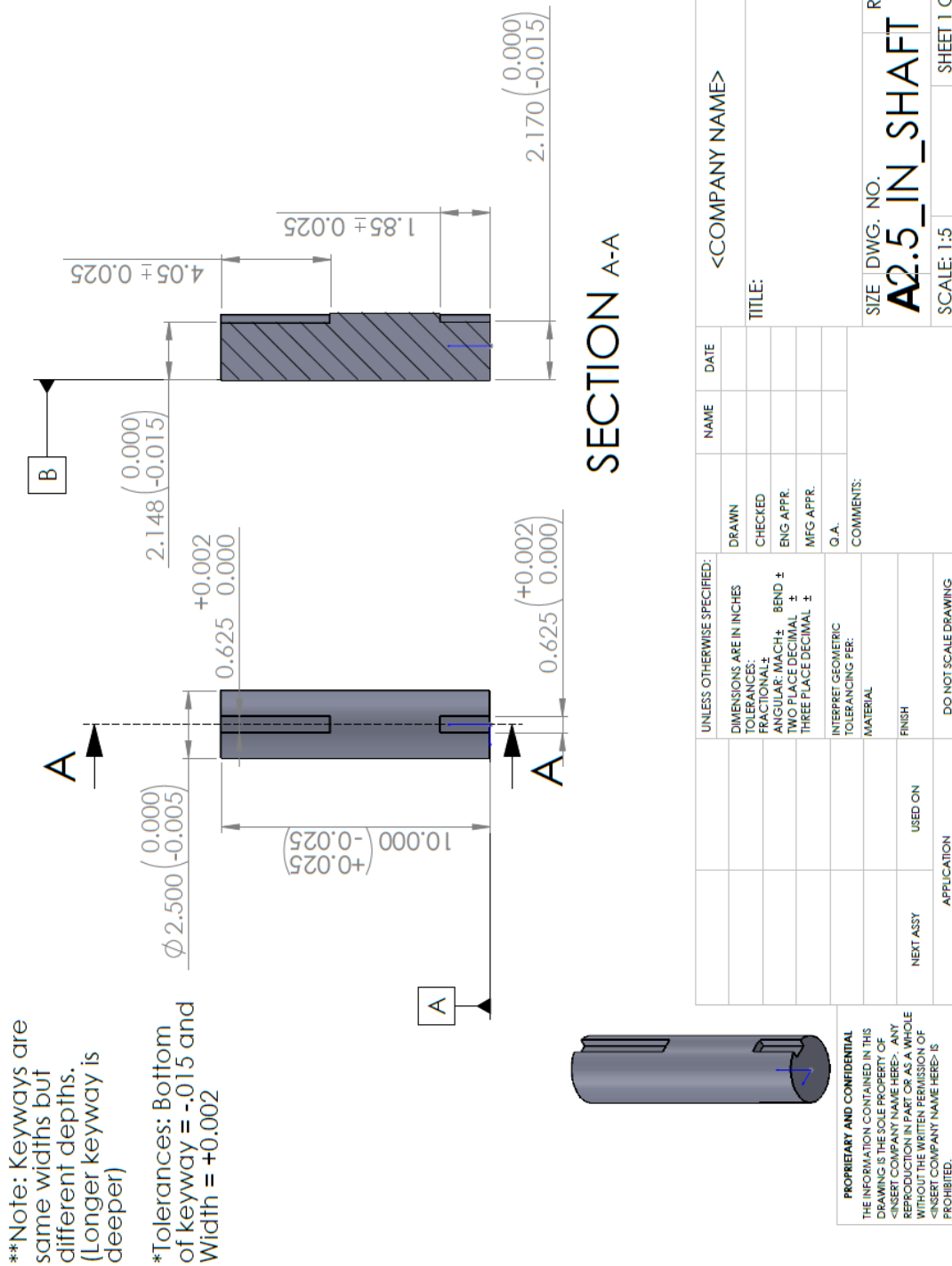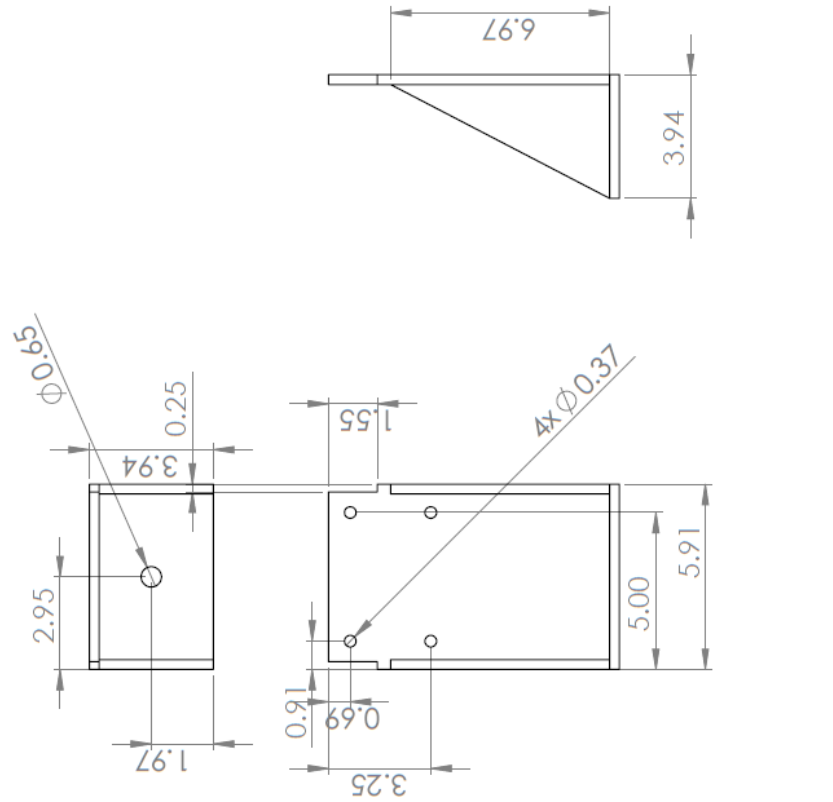
2.5 Inch Custom Designed Driveline Shaft

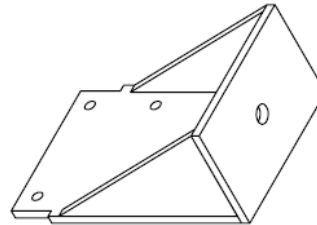Figure B5: Drawing of Driveline Shaft

Front Motor Mounts

Figure B6: Drawing of Front Motor Mounts
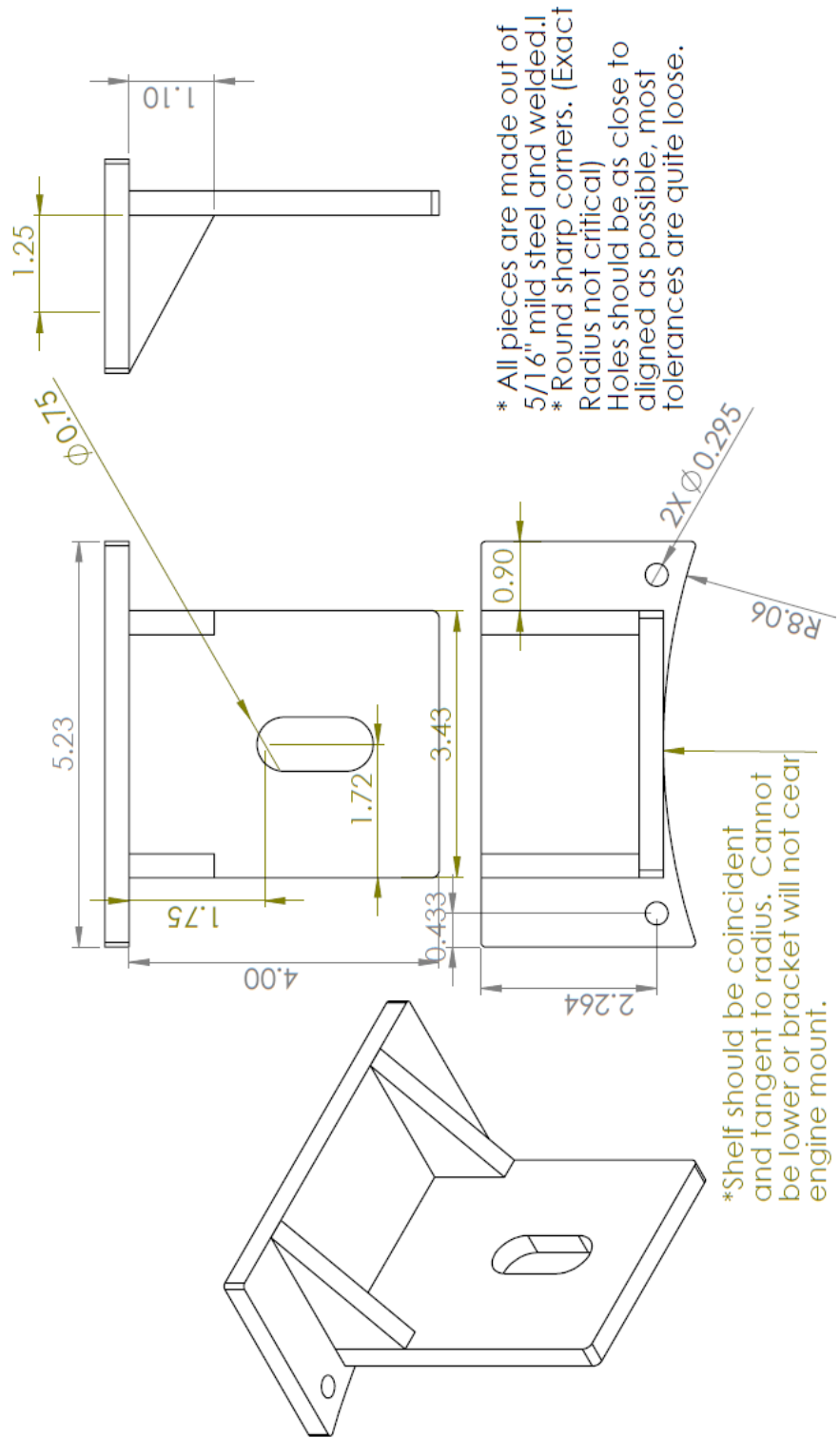
89

Rear Motor Mount Drawing

Figure B7: Drawing of Rear Motor Mounts

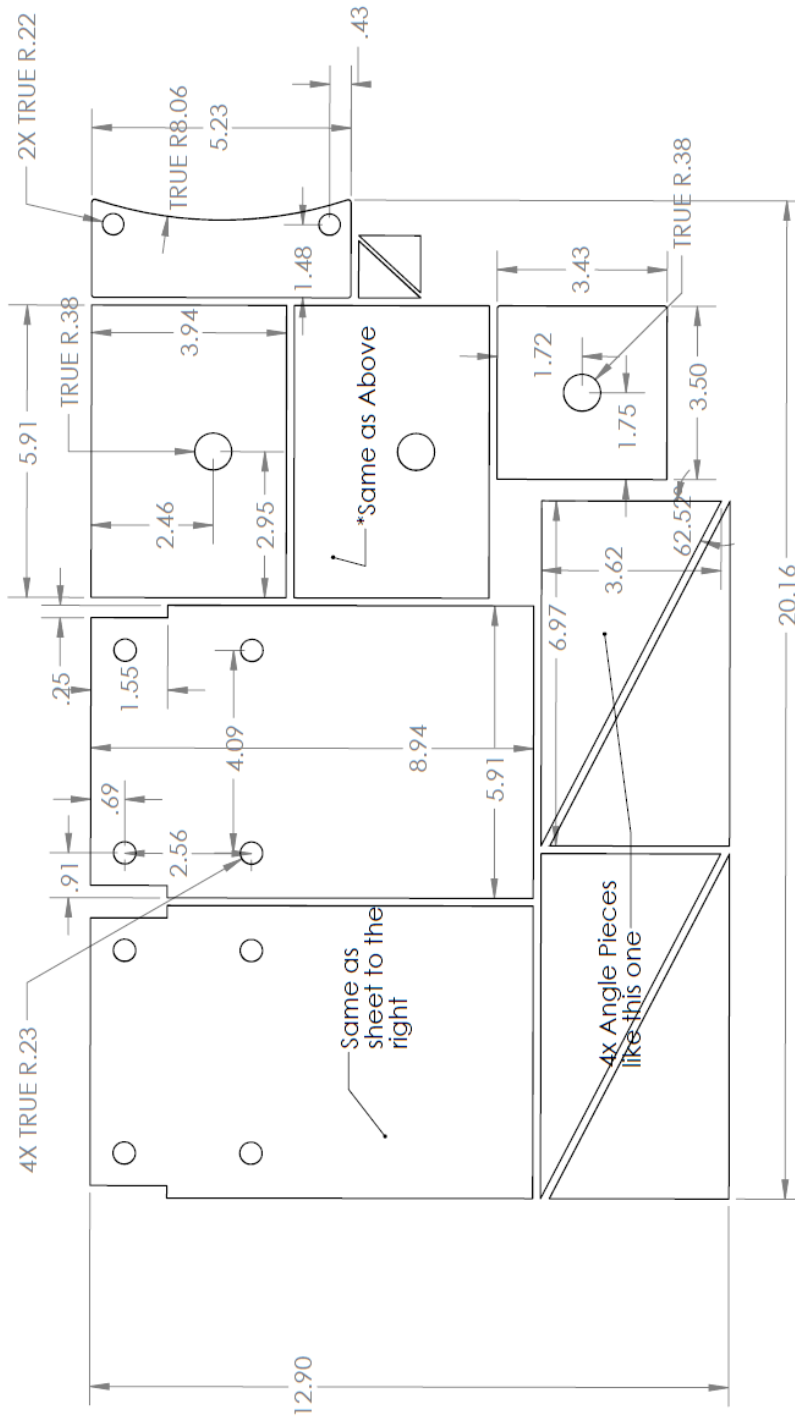**Waterjet Layout for Motor Mounts**

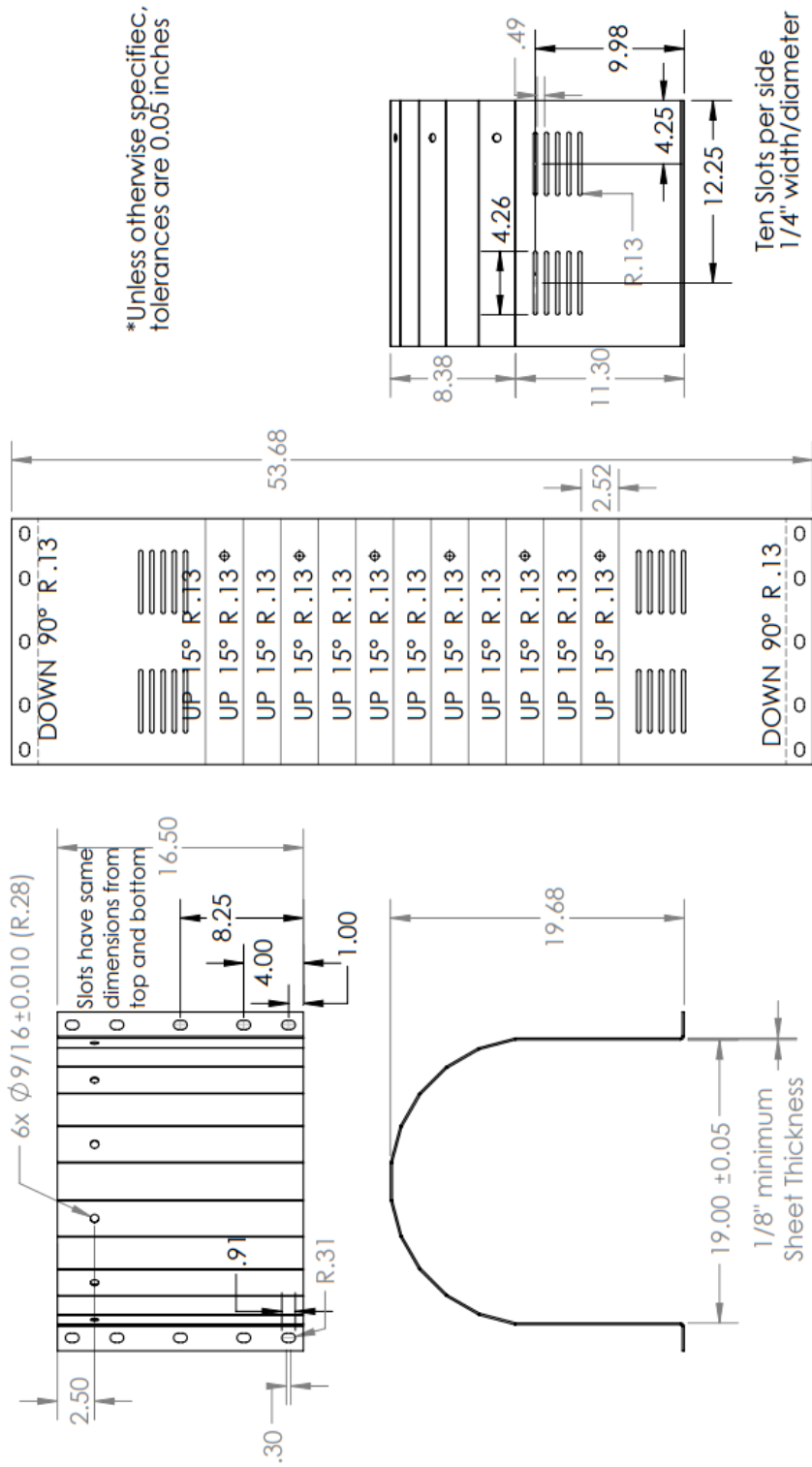Figure B8: Drawing of Motor Mount Water Jet Pattern

Driveline Guard

Figure B9: Drawing for Driveline Guard

92

APPENDIX C. HEAT EXCHANGER SPECIFICATIONS AND DRAWING

Heat Exchanger Specifications from Thermal Transfer Systems (TTS)

Alfa Laval Plate Heat Exchanger Specification

Customer : BYU
Project : 7-20-2018
Item : Item 1   Date   : 8/9/2018

Model: CB110AQ-20L

		Hot Side	Cold Side
Fluid		50.0% Eth.glycol	50.0% Eth.glycol
Volume flow rate	GPM	54.0	12.0
Inlet temperature	°F	202.0	65.0
Outlet temperature	°F	181.7	156.6
Pressure drop	psi	4.71	0.326
Heat exchanged	kBtu/h	485.90	
Density	lb/ft³}	64.6	66.0
Specific heat	Btu/lb,°F	0.858	0.829
Thermal conductivity	Btu/ft,h,°F	0.231	0.237
Viscosity	cP	0.768	1.17

Material plate / brazing	Alloy 316 / Cu
Connection material	Stainless Steel
ConnectionS1 (Cold-out)	Threaded (External)/ 2" NPT (F22) Alloy 316 NPT
ConnectionS2 (Cold-in)	Threaded (External)/ 2" NPT (F22) Alloy 316 NPT
ConnectionS3 (Hot-out)	Threaded (External)/ 2" NPT (F22) Alloy 316
ConnectionS4 (Hot-in)	Threaded (External)/ 2" NPT (F22) Alloy 316 NPT

Pressure vessel code		UL/CRN	
Design Pressure @ -321.000000	Psig	392.	392.
Design Pressure @ 400.000000	Psig	392.	392.
Design Temperature	°F	-320.8/400.0	
Overall length x width x height	in	5 x 8 x 24	
Net weight, empty / operating	lb	45.7 / 55.0	

Figure C1: Specifications for TTS Heat Exchanger
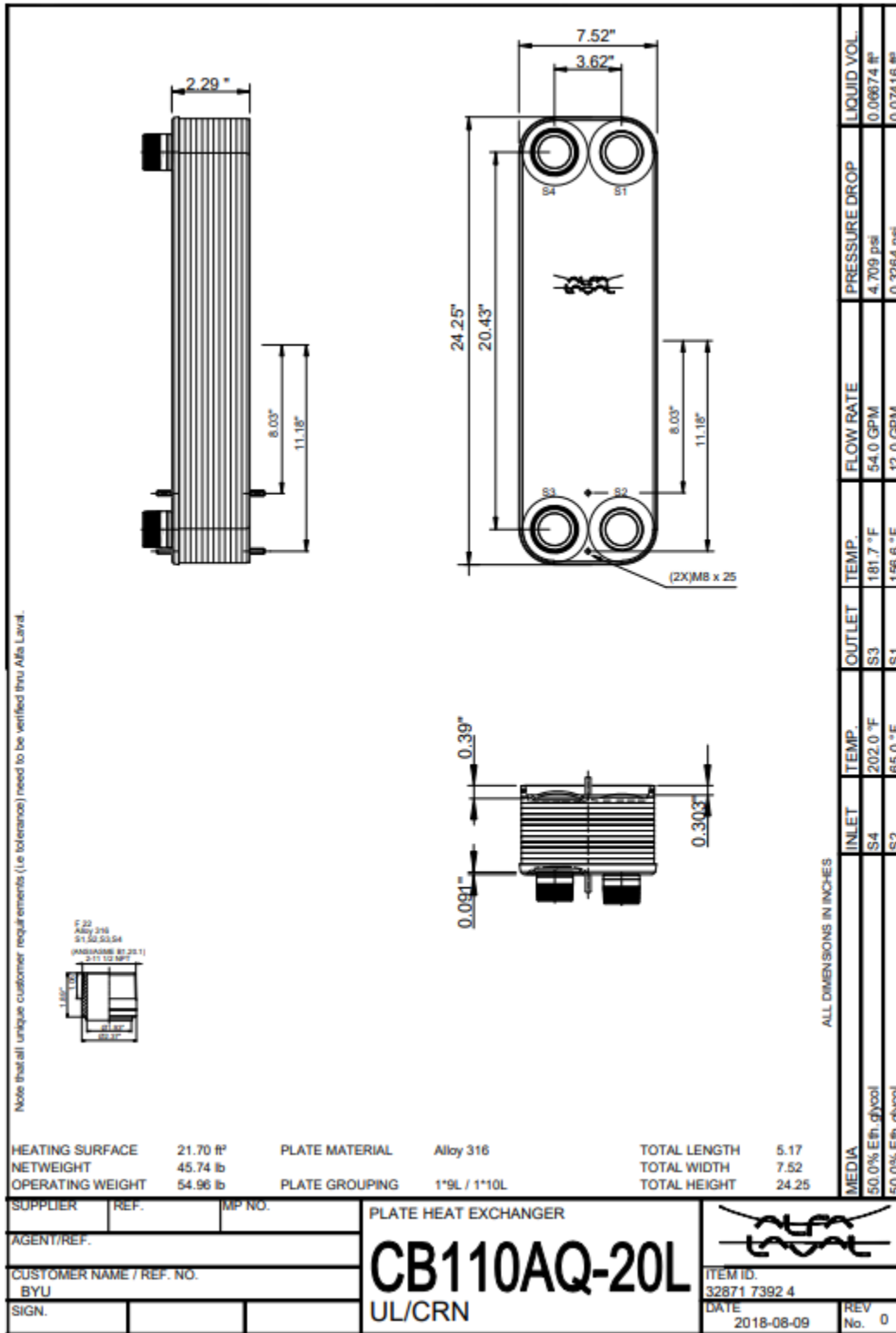
Plate Heat Exchanger Dimensions

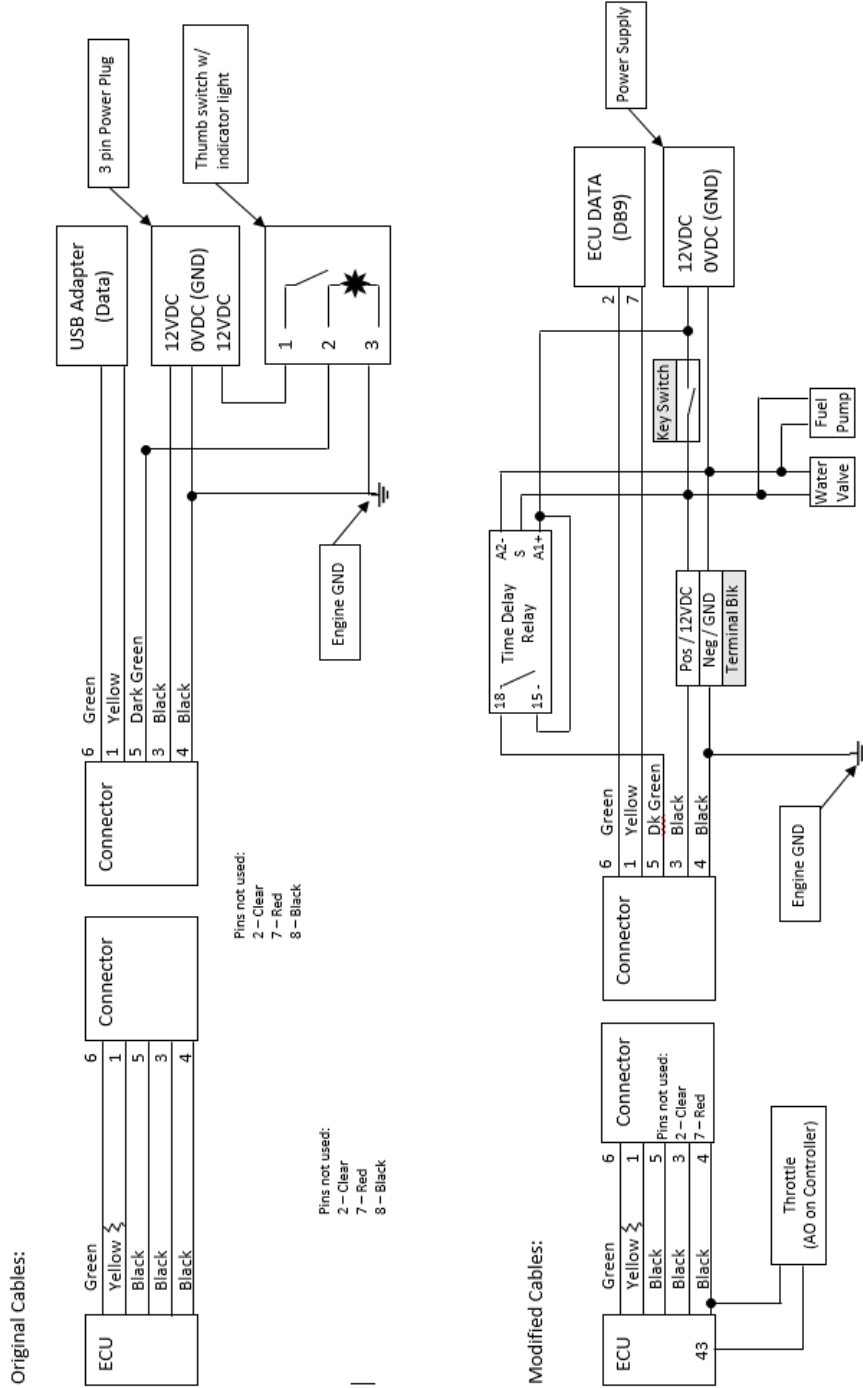Figure C2: Drawing for TTS Heat Exchanger

Figure D1: Wiring Diagram for Controls and Data Acquisition System

APPENDIX E. ENGINE LAB POWER CAPACITY CALCULATIONS

This section explains the calculations behind the power measurements listed in Table 4-1.

Dynamometer

Power capacity comes specified point on the torque curve from the Dynamometer supplier.

Air Intake/Exhaust

Assuming dilute exhaust with air 10:1

$$\dot{V} = \frac{2000 \; scfm}{10} = \frac{200 \; scfm}{0.03531 \; \frac{ft^3}{min}} * \frac{1 \; min}{60 \; sec} = 94.4 \frac{L}{s} * \frac{0.001 \; m^3}{s} = 0.0944 \; \frac{m^3}{s}$$

$$\dot{m} = \rho_{air \, (20°C)} * \dot{V} = 1.204 \; \frac{kg}{m^3} * 0.0944 \; \frac{m^3}{s} = 0.1136 \; \frac{kg}{s}$$

Assuming an A/F = 30:1

$$\dot{m}_{fuel} = \frac{\dot{m}_{air}}{30} = 0.00378 \; \frac{kg}{s}$$

$$\dot{w}_{fuel} = \dot{m}_{fuel} * q_{hv} * \eta_{brake} = 0.00378 \; \frac{kg}{s} * \frac{44000 \; kJ}{kg \; fuel} * 0.35 = 58.3 \; kW$$

Building Cooling Capacity

$$\dot{Q} = \dot{m} * C_p * \Delta T$$

$$\dot{V} = 15 \frac{gal}{min} = 0.00946 \; \frac{m^3}{s}$$

$$T_{avg} = \frac{293 \; K + 313 \; K}{2} \sim 300 \; K$$

Assuming water at Tavg = 300 K: Cp = 4.179 kJ/kg-K and density = 996.6 kg/m³

$$\dot{m} = \rho_{air \, (20°C)} * \dot{V} = 996.6 \frac{kg}{m^3} * 0.00946 \; \frac{m^3}{s} = 0.943 \; \frac{kg}{s}$$

$$\dot{Q} = \dot{m} * C_p * \Delta T = 0.943 \; \frac{kg}{s} * 4.179 \; \frac{kJ}{kg - K} * 40 \; k = 157 \; kW$$

Maximum Fuel Flow Meter Power Rating

$$\dot{w} = \dot{m} * q_{hv} * \eta_{brake} = .0151\frac{kg}{s} * \frac{44000\ kJ}{kg\ fuel} * 0.35 = 233\ \text{kW}$$

Actual maximum power as limited by air supply (with roll-up door closed):

$$\dot{w}_{fuel} = \dot{m}_{fuel} * q_{hv} * \eta_{brake} = 0.0026\frac{kg}{s} * \frac{44000\ kJ}{kg\ fuel} * 0.35 = 40.0\ kW$$

APPENDIX F. DATA SHEETS FOR CUMMINS 2.8 L AND 5.0 L ENGINES

This appendix contains the data sheets for the Cummins 2.8 L and 5.0 L engines. Values used for design shown in Table 4-2 come from the second page of these data sheets where requirements for peak torque and maximum power are found in a table.

Cummins 2.8 L Data Sheet

|	Engine Performance Data Cummins Inc Columbus, Indiana 47202-3005 http://www.cummins.com	Automotive **ISF2.8S 5148** FR93527	110KW @ 2900rmp 360 Nm @ 1500-2900 rpm
			Configuration D0E3002BX03	CPL Code 3726	Revision 09-Aug-2017

| Compression Ratio: 16.9 :1	Displacement: 2.8 L (171 in3)
Fuel System: Bosch Electronic	Aspiration: Turbocharged and Charge Air Cooled

Emission Certification

Rating Types

China MEP NS V, Euro V

Motor Coach, Shuttle Bus, Truck

Torque Output
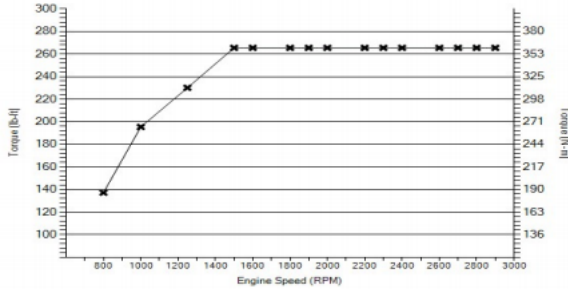
RPM	lb-ft	N-m
800	137	186
1000	195	265
1250	230	312
1500	266	360
1600	266	360
1800	266	360
1900	266	360
2000	266	360
2200	266	360
2300	266	360
2400	266	360
2600	266	360
2700	266	360
2800	266	360
2900	266	360

Power Output
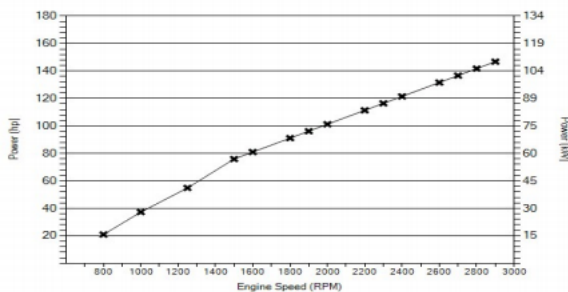
RPM	hp	kW
800	21	16
1000	37	28
1250	55	41
1500	76	57
1600	81	60
1800	91	68
1900	96	72
2000	101	75
2200	111	83
2300	116	87
2400	121	91
2600	132	98
2700	137	102
2800	142	106
2900	147	109

Curves shown above represent gross engine performance capabilities obtained and corrected in accordance with SAE J1995 conditions of 100 kPa (29.61 in Hg) barometric pressure [91 m (300 ft) altitude], 25 deg C (77 deg F) inlet air temperature, and 1 kPa (0.30 in Hg) water vapor pressure with No. 2 diesel fuel.

All data based on the engine operating with fuel system, water pump, lubricating oil pump, air compressor (unloaded) and with inlet restriction and exhaust restriction at or below datasheet limits. Not included are alternator, fan, optional equipment and driven components.

Tolerance within 5 %

Intake Air System

Maximum allowable air temperature rise between ambient air and engine air inlet		27 delta deg F	15 delta deg C

Cooling System

Maximum coolant temperature - engine out	230 deg F	110 deg C
Maximum charge air cooler outlet temperature (pumping mode)	158 deg F	70 deg C
Maximum coolant temperature - engine out (pumping mode)	230 deg F	110 deg C
Maximum coolant pressure (exclusive of pressure cap; closed thermostat at maximum no load speed)	31.2 psi	215 kPa
Minimum cooling capability at nominal fuel rate [Level II] with 30 km/hr (19 mile/hr) ram air speed and 50/50 ethylene glycol/water by volume		
Engine out coolant to ambient at 1500 RPM is 77 delta deg C (138.6 delta deg F)		
Maximum allowable pressure drop across charge air cooler and OEM CAC piping (CACDP)	4 in-Hg	13.5 kPa
Maximum coolant temperature for engine protection controls	237 deg F	114 deg C

Exhaust System

Maximum exhaust back pressure	5.92 in-Hg	20 kPa
Recommended exhaust pipe size (inner diameter)	3 in	76 mm

Fuel System

Engine fuel compatibility (consult Service Bulletin #3379001 for appropriate use of other fuels)	High Speed Diesel

Performance Data

Maximum low idle speed: 800 RPM

Minimum low idle speed: 700 RPM

Nominal no load governed speed: 3200 RPM

Maximum overspeed capability: 4800 RPM

Torque available at clutch engagement	133 lb-ft	180 N-m

Turbo model: HE201W

Turbo frame size: Small

	Governed Power	Maximum Power	Peak Torque
Engine Speed	2900 RPM		1500 RPM
Output Power	110 kW (148 hp)		56 kW (75 hp)
Torque	360 N-m (266 lb-ft)		360 N-m (266 lb-ft)
Turbo Comp. Outlet Pressure	141 kPa (41.8 in-Hg)		108 kPa (32 in-Hg)
Turbo Comp. Outlet Temperature	157 deg C (315 deg F)		127 deg C (260 deg F)
Inlet Air Flow	122 L/s (259 ft3/min)		60 L/s (127 ft3/min)
Charge Air Flow	8.5 kg/min (18.7 lb/min)		4 kg/min (9 lb/min)
Exhaust Gas Flow	297 L/s (629 ft3/min)		142 L/s (302 ft3/min)
Exhaust Gas Temperature	556 deg C (1033 deg F)		440 deg C (824 deg F)
Heat Rejection to Coolant	59 kW (3355 BTU/min)		32.9 kW (1870 BTU/min)
Radiator Coolant Flow*	3.1 L/s (49.1 gpm)		2.1 L/s (32.8 gpm)
Fuel Consumption	23.6 kg/hr (52 lb/hr)		11.4 kg/hr (25.1 lb/hr)
Brake Mean Effective Pressure	1600 kPa (232.1 psi)		1630 kPa (236.4 psi)

*Radiator Coolant Flow is approximately 5% less with a continuously deaerating system.

Cranking System (Cold Starting Capability)

Minimum ambient temperature for unaided cold start	14 deg F	-10 deg C

Change Log

Figure E1: Cummins 2.8 L Data Sheet

Cummins 5.0 L Data Sheet

	Engine Performance Data	Automotive	275 hp (205 kW) @ 3200 rpm
Cummins (logo)	Cummins Inc Columbus, Indiana 47202-3005 http://www.cummins.com	**V5.0 275** FR80027	560 lb-ft (750 N-m) @ 1600 rpm

| | Configuration D0H3004BX03 | CPL Code 4946 | Revision 27-Apr-2017 |

| Compression Ratio: 16.8 :1	Displacement: 5 L (305 in3)
Fuel System: Bosch HPCR	Aspiration: Turbocharged CAC

Emission Certification   EPA 2017
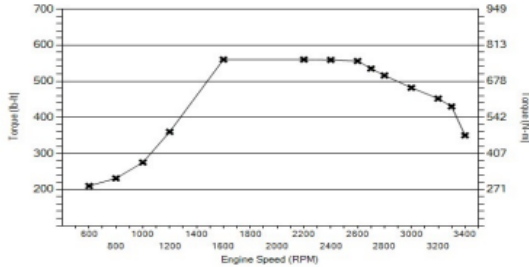
Rating Types   Recreational Vehicle, Truck

Torque Output

RPM	lb-ft	N-m
600	210	285
800	231	313
1000	275	373
1200	360	488
1600	560	759
2200	560	759
2400	559	758
2600	556	754
2700	535	725
2800	516	700
3000	482	654
3200	452	613
3300	430	583
3400	350	475
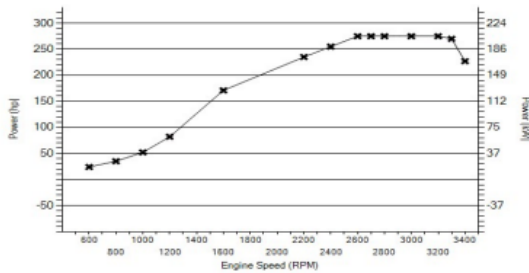
Power Output

RPM	hp	kW
600	24	18
800	35	26
1000	52	39
1200	82	61
1600	171	128
2200	235	175
2400	255	190
2600	275	205
2700	275	205
2800	275	205
3000	275	205
3200	275	205
3300	270	201
3400	227	169

Curves shown above represent gross engine performance capabilities obtained and corrected in accordance with SAE J1995 conditions of 100 kPa (29.61 in Hg) barometric pressure [91 m (300 ft) altitude], 25 deg C (77 deg F) inlet air temperature, and 1 kPa (0.30 in Hg) water vapor pressure with No. 2 diesel fuel.

All data based on the engine operating with fuel system, water pump, lubricating oil pump, air compressor (unloaded) and with inlet restriction and exhaust restriction at or below datasheet limits. Not included are alternator, fan, optional equipment and driven components.

Intake Air System

Maximum allowable air temperature rise between ambient air and engine air inlet	20 delta deg F	11.1 delta deg C

Cooling System

Maximum coolant temperature - engine out	225 deg F	107 deg C
Maximum coolant pressure (exclusive of pressure cap; closed thermostat at maximum no load speed)	20 psi	138 kPa

Minimum cooling capability at nominal fuel rate [Level II] with 24 km/hr (15 mile/hr) ram air speed and 50/50 ethylene glycol/water by volume

Engine out coolant to ambient at 3200 RPM is 66.1 delta deg C (119 delta deg F)

Engine out coolant to ambient at 2000 RPM is 71.1 delta deg C (128 delta deg F)

Charge air cooler outlet to ambient at 3200 RPM is 21.1 delta deg C (38 delta deg F)

Maximum allowable pressure drop across charge air cooler and OEM CAC piping (CACDP)	4 in-Hg	13.5 kPa
Maximum coolant temperature for engine protection controls	240 deg F	116 deg C

Exhaust System

Fuel System

Engine fuel compatibility (consult Service Bulletin #3379001 for appropriate use of other fuels)	ULSD

Performance Data

Maximum low idle speed: 1000 RPM

Minimum low idle speed: 600 RPM

Nominal no load governed speed: 3600 RPM

Maximum overspeed capability: 4750 RPM

	Governed Power	Maximum Power	Peak Torque
Engine Speed	3400 RPM	3200 RPM	2000 RPM
Output Power	169 kW (227 hp)	205 kW (275 hp)	159 kW (213 hp)
Torque	475 N-m (350 lb-ft)	613 N-m (452 lb-ft)	759 N-m (560 lb-ft)
Turbo Comp. Outlet Pressure	165.1 kPa (48.9 in-Hg)	193.5 kPa (57.3 in-Hg)	175.3 kPa (51.9 in-Hg)
Turbo Comp. Outlet Temperature	161 deg C (322 deg F)	181 deg C (358 deg F)	169 deg C (336 deg F)
Inlet Air Flow	235 L/s (498 ft3/min)	256 L/s (543 ft3/min)	156 L/s (331 ft3/min)
Charge Air Flow	19.9 kg/min (43.8 lb/min)	21 kg/min (46 lb/min)	13 kg/min (29 lb/min)
Exhaust Gas Flow	448 L/s (950 ft3/min)	491 L/s (1040 ft3/min)	352 L/s (745 ft3/min)
Exhaust Gas Temperature	461 deg C (862 deg F)	520 deg C (968 deg F)	464 deg C (867 deg F)
Heat Rejection to Coolant	124.8 kW (7100 BTU/min)	142.4 kW (8100 BTU/min)	105.5 kW (6000 BTU/min)
Radiator Coolant Flow*	3.5 L/s (56 gpm)	3.4 L/s (54 gpm)	2.3 L/s (36 gpm)
Fuel Consumption	41.1 kg/hr (90.7 lb/hr)	49.6 kg/hr (109.4 lb/hr)	34.3 kg/hr (75.6 lb/hr)
Brake Mean Effective Pressure	1193 kPa (173 psi)	1538 kPa (223 psi)	1910 kPa (277 psi)

*Radiator Coolant Flow is approximately 5% less with a continuously deaerating system.

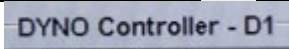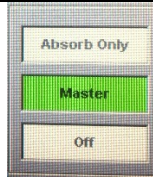**Cranking System (Cold Starting Capability)**
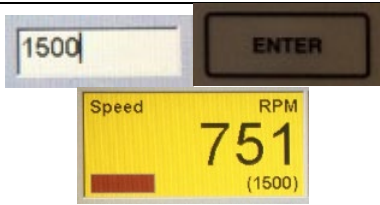
Minimum ambient temperature for unaided cold start   -13 deg F   -25 deg C
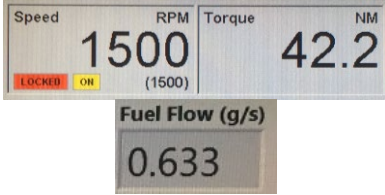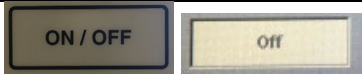
Figure E2: Cummins 5.0 L Data Sheet

APPENDIX G. DIESEL ENGINE OPERATING INSTRUCTIONS

Step	Process	Instruction	Picture
***	Emergency	**During operation, keep an eye on the dyno. If there are any unusual sounds, smells, or leaks, 1) Turn the key "OFF." If problem persists, 2) Press the Dyno "Emergency Stop" button**	
1	Pre-Start	Enter the engine lab. Visually inspect the engine and alert the TA if there are any obvious leaks or problems.	
2	Pre-Start (Dyno VFD in Engine Lab)	Turn on the Dynamometer (Dyno) VFD by ensuring that Emergency Stop is pulled out and press the **Green** button. Wait to hear fans at the top of the unit turn on.	
3	Pre-Start (Exhaust VFD in Engine Lab)	Power on the Exhaust VFD by turning the lower left switch to '**AUTO**'. 1. Place your hand inside the exhaust vent over the engine to ensure that air is being drawn out of the room. BE CAREFUL NOT TO TOUCH THE EXHAUST PIPE AS IT MAY BE HOT!	
4	Pre-Start (Water Lines in Engine Lab)	Verify that water valves on the east wall are open and resemble the picture shown.	
5	Pre-Start (Key in Control Room)	Turn the key switch to the "**ON**" position. You should hear the cooling water start flowing and the fuel pump turn on.	
6	Pre-Start (Computer)	On the computer, open the "Calterm" program. Select "Automatic" and wait for "Coolant_Temperature" value to	

		turn from gray to dark black. (This indicates that Calterm is connected to engine computer)	Coolant_Temperature 43.133
7	Pre-Start (Computer)	Open LabView Program "Flow Meter" on the desktop (click on the Run arrow if it is not already running)	
8	Startup (Dyno)	Ensure that the dyno screen shows "DYNO Controller – D1", if not, press "Control Select"	DYNO Controller - D1
9	Startup (Dyno)	Ensure that the absorb only icon on the screen is off (as shown in the picture), If the icon is green, Press "Absorb Only" to turn it off. This will enable the dyno to spin the engine up to a startup speed.	
10	Startup (Dyno)	Type "800" into the lower right input box and press "On/Off" to turn on the dyno	
11	Startup (Dyno)	Once the engine is running above 700 RPM, press the "Absorb Only" button which should cause the engine to idle at 750 RPM. (The engine will now spin the dyno rather than the dyno spinning the engine.)	
12	Startup (Dyno)	Change the dyno set speed to "1500" and press "Enter". (The engine should continue to idle until it receives additional fuel and tries to exceed the set speed of 1500 RPM.)	
13	Warmup (Dyno)	Switch screens by selecting "Control Select". You should now see "THROTTLE CONTROLLER – T3".	
14	Warmup (Dyno)	Press the "On/Off" button to turn on the throttle control (The Position % icon should light up. If not, touch it.)	
15	Warmup (Dyno)	Enter "20" % and press enter. This will add fuel to the engine causing it to speed up until it reaches the set speed. It will then increase load with additional fuel.	
16	Warmup (Computer)	Wait for the engine "Coolant_Temperature" (in **Calterm**) to reach an operating temperature of **80°C.** This usually takes about 6 minutes when	Coolant_Temperature 22.188 Should reach **80°C**

		cold. (After the engine warms up, the temperature will fluctuate between 78-86℃ as thermostat opens and closes)	
17	Change Load (Dyno)	Set the throttle controller position % to the first desired value and press "Enter." **(% must be between 0-55%)**	See Step #15
18	Take Data (Dyno and Computer)	Wait until torque and fuel data are at steady state and record the following values multiple times: 1. Dyno control screen: speed (RPM), torque (N-m) 2. LabVIEW Program: fuel flow (g/s)	
19	Shutdown (Dyno)	Turn throttle controller position % down to **20**	See Step #15
20	Shutdown (Dyno)	Hit "**On/Off**" to turn "THROTTLE Controller – T3" off (This should slow the engine down to an idle speed)	
21	Shutdown (Dyno)	Hit "**Control Select**" to switch to "DYNO Controller – D1"	
22	Shutdown (Dyno)	Hit "**On/Off**" on the Dyno Controller (Dyno fans will turn off)	
23	Shutdown (Key)	Turn the key to the "**Off**" position to kill the engine, water flow, and fuel pump.	
24	Shutdown (Dyno VFD)	Enter the room and turn off the Dyno VFD using the Red button.	
25	Shutdown (Exhaust VFD)	Turn the Exhaust fan VFD to the "OFF" position. (Everything should be quiet when shut down properly)	
26	Shutdown (Computer)	Close the Calterm and LabView programs	

APPENDIX H. DIESEL ENGINE LABORATORY EXPERIMENT INSTRUCTIONS AND SAMPLE DATA

<u>**Key for**</u> - <u>Diesel Lab 1: Diesel Brake Work, Power, and Efficiency</u>

Assignment

1. Run the lab to take data for Torque and Fuel Flow Rate
2. Calculate the Brake Power (kW) and Fuel Power E_{fuel} (kW) per cycle for each operating condition.
3. Plot torque as a function of fuel flow rate with a single point as the average and error bars showing one standard deviation for the four data points you collected (may not be able to see it if data has a small spread and values are large)
4. Plot the brake fuel conversion efficiency as a function of fuel flow rate (load) showing a single data point for the average and error bars representing plus or minus one standard deviation of the data collected.
5. Discuss why the brake fuel conversion efficiency increases with increasing load?

Answers

The Answers should resemble, the following data, though the lab data will not include the 60 and 70% Pedal Positions. Data (Taken on 9/27/19)

1. Run the lab to take data for Torque and Fuel Flow Rate
2. Calculate the Brake Power (kW) and Fuel Power E_{fuel} (kW) per cycle for each operating condition.

| | | Power Data | | | Calculated Values | |
| | % | | m_dot | | Heating Power | |
RPM	Throttle	Torque (N-m)	(g/s)	Power (kW)	(kW)	Efficiency
750	0	5	0.188	0.39269908	8.272	0.047473
	0	6	0.2	0.4712389	8.8	0.05355
	0	7	0.149	0.54977871	6.556	0.083859
	0	10	0.159	0.78539816	6.996	0.112264
1500	15	51.2	0.717	8.04247719	31.548	0.254928
	15	53.2	0.663	8.35663646	29.172	0.286461
	15	52.2	0.686	8.19955683	30.184	0.271652
	15	52.8	0.71	8.29380461	31.24	0.265487
1500	20	68	0.811	10.681415	35.684	0.299333
	20	69.6	0.774	10.9327424	34.056	0.321023
	20	67.2	0.809	10.5557513	35.596	0.296543
	20	69.4	0.774	10.9013265	34.056	0.3201
1500	30	113	1.195	17.7499985	52.58	0.337581
	30	111.7	1.12	17.545795	49.28	0.356043
	30	112.6	1.171	17.6871666	51.524	0.34328
	30	114.2	1.125	17.9384941	49.5	0.362394
1500	40	157.4	1.445	24.7243342	63.58	0.38887
	40	156.7	1.528	24.6143784	67.232	0.366111
	40	158	1.485	24.818582	65.34	0.379837
	40	156	1.577	24.5044227	69.388	0.353151
1500	50	211	1.95	33.1438025	85.8	0.386291
	50	209	2.001	32.8296432	88.044	0.372878
	50	210	1.995	32.9867229	87.78	0.375789
	50	211.8	2.033	33.2694662	89.452	0.371925
1500	55	227	2.18	35.6570766	95.92	0.371738
	55	224.5	2.15	35.2643775	94.6	0.372774
	55	226.5	2.17	35.5785368	95.48	0.372628
	55	225	2.14	35.3429174	94.16	0.37535

3. Plot torque as a function of fuel flow rate with a single point as the average and error bars showing one standard deviation for the four data points you collected (may not be able to see it if data has a small spread and values are large)
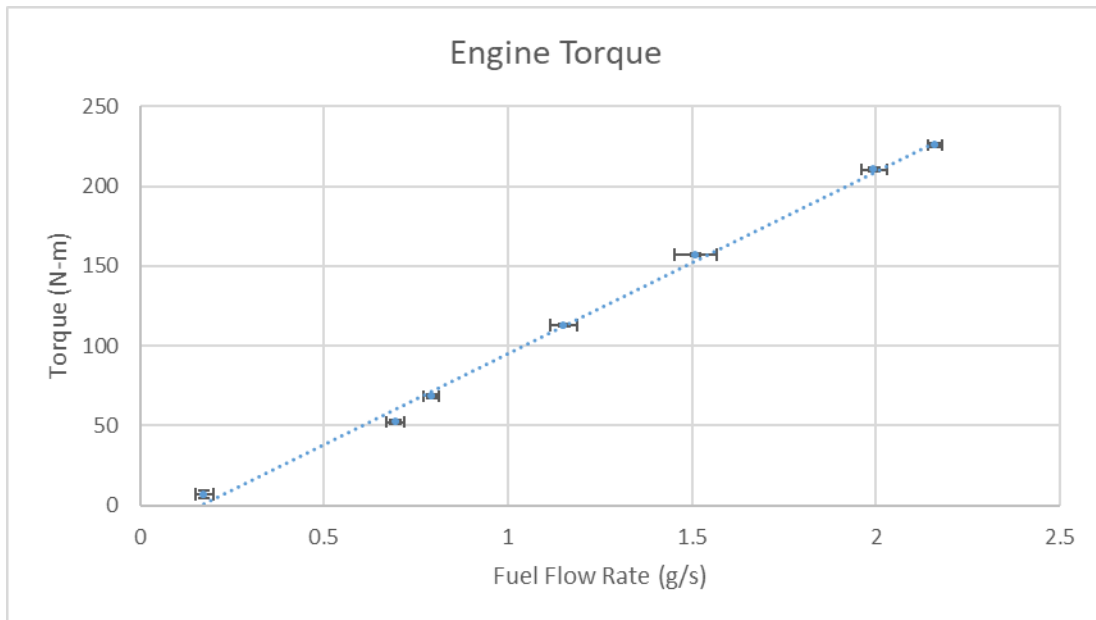
4. Plot the brake fuel conversion efficiency as a function of fuel flow rate (load) showing a single data point for the average and error bars representing plus or minus one standard deviation of the data collected.
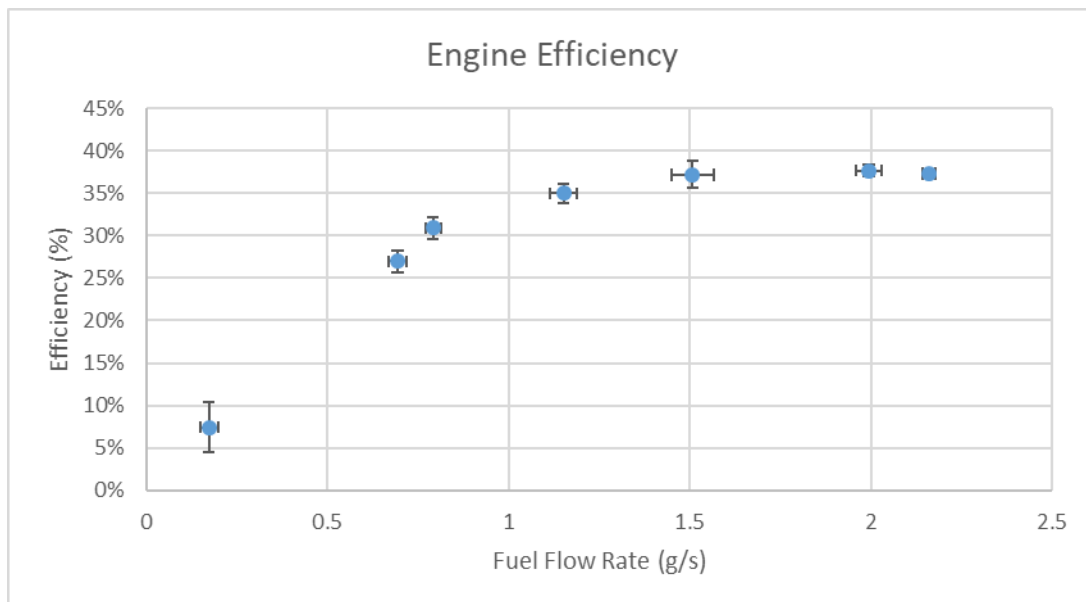
5. Discuss why the brake fuel conversion efficiency increases with increasing load?

$$\eta_b = \frac{\dot{W}_b}{q_{hv} * \dot{m}_f} = \frac{\dot{W}_{i,g} - \dot{W}_p - \dot{W}_f}{q_{hv} * \dot{m}_f} = \frac{\dot{W}_{i,g}}{q_{hv} * \dot{m}_f} - \frac{\dot{W}_p}{q_{hv} * \dot{m}_f} - \frac{\dot{W}_f}{q_{hv} * \dot{m}_f}$$

Of the Terms on the right side, the left term is nearly constant as both the numerator and denominator increase. The middle term is nearly 0 for a diesel engine with no pumping work (or that term even becomes a slight positive for turbocharged engine. The right term decreases or the friction becomes a smaller portion due to the fact that the friction remains nearly constant for a constant engine speed and the denominator keeps increasing with increasing fuel flow.

Additional Plots for Reference

Brake Engine Power
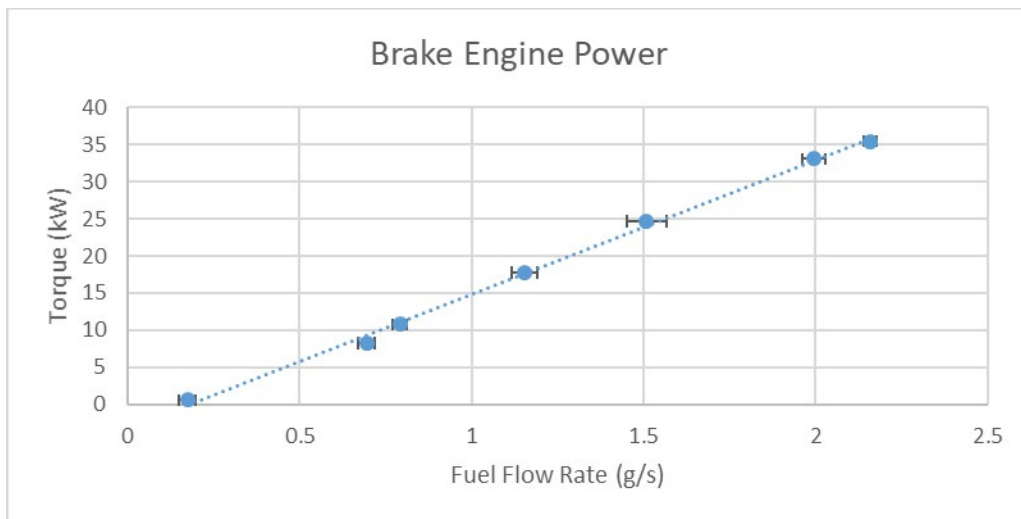
Key for - Diesel Lab 2: Diesel Emissions, Brake Work, and Efficiency

Assignment

1. Run the lab to take data for Torque, Fuel Flow Rate, NOx, CO, CO2, O2.
2. Plot the emissions concentrations as a function of fuel flow with error bars. (Plot both PPM and Vol % on the same chart. Plot PPM (NO_x, SO_2, CO) on the left axis and Vol% (CO_2 and O_2) on the right axis and differentiate each with a legend. If printing in black and white, change the points to stars, boxes, … to clearly differentiate the concentrations.)
3. Discuss trends in emissions verses fuel flow rate (load). Some observations should include:
   a. The scale of NO and CO compared to O2, CO2?
   b. The relationship between CO2 and O2 with change in fuel flow?
   c. How does NOx change with fuel flow?
   d. How does O2 change with fuel flow?
   e. How does CO2 change with fuel flow?
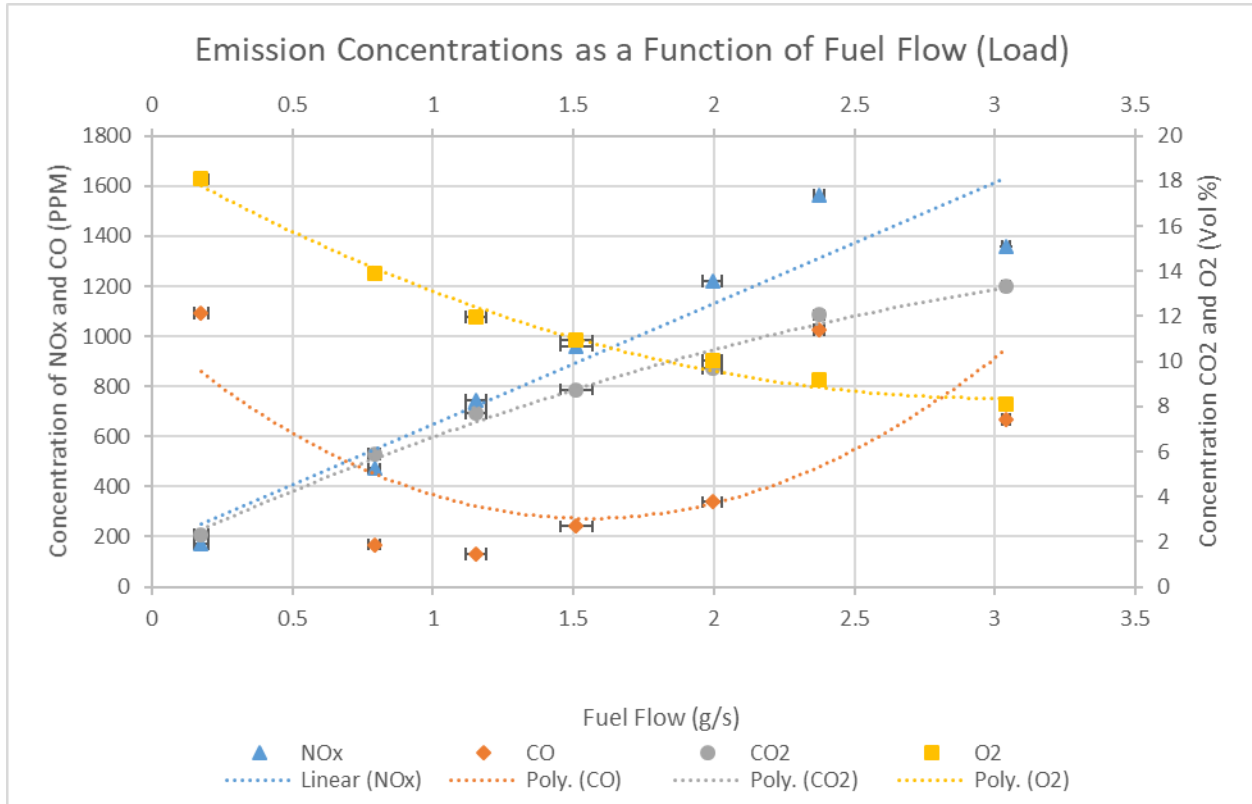   f. How does CO change with change in fuel flow?

Answers

The Answers should resemble, the following data, though the lab data will not include the 60 and 70% Pedal Positions. Data (Taken on 10/2/2019) (Bay door must be opened a bit in order to achieve 60/70% pedal positions)

4. Run the lab to take data for Torque, Fuel Flow Rate, NOx, CO, CO2, O2. – (NOTE: exact values of emissions will change between labs, but the trends should remain the same)

	Power Data			Emissions Data			
RPM	% Throttle	Torque (N-m)	m_dot (g/s)	Nox (PPM)	CO (PPM)	CO2 (Vol%)	O2 (Vol%)
750	0	5	0.188	173	1096	2.31	18.08
	0	6	0.2	172	1088	2.31	18.08
	0	7	0.149	171	1105	2.32	18.08
	0	10	0.159	173	1083	2.33	18.09
1500	20	68	0.811	471	169	5.89	13.89
	20	69.6	0.774	472	168	5.89	13.91
	20	67.2	0.809	473	170	5.9	13.91
	20	69.4	0.774	473	167	5.9	13.89
1500	30	113	1.195	746	134	7.71	11.97
	30	111.7	1.12	745	131	7.7	11.96
	30	112.6	1.171	745	131	7.69	11.97
	30	114.2	1.125	746	130	7.71	11.97
1500	40	157.4	1.445	961	237	8.76	10.93
	40	156.7	1.528	962	241	8.75	10.93
	40	158	1.485	961	246	8.74	10.93
	40	156	1.577	962	243	8.76	10.93
1500	50	211	1.95	1217	326	9.67	10.05
	50	209	2.001	1222	338	9.68	10.03
	50	210	1.995	1223	341	9.69	10.04
	50	211.8	2.033	1221	350	9.7	10.04
1500	60	250	2.37	1555	1015	12.05	9.14
	60	251	2.4	1565	1015	12.05	9.15
	60	252	2.36	1567	1027	12.06	9.17
	60	245	2.37	1568	1049	12.07	9.17
1500	70	320	3.06	1337	642	13.29	8.11
	70	316	3.03	1341	648	13.35	8.1
	70	317	3.04	1378	691	13.32	8.1
	70	319	3.03	1378	690	13.35	8.03

5. Plot the emissions concentrations as a function of fuel flow with error bars. (Plot both PPM and Vol % on the same chart. Plot PPM (NO_x and CO) on the left axis and Vol% (CO_2 and O_2) on the right axis and differentiate each with a legend. If printing in black and white, change the points to stars, boxes, … to clearly differentiate the concentrations.)

Emission Concentrations as a Function of Fuel Flow (Load)

6. Discuss trends in emissions verses fuel flow rate (load). Some observations should include:
   a. The scale of NO and CO compared to O2, CO2?
   b. The relationship between CO2 and O2 with change in fuel flow?
   c. How does NOx change with fuel flow?
   d. How does O2 change with fuel flow?
   e. How does CO2 change with fuel flow?
   f. How does CO change with change in fuel flow?

111

	Question	Answer
A	The scale of NOx and CO compared to O2, CO2?	NOx and CO are in PPM and CO2 and O2 are in Volume %, therefore, it takes 10,000 ppm to make 1%
B	The relationship between CO2 and O2 with change in fuel flow?	As fuel in increases, a larger amount of O2 is converted to CO2, and CO is a minimal emission product, therefore the percent of O2 decreases as the percent of CO2 increases. They can cross each other, but don't normally cross for the lab values of 0-50% pedal position.
C	How does NOx change with fuel flow?	NOx increases linearly with fuel flow. As load increases, NOx increases. *Note: emissions analyzer couldn't read the NOx at the maximum 70% position
D	How does O2 change with fuel flow?	O2 Decreases
E	How does CO2 change with fuel flow?	CO2 Increases
F	How does CO change with change in fuel flow?	Engine emits much more CO2 at idle then it decreases down to a minimum around 30% pedal position then increases with load

Additional Plots for Reference

Brake Engine Torque

Brake Engine Power

Engine Efficiency